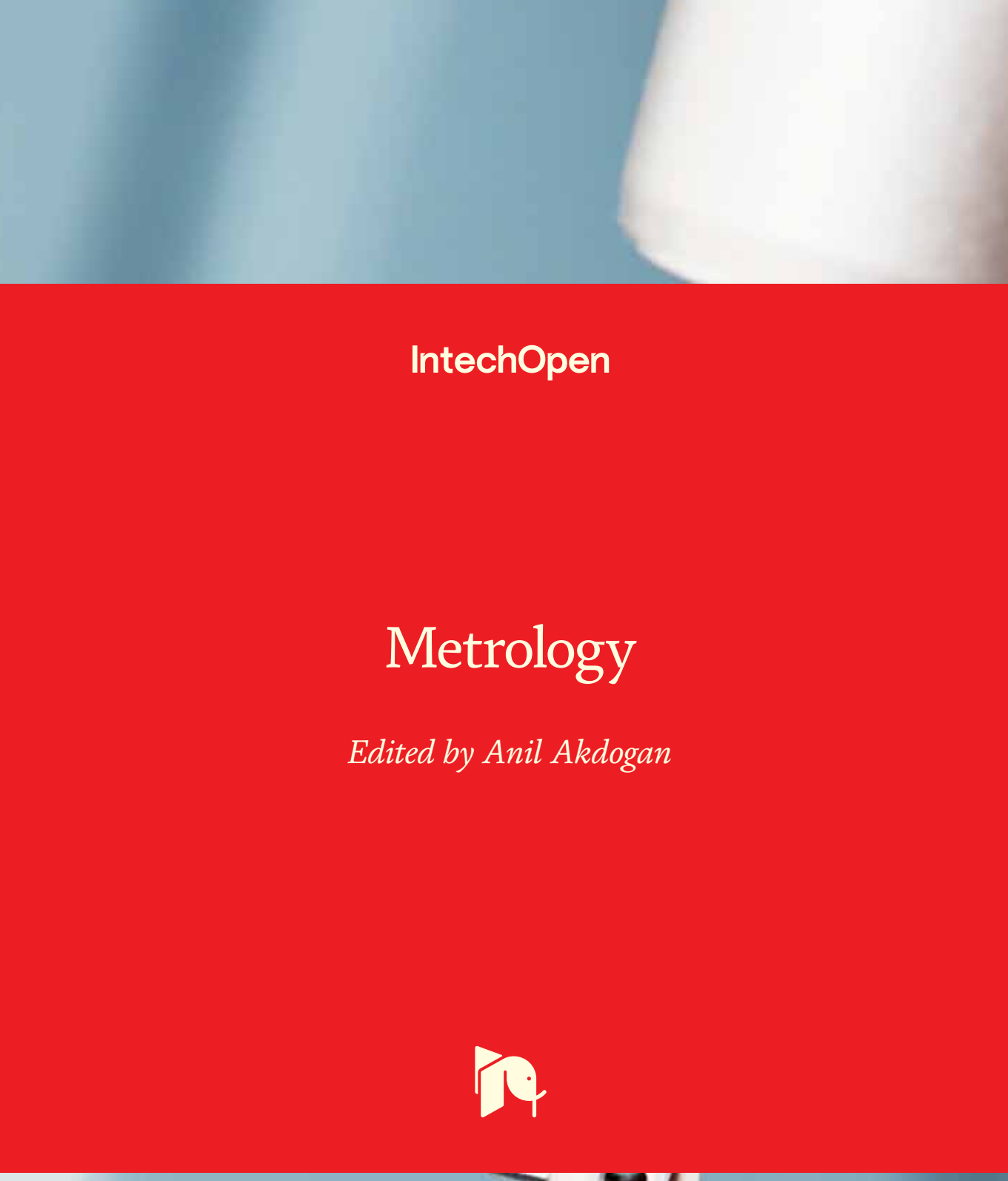

IntechOpen

Metrology

Edited by Anil Akdogan

METROLOGY

Edited by **Anil Akdogan**

Metrology
http://dx.doi.org/10.5772/intechopen.71144
Edited by Anil Akdogan

Contributors

Anil Akdogan, Manal A. Haridy, Affia Aslam, Eugene Charnukha, Jailton Damasceno, Paulo Guimarães Couto, Michael Surdu, Andrea De Marchi

Notice

First published in London, United Kingdom, 2018 by IntechOpen
eBook (PDF) Published by IntechOpen, 2019
IntechOpen is the global imprint of INTECHOPEN LIMITED, registered in England and Wales, registration number: 11086078, The Shard, 25th floor, 32 London Bridge Street
London, SE19SG – United Kingdom
Printed in Croatia

British Library Cataloguing-in-Publication Data
A catalogue record for this book is available from the British Library

Additional hard and PDF copies can be obtained from orders@intechopen.com

Metrology
Edited by Anil Akdogan

p. cm.

Print ISBN 978-1-78923-595-1

Online ISBN 978-1-78923-594-4

eBook (PDF) ISBN 978-1-83881-517-2

Meet the editor

Assoc. Prof. Anil Akdogan was born in Antalya, Turkey in 1976. She received her Bachelor of Science degree in Mechanical Engineering in 1996 and her PhD degree in Mechanical Engineering in 2005 from the Yildiz Technical University, Mechanical Engineering Department, Istanbul, Turkey. She has over 20 years of experience in teaching at the Mechanical Engineering Faculty, Yildiz Technical University. She has lectured courses in "Measurement Techniques and Evaluation," "Quality in Industry," "Manufacturing Technologies" and "Measurement Techniques and Quality Management" for many years. She has published many manuscripts in international journals and presented proceedings at different international conferences about manufacturing technologies and industrial metrology.

Contents

Preface

Metrology is the science of measurement. It covers all the practical and theoretical topics based on measurement, regardless of accuracy level and application area. Measurement processes, measurement methods and procedures, instrumentation, calibration, determination of measurement systems, verification, measurement accuracy, measurement precision, measurement error, data acquisition, evaluation of measurement results, the formation of statistical evaluations and quality determinations are the main subjects of metrology. Metrology is crucial for many sciences and technological developments as well. Since metrology helps to improve many other sciences, the book reflects in general metrology and some special metrological approaches at different fields such as radiation and frequency measurements in detail. This book also focuses on technical testing and control applications in the industry and intends the fundamentals of metrology concerning the related standards and systems of units. In addition, the book considers the calibration of measurement instruments and measurement uncertainties as the basic requirements of the related quality standards. Thanks go to all metrology scientists working for closer results to the reals.

Anil Akdogan
Yildiz Technical University
Department of Mechanical Engineering
Istanbul, Turkey

Section 1

Metrology in General

Chapter 1

Introductory Chapter: Metrology

Anil Akdogan

Additional information is available at the end of the chapter

http://dx.doi.org/10.5772/intechopen.75541

1. Introduction

Metrology, the science of measurement, is crucial for manufacturing technologies. Since manufacturing has made huge leaps depending on the improvements in metrology, the book reflects recent developments in metrology in detail. This book focuses on dimensional and geometric measurements as well as technical testing and quality control applications in industry. It also intends the fundamentals of metrology concerning the related standards and systems of units. In addition, the book considers the calibration of measurement instruments and measurement uncertainties as the basic requirements of the related quality standards. Furthermore, it mentions the trends in micro and nanometrology and microscopic examinations. Topics covered in this book are of course not limited to them. The readers can find chapters about Metrology in a wide frame.

Physical properties such as length, weight, and temperature are determined by comparison with known quantities. In addition, measurement techniques are available in all engineering disciplines and allow for the creation and operation of all other scientific branches. In particular, measurement techniques are required at all levels of laboratory works. In fact, we practically measure many things: the weight of our body, the volume of our fuel oil, the temperature of the house, the noise at the factory, the distance between two points, etc. In addition to having an important place in our daily life, the measurement technique is the basis of almost all science branches such as Physics, Chemistry, and Biology. Measurement techniques are used to solve technical problems at all science branches. Theoretical hypotheses are supported by proving correctness by means of measurement technique by making necessary experiments and observations.

Metrology is the science of measurement. It covers all the practical and theoretical topics based on measurement, regardless of accuracy level and application area [1]. Measurement processes, measurement methods and procedures, instrumentation, calibration, determination of

measurement systems, verification, measurement accuracy, measurement precision, measurement error, data acquisition, evaluation of measurement results, the formation of statistical evaluations, and quality determinations are the main subjects of metrology.

The recognition that a measurement made by an industrial device is recognized worldwide and is the same as any other measurement made possible by achieving the highest precision basic measurement standard with a measurement reference chain. By fulfilling this, it is ensured that all the measurements carried out are accepted nationally and/or internationally. As a result, the calibration and verification processes have gained a great deal of importance. Calibration is a process of establishing a link between the values indicated by a measuring instrument or measuring system under certain conditions and the values obtained by a measuring instrument and corresponding values of corresponding measured values. With calibration, the measurement of a less precise measuring instrument or standard is carried out using an accepted standard of accuracy [2]. National metrology institutes are operating at the highest level, linked to the system by reference chain. These institutions are also linked to the Bureau International des Poids et Measure (BIPM) in central Paris in order to ensure that the measurements are internationally recognizable in a hierarchical structure. In the process of industrialization which started with serial production, it has become very important to establish a whole by combining the parts produced in different places, initiate specialization forms in the subsidiary industry and production, and make the measurements internationally recognizable.

The reliability of measuring instruments has increased at the same rate as the widespread use of microelectronics. Nowadays, measurement techniques are required to meet demands for faster, more accurate, and more flexible measurements. The documentation of measurement results is equally important. The development of precise manufacturing technology brings the need for more precise measuring technology. The developments in technology, especially in the field of measuring technology, have been the main reason for the increasing demands on the accuracy of the measurement. As micro and nanotechnologies have been used, it has become inevitable to develop devices and instruments that enable the measurement operations to be carried out at these accuracies.

New dimensions and research opportunities have been born in many scientific fields such as being in the electronics or molecular biology with nanotechnology. All of these disciplines are doing nanoscience studies on their own terms, and the opportunity to share all these different windows and share tools and techniques that develop independently is attractive to all sciences today. The placement of the atoms in the prescribed positions with the aid of nanotechnology is realized in this technology. Today the word "Nano" indicates a technique related to length measurements of very small objects in metrology, microtechnology, semiconductors, and nanotechnology fields. In nanometrology, the measurement size is typically specified as a nanometer. All applied methods are based on microscope technique with nano-position systems and position measurements at high accuracy. For instance, in mechanical engineering, nanotechnology and nanometrology are the necessary technologies to make a crystal perfect. The ability to precisely control the alignment of imprints and errors with respect to each other and the ability to integrate perfectly inorganic and organic nanostructures will lead to the emergence of a whole new generation of advanced composites. The improvements in technology intended to use the term *picotechnology* is a combination of picometer

and technology, parallel the term nanotechnology. Basic speckle metrology and autonomic computing resources are of course the most realistic uses of picotechnology. The ability to examine and manipulate resources at this level is quite useful. Of course, it is not difficult to imagine the tangible advantages of this type of technology.

2. Standardization in metrology

Standards are considered as measurement references. The basic standards about metrology are the basis of the traceability which is defined as a measurement whereby the result can be related to a reference through an unbroken chain of calibrations. Using internationally standardized systems of units, Vocabulary of Metrology (VIM), Guide to the International Uncertainty Measurements (GUM), or Internationally Standardized Measurement Management Systems [3] helps to improve the reliability of the results.

2.1. Unit of measurement

The most important condition of each measuring process and the manufacturing technique is the presence of units which are exactly defined according to the required quantities, and these units must be determined in accordance with internationally established rules. M*easurement* is a process that uses numbers to describe a physical quantity done to be able to compare them to each other. The results can be explained by a "*unit* of *measurement*," which is a definite magnitude of a quantity. The *SI,* The International System of *Units,* is the modern form of the metric system, and the most widely used system of measurement is made up of 7 base *units* that define the 22 derived *units* with special names and symbols. Base units provide the reference used to define all the measurement units of the system, while the derived units are products of base units and are used as measures of derived quantities. Derived units are the units obtained by algebraic operations from basic and auxiliary units. Certain derived units have special names and symbols like acceleration, meter per second squared, m s^{-2}.

2.2. Uncertainty of measurement

The uncertainty of a measurement is a predicament that characterizes the range of values, including the true value of the measure. *Measurement uncertainty* is an important topic for all measurement fields. All measurements have error. The error of a measurement is unknowable because one cannot know the error without knowing the true value of the quantity being measured. The *Evaluation of Measurement Data: Guide to the Expression of Uncertainty in Measurement* (GUM) provides general rules for evaluating and expressing uncertainty in measurement. The uncertainty of measurement generally includes many components. Some of these components can be estimated on the basis of the statistical distribution of series measurement results and can be characterized by empirical standard deviations. The estimates of the other components are based solely on the main information or experiences. The uncertainty of measurements should be evaluated and reported according to the related international standards.

2.3. Calibration

The purpose of calibration is to determine and document how much of the equipment is in error with the actual value. The correct value is obtained by considering the amount of error in the result. Calibration is the process of determining the relationship between the value read in a gauge and the gauge size. Calibration and control of measuring, inspection, and control equipments ensure the appropriateness of measurements made during manufacturing. The continuity of this safety is ensured by the regular and identifiable calibration of the equipment in question. Calibration is performed by comparison with a measurement of normality known to the measurement magnitude. To sum up, calibration is explained in the related standard: under specified conditions, the series of operations in which the relationship between the values indicated by a measuring instrument or device and the values indicated by a material measurement or reference material is established [3]. In order to supply traceability in measurements, calibration hierarchy in **Figure 1** should be followed up carefully.

3. Data evaluation

Metrology and inspection together serve as the control function of the quality of conformance. Inspection helps to evaluate the degree of conformance or nonconformance to specifications, provides for reporting of deficiencies early in the production process, and helps to assure that desired quality requirements have been met. The field of knowledge concerned with measurement. Metrology includes all aspects of both theoretical and practical with reference to measurements, whatever their level of accuracy, and in whatever fields of science or technology they occur. Since quality performance decisions are based on inspection and measurement, undesirable consequences may result if these tasks are not performed properly. Not only incorrect measurements lead to wrong decisions, which can have serious consequences, but also improper data evaluations can cause undesirable consequences. Since Statistical Process Control is the utilization of statisti-

Figure 1. Hierarchy of calibration/traceability pyramid.

cal tools and methods to acquisite and to analyze data in order to monitor process capabilities, it is widely used in data evaluation. Quality control charts and the other statistical tools are used to analyze processes enabling appropriate actions to achieve improved or stabilized processes. They help to ensure that the process operates efficiently and allow organizations to understand variation in their processes, differentiating common causes from special or assignable causes of variation.

4. Conclusions

Metrology is a crucial science including its standards, systems of units, instruments, calibration procedures, uncertainties, inspection, and quality control topics in many industries such as automotive, aerospace, mechanical engineering, surface engineering, etc. and in many sciences like natural and applied sciences in different sizes like micro and nanometrology serving for sustainable improvements. Like being in today, there will always be valuable researches in the field of metrology, with the help of technological developments to support the scientific researches in the future. Care taken in the reliability of measurements and their traceability will always be crucial. Metrology is such useful for humanity if it is conducted according to its rules and international standards.

Acknowledgements

I would like to thank the authors for their contributions and the publisher that provided this opportunity.

Author details

Anil Akdogan

Address all correspondence to: nomak@yildiz.edu.tr

Mechanical Engineering Department, Yildiz Technical University, İstanbul, Turkey

References

[1] International Vocabulary of Metrology: Basic and General Concepts and Associated Terms. 3rd ed. VIM; 2012. JCGM 200:2012

[2] Uncertainty of measurement: Part 3: Guide to the expression of uncertainty in measurement. GUM; 1995. ISO/IEC Guide 98-3:2008

[3] Measurement management systems: Requirements for measurement processes and measuring equipment. 2003. ISO 10012:2003

Chapter 2

Methods for Evaluation of Measurement Uncertainty

Jailton Carreteiro Damasceno and Paulo R.G. Couto

Additional information is available at the end of the chapter

http://dx.doi.org/10.5772/intechopen.74873

Abstract

This chapter presents and explains the most used methodologies for the evaluation of measurement uncertainty in metrology with practical examples. The main topics are basic concepts and importance, existing documentation, the harmonized methodology of the Guide to the Expression of Uncertainty in Measurement, types of uncertainty, modeling of measurement systems, use of alternative methods (including the GUM supplement 1 Monte Carlo numerical method), evaluation of uncertainty for calibration curves, correlated uncertainties, uncertainties arising from the calibration of instruments, and the main proposals for the new revised GUM. The chapter also discusses the GUM as a tool for the technical management of measurement processes.

Keywords: metrology, measurement, uncertainty, GUM, Monte Carlo

1. Introduction

Measurement uncertainty is a quantitative indication of the quality of measurement results, without which they could not be compared between themselves, with specified reference values or to a standard. Uncertainty evaluation is essential to guarantee the metrological traceability of measurement results and to ensure that they are accurate and reliable. In addition, measurement uncertainty must be considered whenever a decision has to be taken based on measurement results, such as in accept/reject or pass/fail processes.

Considering the context of globalization of markets, it is necessary to adopt a universal procedure for evaluating uncertainty of measurements, in view of the need for comparability of results between nations and for mutual recognition in metrology. As an example, laboratories accredited under the ISO/IEC 17025:2017 standard [1] need to demonstrate their technical

competence and the ability to properly operate their management systems, and so they are required to evaluate the uncertainty for their measurement results.

In addition, the use of uncertainty evaluation methods as a tool for technical management of measurement processes is extremely important to reduce, for example, the large number of losses that occurs in the industry, which can be highly significant in relation to the gross domestic product (GDP) of some countries. One of the probable causes of the waste can be attributed to instruments whose accuracy is inadequate to the tolerance of a certain measurement process.

In this chapter, detailed steps for uncertainty evaluation are given.

2. Main references for uncertainty evaluation

In order to harmonize the uncertainty evaluation process for every laboratory, the *Bureau International des Poids et Mesures* (BIPM) published in 1980 the Recommendation INC-1 [2] on how to express uncertainty in measurement. This document was further developed and originated the "Guide to the Expression of Uncertainty in Measurement"—GUM in 1993, which was revised in 1995 and lastly in 2008. This document provides complete guidance and references on how to treat common situations on metrology and how to deal with uncertainties in metrology. Currently, it is published by International Organization for Standardization (ISO) as the ISO/IEC Guide 98-3 "Uncertainty of measurement—Part 3: Guide to the expression of uncertainty in measurement" (GUM), and by the Joint Committee for Guides in Metrology (JCGM) as the JCGM 100:2008 guide [3]. The JCGM was established by BIPM to maintain and further develop the GUM. They are in fact currently producing a series of documents and supplements to accompany the GUM, four of which are already published [4–7].

Evaluation of uncertainty, as presented by the JCGM 100:2008, is based on the law of propagation of uncertainties (LPU). This methodology has been successfully applied for several years worldwide for a range of different measurement systems and is currently the most used procedure for uncertainty evaluation in metrology. However, since its twentieth anniversary in 2013, JCGM decided to revise it again [8–10]. In this new revision, uncertainty terms and concepts [11] will be aligned with the current International Vocabulary of Metrology (VIM) [12] and with the new GUM supplements [5, 6]. Aspects such as a new Bayesian approach, the redefinition of coverage intervals and the elimination of the Welch-Satterthwaite formula to evaluate the effective degrees of freedom will be covered [9]. In late 2014, a first draft of the newly revised version of the GUM was circulated among National Metrology Institutes. Remarkable changes were made that could affect the way laboratories deal with the measurement uncertainty results. This revision is still being discussed, and some information about it has also been released elsewhere [10].

In the field of analytical chemistry, there is also another document worth mentioning that is the "Quantifying Uncertainty in Analytical Measurement" guide [13], produced by a joint

EURACHEM/CITAC Measurement Uncertainty Working Group. This document was first published in 1995 and further revised in 2000 [14]. This last edition had a widespread implementation and is among the most highly cited publications in chemical metrology area [14]. Recently, a new revised edition was published in 2012 with improved content and added information on developments in uncertainty evaluation [14]. This document basically presents the uncertainty evaluation process following the suggestions of the GUM, but also contains several examples in the analytical chemistry area.

3. Using the GUM approach on uncertainty evaluation

The following main steps summarize the methodology presented by the GUM.

3.1. Definition of the measurand and of input quantities

It must be clear to the analyst which quantity will be the final object of the measurement in question. This quantity is known as the measurand. In addition, it is important to identify all the variables that directly or indirectly influence the measurand. These variables are known as the input quantities. As an example, Eq. (1) shows a measurand y as a function of three different input quantities: x_1, x_2, and x_3.

$$y = f(x_1, x_2, x_3) \tag{1}$$

3.2. Modeling the measurement process

In this step, the measurement procedure should be modeled in order to have a functional relationship expressing the measurand as a result of all the input quantities. The measurand y in Eq. (1) could be modeled, for example, as in Eq. (2)

$$y = \frac{x_1 x_2}{x_3^2} \tag{2}$$

The modeling step is critical for the uncertainty evaluation process as it defines how the input quantities impact the measurand. The better the model is defined, the better its representation of reality will be, including all the sources that impact the measurand on the uncertainty evaluation. The modeling process can be easily visualized by using a cause-effect diagram (**Figure 1**).

Example: To illustrate these steps, let us consider a measurement model for a torque test. Torque is a quantity that represents the tendency of a force to rotate an object about an axis. It can be mathematically expressed as the product of a force and the lever-arm distance. In metrology, a practical way to measure it is by loading a known mass to the end of a horizontal arm while keeping the other end fixed (**Figure 2**).

Note: This example is also presented, with a few adaptations, in other publications by the same authors [15].

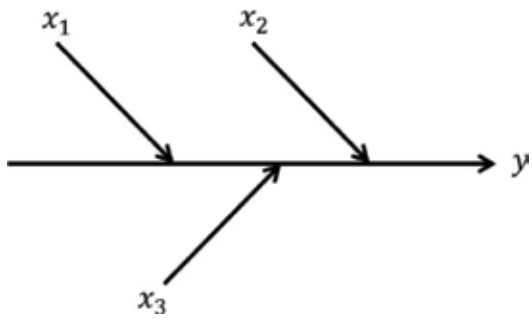

Figure 1. A cause-effect diagram representing the model from Eq. (2).

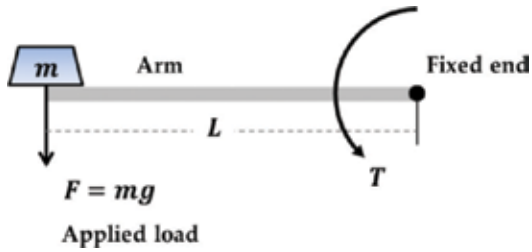

Figure 2. A conceptual illustration of the experimental setup for a measurement of torque (T), where F is the applied force, m is the mass of the load, g is the local gravity acceleration, and L is the length of the arm.

A simple model that describes this experiment can be expressed as follows:

$$T = mgL \tag{3}$$

where T is the torque (N.m), m is the mass of the applied load (kg), g is the local gravity acceleration (m/s^2), and L is the total length of the arm (m). Thus, m, g, and L are the input quantities for this model. This example will be further discussed in the subsections ahead.

3.3. Evaluating the uncertainties of the input quantities

This step is also of great importance. Here, uncertainties for all the input quantities are individually evaluated. The GUM classifies uncertainty sources as being of two main types: Type A, which usually originates from some statistical analysis, such as the standard deviation obtained in a repeatability study; and Type B, which is determined from any other source of information, such as a calibration certificate or deduced from personal experience.

Type A uncertainties from repeatability studies are evaluated by the GUM as the standard deviation of the mean obtained from the repeated measurements. For example, if a set of n indications x_i about a quantity x are available, the uncertainty u_x due to repeatability of the measurements can be expressed by $s(\overline{x})$ as follows in Eq. (4):

$$u_x = s(\overline{x}) = \frac{s(x_i)}{\sqrt{n}} \tag{4}$$

where $\overline{x}$ is the mean value of the repeated measurements, $s(x_i)$ is its standard deviation, and $s(\overline{x})$ is the standard deviation of the mean. As such, the statistical distribution associated with this input source is considered to be normal or Gaussian.

Note: This evaluation is not consistent with the GUM supplement 1 [5], where repeated indications are treated as Student's *t*-distributions to account for the lack of degrees of freedom or a low number of indications. In this way, the new proposal for the draft GUM is to consider repeated indications as *t*-distributions, just like in supplement 1. Therefore, its uncertainty would be evaluated as in Eq. (5). This equation takes the degrees of freedom for the indications $(n-1)$ into account, raising the uncertainty for a low number of indications. This correction would then be in accordance with the approach suggested by the other GUM supplements for this type of uncertainty

$$u_x = \left(\frac{n-1}{n-3}\right)^{1/2} \frac{s(x_i)}{\sqrt{n}} \tag{5}$$

It is important to note that the evaluation of uncertainties of Type B input sources must be based on careful analysis of observations or in an accurate scientific judgment, using all available information about the measurement procedure. This uncertainty type is generally used when repeated experiments would not be possible, not available, or would be too costly or time-consuming. In this case, the GUM also suggests the use of two more types of statistical distributions: the uniform and the triangular distributions.

The uniform distribution should be used when only a range of values are available, that is, an interval with the minimum and maximum values, and no detailed information about the probability of values within this interval is available. The standard uncertainty associated with such an interval is given by Eq. (6):

$$u_x = \frac{b-a}{\sqrt{12}} \tag{6}$$

where b is the maximum and a is the minimum values for the range. For example, if the only information about the room temperature of a laboratory is known to be $(20 \pm 2)^{\circ}$C, then $b - a = 22 - 18 = 4^{\circ}$C and the standard uncertainty associated with the room temperature would be evaluated as $u_\theta = 4/\sqrt{12}^{\circ}\text{C} = 1.15^{\circ}\text{C}$.

The triangular distribution can be used when there is a strong evidence that the most probable value lies in the middle of a given interval, but still without knowing exactly how this probability behave within the interval. In chemistry, for example, the uncertainty associated with the volume of a measuring flask could be evaluated by a triangular distribution. The standard uncertainty for a triangular distribution is given by Eq. (7):

$$u_x = \frac{a}{\sqrt{6}} \tag{7}$$

where a is the semi-interval for the total range of the triangular distribution.

Another common Type B source of uncertainty is due to calibration certificates, related to a standard or to a calibrated instrument. In this case, the standard uncertainty to be used is normally obtained by dividing the expanded uncertainty U by the coverage factor k, both provided by the calibration certificate (Eq. (8))

$$u_x = \frac{U}{k} \tag{8}$$

Several good examples on how to treat some of the most common uncertainty sources can be found on the GUM [3], the EURACHEM/CITAC guide [13], and elsewhere [16].

Example: Returning to the example of torque measurement and considering the model defined in Eq. (3), the following sources of uncertainty are considered:

Mass (*m*). The mass m was repeatedly measured 10 times in a calibrated balance. The average mass was 35.7653 kg, with a standard deviation of 0.3 g. This source of uncertainty is purely statistical and is classified as being of Type A according to the GUM. The standard uncertainty (u_{m_R}) that applies in this case is obtained by Eq. (4), that is, $u_{m_R} = 0.3\ \text{g}/\sqrt{10} = 9.49 \times 10^{-5}$ kg.

In addition, the balance used for the measurement has a certificate stating an expanded uncertainty for this range of mass of U_m = 0.1 g, with a coverage factor k = 2 and a coverage probability of 95%. The uncertainty of the mass due to the calibration of the balance constitutes another source of uncertainty involving the same input quantity (mass). In this case, the standard uncertainty (u_{m_C}) is calculated by using Eq. (8), that is, $u_{m_C} = U_m/k = 0.1\ \text{g}/2 = 0.00005$ kg.

Local gravity acceleration (*g*). The value for the local gravity acceleration is stated in a certificate of measurement as 9.80665 m/s^2, as well as its expanded uncertainty of U_g = 0.00002 m/s^2, for k = 2 and p = 95%. Again, Eq. (8) is used to calculate the standard uncertainty (u_g), that is, $u_g = U_g/k = \left(0.00002\ \text{m/s}^2\right)/2 = 0.00001\ \text{m/s}^2$.

Length of the arm (*L*). Let us suppose that in this hypothetical case, the arm used in the experiment has no certificate of calibration, indicating its length value and uncertainty, and that the only measuring method available for the arm's length is by the use of a ruler with a minimum division of 1 mm. The use of the ruler leads then to a measurement value of 2000.0 mm for the length of the arm. However, in this situation, very poor information about the measurement uncertainty of the arm's length is available. As the minimum division of the ruler is 1 mm, one can assume that the reading can be done with a maximum accuracy of up to 0.5 mm, which can be thought as an interval of ±0.5 mm as limits for the measurement. As no information of probabilities within this interval is available, the assumption of a uniform distribution is the best option, on which there is equal probability for the values within the whole interval. Thus, Eq. (6) is used to determine the standard uncertainty (u_L), that is, $u_L = (2000.5 - 1999.5)\ \text{mm}/\sqrt{12} = 0.000289$ m.

In practice, one can imagine several more sources of uncertainty for this experiment, like, for example, the thermal dilatation of the arm as the room temperature changes. However, the objective here is not to exhaust all the possibilities, but instead to provide basic notions of how to implement the methodology of the GUM on a simple model.

3.4. Propagation of uncertainties

3.4.1. The law of propagation of uncertainties

The GUM uncertainty approach is based on the law of propagation of uncertainties (LPU). This methodology encompasses a set of approximations to simplify the calculations and is valid for a range of simplistic models.

According to the LPU, the propagation of uncertainties is accomplished by expanding the measurand model in a Taylor series and simplifying the expression by considering only the first-order terms. This approximation is viable as uncertainties are very small numbers compared with the values of their corresponding quantities. In this way, the treatment of a model where the measurand y is expressed as a function of N variables $x_1, \ldots, x_N$ (Eq. (9)) leads to the general expression for the propagation of uncertainties shown in Eq. (10)

$$y = f(x_1, \ldots, x_N) \tag{9}$$

$$u_y^2 = \sum_{i=1}^{N} \left(\frac{\partial y}{\partial x_i}\right)^2 u_{x_i}^2 + 2\sum_{i=1}^{N-1}\sum_{j=i+1}^{N} \left(\frac{\partial y}{\partial x_i}\right)\left(\frac{\partial y}{\partial x_j}\right) COV(x_i, x_j) \tag{10}$$

where u_y is the combined standard uncertainty for the measurand y and u_{x_i} is the uncertainty for the ith input quantity. The second term of Eq. (10) is due to the correlation between the input quantities. If there is no supposed correlation between them, Eq. (10) can be further simplified as

$$u_y^2 = \sum_{i=1}^{N} \left(\frac{\partial y}{\partial x_i}\right)^2 u_{x_i}^2 \tag{11}$$

The partial derivatives of Eq. (11) are known as sensitivity coefficients and describe how the output estimate y varies with changes in the values of the input estimates $x_1, x_2, \ldots, x_N$. It also converts the units of the inputs to the unit of the measurand.

Another important observation regarding the sensitivity coefficient occurs when the mathematical model that defines the measurand does not contemplate a given quantity, known as influence quantity. In this case, the determination of the sensitivity coefficient of the measurand in relation to the input quantity must be done experimentally. For example, biodiesel is susceptible to oxidation when exposed to air, and this oxidation process affects fuel quality. The oxidation time is determined by measuring the conductivity of an oil sample when inflated with air at a given flow rate. There are a number of influence quantities that impact the oxidation time of biodiesel such as temperature, air flow, conductivity, sample mass, and so on. In this case, the sensitivity coefficients for oxidation time with respect to each of these influence quantities are determined from an interpolation function obtained with experimental data. For example, **Figure 3** presents the table and its resulting graph, which shows the model of the function that relates the oxidation time to the temperature of a biofuel sample (case study of the authors).

Temperature [°C]	Oxidation time [h]
100	17.31
100	16.60
100	17.00
110	9.14
110	9.19
110	9.27
120	4.06
120	4.01
120	3.93

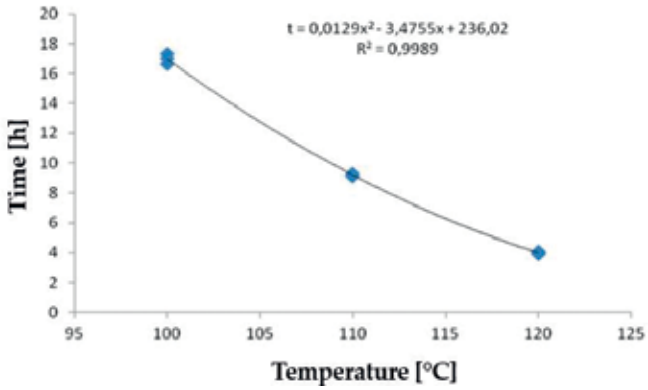

Figure 3. A table and a graph representing the variation of the oxidation time of a biofuel sample as a function of temperature.

Example: On returning to the torque measurement example, assuming that all the input quantities are independent, the combined standard uncertainty for the torque is calculated by using the LPU (Eq. (11)). The final expression is then

$$u_T = \sqrt{\left(\frac{\partial T}{\partial m}\right)^2 u_{m_R}^2 + \left(\frac{\partial T}{\partial m}\right)^2 u_{m_C}^2 + \left(\frac{\partial T}{\partial g}\right)^2 u_g^2 + \left(\frac{\partial T}{\partial L}\right)^2 u_L^2} = 0.096 \text{ N m} \tag{12}$$

It is important to note that the terms (not squared) of Eq. (12), that is, each sensitivity coefficient multiplied by its corresponding uncertainty, are known as uncertainty components. These components can be compared to each other as they are in the same units of the measurand. **Figure 4** shows the comparison between the uncertainty components for the torque measurement model.

As can be noted, the dominant uncertainty component is due to the uncertainty associated with the measurement of the arm length, which was taken as the resolution of the non-calibrated

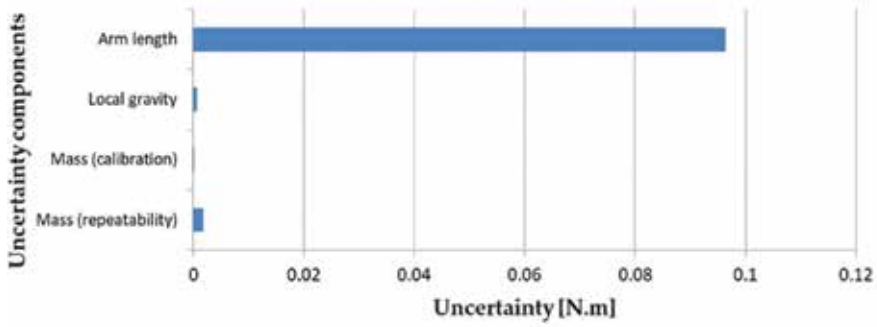

Figure 4. Uncertainty component balance for the input quantities in the torque measurement model.

ruler used in the measurement. This analysis shows to the analyst that, to reduce the final uncertainty and improve the measurement system, a calibrated ruler, with a better uncertainty, should be used. This represents the importance of the GUM as a management tool to the measurement process.

3.4.2. The Kragten method

The Kragten method is an approximation that facilitates the calculation of the combined uncertainty using finite differences in place of the derivatives [13]. This approximation is valid when the uncertainties of the inputs are relatively small compared to the respective values of the input quantities, generating discrepancies in the final result in relation to the LPU that occur in decimals that can be ignored.

Assuming a measurand y, which is calculated from the input quantities x_1, x_2 and x_3 according to the mathematical model of Eq. (2), the uncertainties u_{x_1}, u_{x_2} and u_{x_3} for the input quantities are evaluated normally, according to methodologies already explained previously. From there, the calculations of the measurand are performed individually for each input magnitude (y_{x_1}, y_{x_2} and y_{x_3}) so that each time their respective values are added with their uncertainties, as shown in Eqs. (13)–(15)

$$y_{x_1} = \frac{(x_1 + u_{x_1})x_2}{x_3^2} \tag{13}$$

$$y_{x_2} = \frac{x_1(x_2 + u_{x_2})}{x_3^2} \tag{14}$$

$$y_{x_3} = \frac{x_1 x_2}{(x_3 + u_{x_3})^2} \tag{15}$$

The value of the measurand y varies for y_{x_i} due to the addition of the uncertainty u_{x_i} to the value of its respective input quantity. Thus, the uncertainty component of each input source in the unit of the measurand y is defined by the difference $\left|y_{x_i} - y\right|$, according to Eqs. (16)–(18)

$$u_y(x_1) = \left|y_{x_1} - y\right| \tag{16}$$

$$u_y(x_2) = \left|y_{x_2} - y\right| \tag{17}$$

$$u_y(x_3) = \left|y_{x_3} - y\right| \tag{18}$$

Thus, the combined standard uncertainty of y is finally evaluated as

$$u_y = \sqrt{\sum_{i=1}^{N} u_y^2(x_i)} \tag{19}$$

or by Eq. (20), if there are correlated uncertainties

$$u_y = \sqrt{\sum_{i=1}^{N} u_y^2(x_i) + 2\sum_{i=1}^{N-1}\sum_{j=i+1}^{N} u_y(x_i)u_y(x_j)r(x_i,x_j)} \tag{20}$$

where $r(x_i, x_j)$ is the correlation coefficient between x_i and x_j.

3.5. Evaluation of the expanded uncertainty

The result provided by Eqs. (10) and (11) corresponds to an interval that contains only one standard deviation (or approx. 68.2% of the measurements for a normal distribution). In order to have a better coverage probability for the result, the GUM approach expands this interval by assuming that the measurand follows the behavior of a Student's *t*-distribution. An effective degrees of freedom v_{eff} for the *t*-distribution can be obtained by using the Welch-Satterthwaite formula (Eq. (21))

$$v_{eff} = \frac{u_y^4}{\sum_{i=1}^{N} \frac{\left(\frac{\partial y}{\partial x_i}\right)^4 u_{x_i}^4}{v_{x_i}}} \tag{21}$$

where v_{x_i} is the degrees of freedom for the *i*th input quantity.

The effective degrees of freedom is used to obtain a coverage factor k that depends also of a chosen coverage probability p, which is often 95%. The expanded uncertainty U_y is then evaluated by multiplying the combined standard uncertainty by the coverage factor k that finally expands it to a coverage interval delimited by a *t*-distribution with a coverage probability p (Eq. (22))

$$U_y = ku_y \tag{22}$$

Note: The draft for the new GUM proposal suggests that the final coverage interval cannot be reliably determined if only an expectation y and a standard deviation u_y are known, mainly if the final distribution deviates significantly from a normal or a *t*-distribution. Thus, they propose distribution-free coverage intervals in the form of $y \pm U_p$, with $U_p = k_p u_y$: (a) if no information is known about the final distribution, then a coverage interval for the measurand Y for coverage probability of at least p is determined using $k_p = 1/(1-p)^{1/2}$. If $p = 0.95$, a coverage interval of $y \pm 4.47u_y$ is evaluated. (b) If it is known that the distribution is unimodal and symmetric about y, then $k_p = 2/\left[3(1-p)^{1/2}\right]$ and the coverage interval $y \pm 2.98u_y$ would correspond to a coverage probability of at least $p = 0.95$.

Example: The effective degrees of freedom for the torque measurement example is calculated using Eq. (21). As the number of degrees of freedom for Type B uncertainties is considered infinite, only Type A uncertainties are accounted. In this case,

$$v_{eff} = \frac{u_T^4}{\frac{\left(\frac{\partial T}{\partial m_R}\right)^4 u_{m_R}^4}{v_{m_R}}} = 6.5 \times 10^7 \tag{23}$$

Using *t*-distribution tables, the coverage factor for this value of v_{eff} and p = 95% is k = 1.96. Therefore, the expanded uncertainty is calculated as $U = ku_T = 1.96 \times 0.096 = 0.2$ N m, and the measurement result is expressed as 668.0 ± 0.2 N m. The GUM recommends that the final uncertainty should be expressed with one or at most two significant digits.

4. Calibration curve and correlated uncertainties

One of the most valuable tools for the metrologist is the calibration curve. It is widely used in measurement systems on which one cannot directly obtain the property value to be measured of an object. Instead, a response from the system is measured. In this way, a calibration curve is used to correlate the response from the system with well-known property values, usually calibration standards (see **Figure 5**).

With a calibration curve in hands, the property value for a new unknown sample can be directly determined by using the equation for the fitted curve, which is usually adjusted by a linear regression. However, the calibration curve contains errors due to the lack of fit for the experimental data, causing an uncertainty source to arise. Thus, when evaluating the uncertainty for a predicted property value of x_o corresponding to a new observation y_o (for a new unknown sample, for example), the LPU with correlation terms is applied on the linear regression model in the form of Eq. (24). Eq. (25) represents the model for a predicted value y_o corresponding to a new observed value x_o, in the case of the inverse process

$$x_0 = \frac{y_o - a}{b} \tag{24}$$

$$y_o = a + bx_0 \tag{25}$$

where a and b are, respectively, the intercept and the slope parameters of the linear regression.

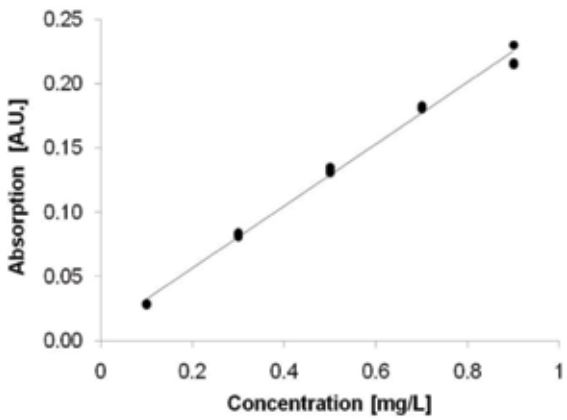

Figure 5. An example of a linear calibration curve for atomic absorption spectroscopy: the absorption signals (instrument responses) are plotted against the concentrations for a specific analyte.

The application of the LPU with the correlation term to Eqs. (24) and (25) leads to Eqs. (26) and (27), respectively, for both cases:

$$u_{x_o} = \sqrt{\left(\frac{\partial x_o}{\partial y_o}\right)^2 u_{y_o}^2 + \left(\frac{\partial x_o}{\partial a}\right)^2 u_a^2 + \left(\frac{\partial x_o}{\partial b}\right)^2 u_b^2 + 2\left(\frac{\partial x_o}{\partial a}\right)\left(\frac{\partial x_o}{\partial b}\right) u_a u_b r_{a,b}} \tag{26}$$

$$u_{y_o} = \sqrt{\left(\frac{\partial y_o}{\partial x_o}\right)^2 u_{x_o}^2 + \left(\frac{\partial y_o}{\partial a}\right)^2 u_a^2 + \left(\frac{\partial y_o}{\partial b}\right)^2 u_b^2 + 2\left(\frac{\partial y_o}{\partial a}\right)\left(\frac{\partial y_o}{\partial b}\right) u_a u_b r_{a,b}} \tag{27}$$

For Eq. (26), u_{x_o} is the combined uncertainty for the predicted value x_o and u_{y_o} is the uncertainty for the new observed response y_o. For Eq. (27), u_{y_o} is the combined uncertainty for the predicted value y_o and u_{x_o} is the uncertainty for the new observed response x_o. In both cases, u_a and u_b are, respectively, the uncertainties for the intercept and the slope, and $r_{a,b}$ is the correlation coefficient between a and b. These last equations can also be found in the ISO/TS 28037 [17], concerning the use of straight-line calibration functions.

The uncertainties for a and b can be obtained by Eqs. (28) and (29), respectively, while the correlation coefficient $r_{a,b}$ is given by Eq. (30)

$$u_a = S_e \sqrt{\frac{\sum x_i^2}{n\sum x_i^2 - \left(\sum x_i\right)^2}} \tag{28}$$

$$u_b = S_e \sqrt{\frac{n}{n\sum x_i^2 - \left(\sum x_i\right)^2}} \tag{29}$$

$$r_{a,b} = -\frac{\sum x_i}{\sqrt{n\sum x_i^2}} \tag{30}$$

where n is the number of points used to construct the curve, x_i are the values for the independent variable of the linear equation for each y_i, and S_e^2 is the residual variance of the fitted curve, obtained by Eq. (31)

$$S_e^2 = \frac{\sum \left(y_i - \widehat{y}_i\right)^2}{n-2} \tag{31}$$

where $\widehat{y}_i$ are the interpolated values in the fitted curve for each x_i, that is, $\widehat{y}_i = a + bx_i$.

Example: This time, let us consider that the calibration certificate of a thermometer presents the results shown in **Table 1**.

For the data shown in **Table 1**, the calibration curve of the thermometer is expressed by $\widehat{y}_o = 1.1484 + 0.9578x_o$. For a temperature value indicated by the thermometer of x_o = 22°C, applying the equation of the calibration curve yields a reference value of $\widehat{y}_o$ = 22.22°C.

Indication (x_i) (°C)	Reference value (y_i) (°C)
20	20.3
21	21.3
22	22.2
23	23.1
24	24.2
25	25.1
27	27.0

Table 1. Values of the calibration certificate of a thermometer.

Using Eqs. (28)–(31), it is possible to calculate the values of **Table 2** that shows the statistical data for the thermometer calibration curve.

Considering that there is no uncertainty for the observed point x_o = 22°C, that is, u_{x_o} = 0, the uncertainty of y_o arising from the interpolation process of the point x_o = 22°C can then be calculated by applying Eq. (27) and the data from **Table 2**, resulting in the following: $u_{y_o} = \sqrt{1^2 \cdot 0.1943^2 + 22^2 \cdot 0.0084^2 + 2 \cdot 1 \cdot 22 \cdot 0.1943 \cdot 0.0084 \cdot (-0.995)} = 0.021°\text{C}$.

Another frequently used expression for the standard uncertainty of the predicted value u_{x_o} is given by Eq. (32) [13, 18]:

$$u_{x_o} = \frac{S_e}{b}\sqrt{\frac{1}{m} + \frac{1}{n} + \frac{\left(\overline{y}_o - \overline{y}\right)^2}{b^2 \sum \left(x_i - \overline{x}\right)^2}} \tag{32}$$

where S_e is the residual standard deviation of the fitted line, m is the number of observations of y_o, n is the number of points composing the calibration curve, and $\overline{y}_o$ is the average value obtained from the observations of y_o. In this expression, the uncertainty component due to the observations of y_o is evaluated by [19]

$$u_{y_o} = \frac{S_e}{\sqrt{m}} \tag{33}$$

However, Hibbert [19] suggests that if the standard deviation of the indications is known from consistent data, u_{y_o} can be better evaluated by

Data	Value	Unit
S_e^2	0.0024	°C^2
u_a	0.1943	°C
u_b	0.0084	
$r_{a,b}$	−0.995	

Table 2. Statistical data for the calibration curve of a thermometer.

$$u_{y_o} = \frac{S_{y_o}}{\sqrt{m}} \tag{34}$$

where S_{y_o} is the standard deviation of the observations of y_o, and Eq. (32) is then expressed as Eq. (35) [18, 19]:

$$u_{x_o} = \frac{1}{b}\sqrt{\frac{S_{y_o}^2}{m} + \frac{S_e^2}{n} + \frac{S_e^2\left(\overline{y}_o - \overline{y}\right)^2}{b^2\sum\left(x_i - \overline{x}\right)^2}} \tag{35}$$

5. Assessment of uncertainty in instrument calibration

The methodology presented in the GUM can also be used to evaluate the uncertainty in the calibration of a measuring instrument. Following the steps of the GUM, the measurand for the model used in the calibration must be defined by the quantity that evaluates the systematic error of an instrument over its entire measurement range. Thus, Eq. (36) can be generally used for the evaluation of uncertainty in a calibration process:

$$e = V_{ind} - V_{ref} \tag{36}$$

where e is the systematic error of the instrument for a fixed range, V_{ind} is the value indicated by the instrument, and V_{ref} is the reference value corresponding to the indicated value.

From Eq. (36), a basic cause-and-effect diagram can be assembled for the calibration uncertainty assessment of an instrument, as shown in **Figure 6**.

The sources of uncertainty in this case involve the repeatability of indicated values, the resolution of the instrument in calibration, and the certificate of calibration of the reference values. Thus, an evaluation of the uncertainty about the systematic error should be done for each nominal value of the instrument in calibration. The combined standard uncertainties u_{ei} for each calibrated nominal value are obtained by applying the LPU, as shown in Eq. (37)

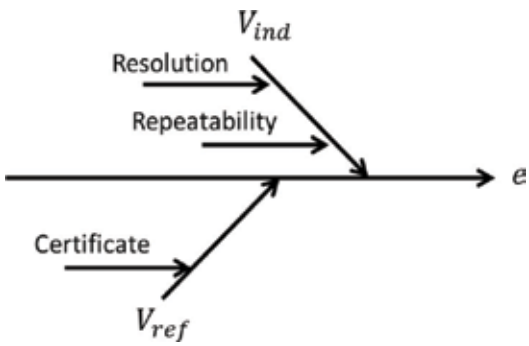

Figure 6. A general cause-and-effect diagram for the calibration of an instrument.

$$u_{e_i} = \sqrt{\left(\frac{\partial e_i}{\partial V_{ind}}\right)^2 u^2_{V_{ind_{Res}}} + \left(\frac{\partial e_i}{\partial V_{ind}}\right)^2 u^2_{V_{ind_{Rep}}} + \left(\frac{\partial e_i}{\partial V_{ref}}\right)^2 u^2_{V_{ref}}} \tag{37}$$

where $u_{V_{ind_{Res}}}$, $u_{V_{ind_{Rep}}}$, and $u_{V_{ref}}$ are, respectively, standard uncertainties due to resolution of the instrument, repeatability of indication values, and certificate of calibration of the reference. These standard uncertainties are obtained as described in Section 3.

The final calibration result can then be presented according to **Table 3**. In addition, correction values or systematic errors can also be reported.

6. Monte Carlo simulation applied to metrology

This section presents the limitations of the GUM and shows an alternative methodology based on the propagation of distributions that overcome those limitations. For further details, please refer to the authors' publication that addresses the use of the Monte Carlo methodology applied to uncertainty in measurement [15] or to the JCGM 101:2008 guide [5]. Also, in the field of analytical chemistry, the latest version of EURACHEM/CITAC guide (2012) was updated with procedures to use Monte Carlo simulations [13].

6.1. Limitations of the GUM approach

As mentioned earlier, the approach to evaluate measurement uncertainties using the LPU as presented by the GUM is based on some approximations that are not valid for every measurement model [5, 20–22]. These approximations comprise (1) the linearization of the measurement model made by the truncation of the Taylor series, (2) the use of a *t*-distribution as the distribution for the measurand, and (3) the calculation of an effective degrees of freedom for the measurement model based on the Welch-Satterthwaite formula, which is still an unsolved problem [23]. Moreover, the GUM approach usually presents deviated results when one or more of the input uncertainties are relatively much larger than others, or when they have the same order of magnitude than its quantity.

The limitations and approximations of the LPU are overcome when using a methodology that relies on the propagation of distributions. This methodology carries more information than the simple propagation of uncertainties and generally provides results closer to reality. It is

Range	Indicated value	Reference value	Expanded uncertainty	Coverage factor
Range 1	V_{ind1}	V_{ref1}	U_1	k_1
Range 2	V_{ind2}	V_{ref2}	U_2	k_2
…	…	…	…	…
Range N	V_{indN}	V_{refN}	U_N	k_N

Table 3. A typical format for the result of calibration of an instrument.

described in detail by the JCGM 101:2008 guide (Evaluation of measurement data—Supplement 1 to the "Guide to the expression of uncertainty in measurement"—propagation of distributions using a Monte Carlo method) [5], providing basic guidelines for using Monte Carlo numerical simulations for the propagation of distributions in metrology. This method provides reliable results for a wider range of measurement models as compared to the GUM approach and is presented as a fast and robust alternative method for cases where the GUM approach does not present good results.

6.2. Running Monte Carlo simulations

The propagation of distributions as presented by the JCGM 101:2008 involves the convolution of the probability distributions for the input sources of uncertainty through the measurement model to generate a distribution for the output (the measurand). In this process, no information is lost due to approximations, and the result is much more consistent with reality.

The main steps of this methodology are similar to those presented in the GUM. The measurand must be defined as a function of the input quantities through a model. Then, for each input, a probability density function (PDF) must be assigned. In this step, the concept of maximum entropy used in the Bayesian statistics should be used to assign a PDF that does not contain more information than that which is known by the analyst. A number of Monte Carlo trials are then chosen and the simulation can be set to run.

Results are expressed in terms of the average value for the output PDF, its standard deviation, and the end points that cover a chosen probability p.

Example: Returning once more to the torque measurement example, one can consider the following PDFs for the input sources:

Mass (m). For repeated indications, the JCGM 101:2008 suggests the use of a scaled and shifted t-distribution. Thus, the distribution should use 35.7653 kg as its average, a scale value of $s/\sqrt{n} = 0.3\ \text{g}/\sqrt{10} = 9.49 \times 10^{-5}$ kg, and $n - 1 = 9$ degrees of freedom.

For the calibration component, the supplement 1 recommends the use of a normal distribution if the number of degrees of freedom is not available. In this case, the mass value of 35.7653 kg is taken as the mean and a standard deviation of $U_m/k = 0.1\ \text{g}/2 = 0.00005$ kg should be used. However, to facilitate the calculation of the final mean value of the measurand, the mean should be shifted to zero, since both values for the mass sources will be added together.

Local gravity acceleration (g). This case is similar to the case of the balance certificate, for which we have values of expanded uncertainty and coverage factor without information on the number of effective degrees of freedom. Thus, a normal distribution with a mean of 9.80665 m/s^2 and a standard deviation of $U_g/k = (0.00002\ \text{m/s2})/2 = 0.00001$ m/s^2 are assumed.

Length of the arm (L). In this case, as poor information about the interval is available (± 0.5 mm), an uniform distribution is assumed with a minimum value of 1999.5 mm and a maximum value of 2000.5 mm.

Uncertainty source	Type	PDF	PDF parameters
Mass (repeatability)	A	*t*-distribution	Mean: 35.7653 kg; scale: 9.49 x 10^{-5} kg; degrees of freedom: 9
Mass (certificate)	B	Normal	Mean: 0 kg; standard deviation: 0.00005 kg
Local gravity	B	Normal	Mean: 9.80665 m/s^2; standard deviation: 0.00001 m/s^2
Arm length	B	Uniform	Minimum: 1999.5 mm; maximum: 2000.5 mm

Table 4. A summary of sources of uncertainty and their associated distributions for the measurement of torque.

Table 4 resumes the input information for the simulation, which was executed for $M = 200,000$ trials, generating the output distribution shown in **Figure 7**.

Table 5 summarizes the statistical data of the output distribution, including the upper and lower limits of a probabilistically symmetric range for a 95% coverage probability.

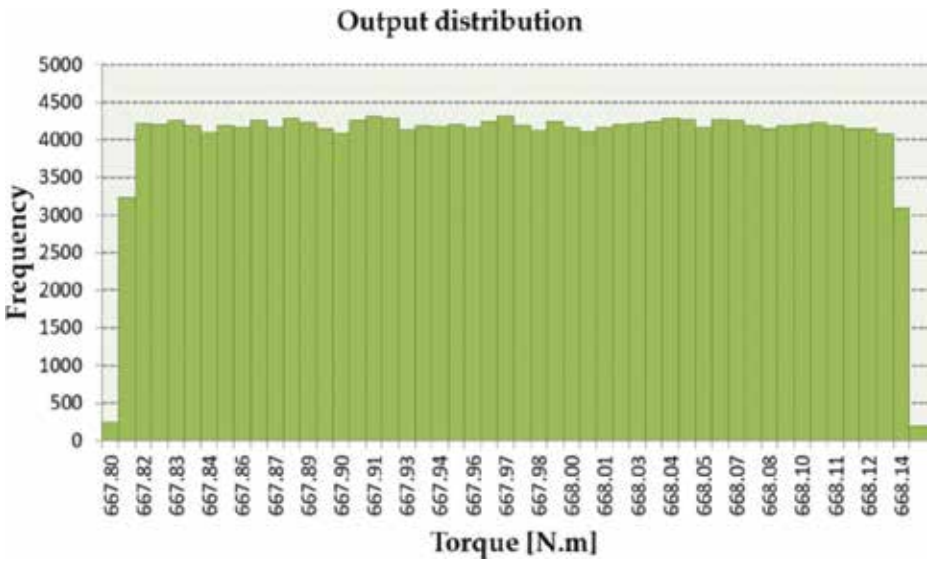

Figure 7. Output distribution resulting from the Monte Carlo simulation for the evaluation of uncertainty of measurement of torque.

Statistical data	Value (N m)
Mean	667.970
Standard deviation	0.096
Lower limit for p = 95%	667.812
Upper limit for p = 95%	668.129

Table 5. A summary of the statistical data for the output distribution for the measurement of torque.

7. Conclusions

Measurement uncertainty and metrological traceability are interdependent concepts. The evaluation of uncertainties of measurement results is essential to ensure that they are reliable and comparable. Moreover, the process that involves the modeling of measurement systems and evaluation of their uncertainties is of great importance for the metrologist as it constitutes a tool for the management of the measurement laboratory, since it can indicate exactly where to invest to get better, more qualified results.

The GUM and the application of the LPU continue to be the most used and widespread methodology for bottom-up uncertainty evaluation in metrology. It is adopted worldwide and provides a strong base for comparability of measurement results between laboratories. On the other hand, a new version for the GUM is currently under revision. This version should be aligned with its supplements in a more harmonized way, incorporating concepts from Bayesian statistics and resolving some inconsistencies. As a consequence, if the mentioned distribution-free coverage intervals are maintained, results for the expanded uncertainty will be greatly overestimated compared to the current version of the GUM.

In this way, the best alternative for a more realistic and lean uncertainty assessment would be through a numerical simulation using the Monte Carlo method, which should lead to a smaller and more reliable uncertainty result.

Author details

Jailton Carreteiro Damasceno* and Paulo R.G. Couto

*Address all correspondence to: jcdamasceno@inmetro.gov.br

National Institute of Metrology, Quality and Technology (Inmetro), Rio de Janeiro, Brazil

References

[1] ISO/IEC 17025. 2005. General Requirements for the Competence of Testing and Calibration Laboratories. ISO: Geneva

[2] Kaarls R. BIPM Proc.-Verb. Com. Int. Poids et Mesures 49:A1–12 (in French), Giacomo P (1981). Metrologia. 1981;**17**:73-74 (in English)

[3] JCGM 100:2008. Evaluation of measurement data—Guide to the expression of uncertainty in measurement. Joint Committee for Guides in Metrology, 2008

[4] JCGM 104:2009. Evaluation of measurement data—An introduction to the "Guide to the expression of uncertainty in measurement" and related documents. Joint Committee for Guides in Metrology. 2009

[5] JCGM 101:2008. Evaluation of measurement data—Supplement 1 to the "Guide to the expression of uncertainty in measurement"—Propagation of distributions using a Monte Carlo method. Joint Committee for Guides in Metrology. 2008

[6] JCGM 102:2011. Evaluation of measurement data—Supplement 2 to the "Guide to the expression of uncertainty in measurement"—Extension to any number of output quantities. Joint Committee for Guides in Metrology. 2011

[7] JCGM 106:2012. Evaluation of measurement data—The role of measurement uncertainty in conformity assessment. Joint Committee for Guides in Metrology. 2012

[8] Bich W, Cox MG, Dybkaer R, Elster C, Estler WT, Hibbert B, Imai H, Kool W, Michotte C, Nielsen L, Pendrill L, Sidney S, van der Veen AMH, Woger W. Revision of the 'guide to the expression of uncertainty in measurement'. Metrologia. 2012;**49**:702-705

[9] Bich W. Revision of the 'guide to the expression of uncertainty in measurement'—Why and how. Metrologia. 2014;**51**:S155-S158

[10] Bich W, Cox M, Michotte C. Towards a new GUM—An update. Metrologia. 2016;**53**:S149-S159

[11] Ehrlich C. Terminological aspects of the guide to the expression of uncertainty in measurement (GUM). Metrologia. 2014;**51**:S145-S154

[12] JCGM 200:2012. International vocabulary of metrology—basic and general concepts and associated terms (VIM). Joint Committee for Guides in Metrology. 2012

[13] EURACHEM/CITAC Guide CG4. Quantifying uncertainty in analytical measurement. EURACHEM/CITAC. 2012

[14] Ellison SLR. Implementing measurement uncertainty for analytical chemistry: The Eurachem guide for measurement uncertainty. Metrologia. 2014;**51**:S199-S205

[15] Couto PRG, Damasceno JC, Oliveira SP. Chapter 2—Monte Carlo simulations applied to uncertainty in measurement. In: Chan V, editor. InTech: Theory and Applications of Monte Carlo Simulations; 2013

[16] Meyer VR. Measurement uncertainty. Journal of Chromatography. A. 2007;**1158**:15-24

[17] ISO/TS 28037. Determination and Use of Straight-line Calibration Functions. Geneva: ISO; 2010

[18] Massart DL, Vandeginste BGM, Buydens LMC, Jong S, Lewi PJ, Smeyers-Verbeke J. Data Handling in Science and Technology. v. 20. Handbook of Chemometrics and Qualimetrics: Part A. Amsterdam: Elsevier; 1997

[19] Hibbert DB. The uncertainty of a result from a linear calibration. Analyst. 2006;**131**:1273-1278

[20] Harris PM, Cox MG. On a Monte Carlo method for measurement uncertainty evaluation and its implementation. Metrologia. 2014;**51**:S176-S182

[21] Possolo A. Statistical models and computation to evaluate measurement uncertainty. Metrologia. 2014;**51**:S228-S236

[22] Gonzalez AG, Herrador MA, Asuero AG. Uncertainty evaluation from Monte-Carlo simulations by using Crystal-Ball software. Accreditation and Quality Assurance. 2005; **10**:149-154

[23] Lepek A. A computer program for a general case evaluation of the expanded uncertainty. Accreditation and Quality Assurance. 2003;**8**:296-299

Chapter 3

Variational Calibration

Michael Surdu

Additional information is available at the end of the chapter

http://dx.doi.org/10.5772/intechopen.74220

Abstract

The approach to the improving the accuracy of the impedance parameter measurements is described. This approach is based on the well-known variations of the influence of the disturbing factors on the results of measurement. Using these variations, measurement circuit provides the additional number of measurements, equal to the number of the disturbing factors. System of equations describes these results of measurements. The solution of this system eliminates the influence of the appropriate uncertainty sources on the results of measurement and gets the true result of the measured value. In addition, the solution of this system also gets the values of the uncertainty components in every measurement and possibility to monitor the properties of the measurement circuit. Examples of the realization of this method for improving the accuracy of the impedance parameter measurements in different bridges are given.

Keywords: impedance, variation calibration, uncertainty, measurement, algorithm, comparison, quadrature, standard, digital synthesis, frequency range, transfer's function

1. Introduction

History of the electricity science is the history of the development, in sufficient part, of the new methods of measurements. These methods are described perfectly well, for example, in [1]. Widely used replacing and substitution methods entered in all handbooks [2]. Bridge methods are described in many monographs [3, 4]. Monographs [5, 6] describe different methods of bridges' accurate balance. Many methods of uncertainty correction are described in [7, 8]. All these methods have their widely discussed advantages and disadvantages. There exists no method that could decide all problems, which appears in measuring practice. This chapter describes the method of the variational calibration [9] in the impedance measurements. This method is based on the *sequential* variation of the influence of the disturbing factors on the

results of measurement. System of equations describes these results. Solution of this system eliminates influences of the disturbing factors and gets the accurate results of measurement. This method significantly simplifies the accurate devices, reducing their weight, dimension and cost, but increases the time of measurement.

2. The variational calibration

2.1. Theoretical basis of the variational calibration

Every measuring circuit (MC) has the input value, which has to be measured and generates measured output value. In an ideal case, the results of measurement depend on the input value and the transfer function ***k*** of the MC only.

Formula (1) describes the result of measurement of ideal MC:

$$Z_x = kZ_0 \tag{1}$$

Formula (2) describes the standard uncertainty δ_{id} of such measurement:

$$\delta_{id} = \sqrt{\delta_0^2 + \delta_s^2} \tag{2}$$

Here δ_0 and δ_s are the uncertainties, of the standard Z_0 and the uncertainty, caused by the sensitivity of the MC.

In the real MC, the results of measurement Z_{x0} also depend on the complex of the disturbing factors $z_1 \ldots z_i \ldots z_j$ as well (for simplicity of the description, these factors on the **Figure 1** are shown being out of MC). These factors create proper complex of the uncertainties of measurements $\delta_1 \ldots \delta_i \ldots \delta_j$ and shift the appropriate result Z_{x0} of measurement from its ideal value Z_x.

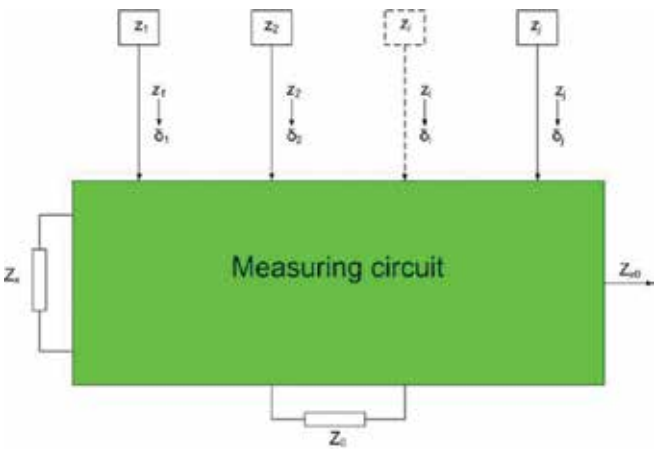

Figure 1. Real measuring circuit.

http://dx.doi.org/10.5772/intechopen.74220

The much more complicated mathematic model (3) of the real MC now describes the results of measurement:

$$Z_{x0} = \gamma\left(Z_x; \delta_1 \ldots \delta_i \ldots \delta_j; \delta_0; \delta_s\right) \tag{3}$$

Usually the model (3) is well known from preliminary investigations of the MC.

In the simplest case, every disturbing factor $z_1..z_i..z_j$ creates appropriate uncertainty components $\delta_1 \ldots \delta_i \ldots \delta_j$. In more complicated cases, some disturbing factors $z_1 \ldots z_i$ can influence some complex $Z_i \ldots Z_{i+m}$ of the results of measurement. But we know functions $\delta_i = f_i(z_1 \ldots z_i \ldots z_n)$ and do not know just the constant coefficients, which enters into these dependences.

Formula (4) describes the standard uncertainty δ_r of the measurement of the real MC:

$$\delta_r = \sqrt{\delta_0^2 + \Sigma_1^j \delta_i^2 + \delta_s^2} \tag{4}$$

To eliminate the influence of the uncertainties $\delta_1 \ldots \delta_i \ldots \delta_j$ on the results of measurement, the variation method was developed (VM) [9]. **Figure 2** illustrates this method. Here, MC contains **n** additional variators $V_1 \ldots V_j$. Last ones influence the uncertainty sources $z_1 \ldots z_j$ and change the uncertainty $\delta_1 \ldots \delta_j$. It creates the output of the proper results of MC measurement $Z_{x1} \ldots Z_{xj}$.

Variators cannot change the uncertainties δ_0 and δ_s. These uncertainties are supposed to be known or equal to zero during the VM calibration.

VM consists of the following steps:

1. First, MC measures initial value Z_{x0} of the input value Z_x.
2. Then, MC consequently varies the influence of the disturbing factor z_i on the well-known value α_i.

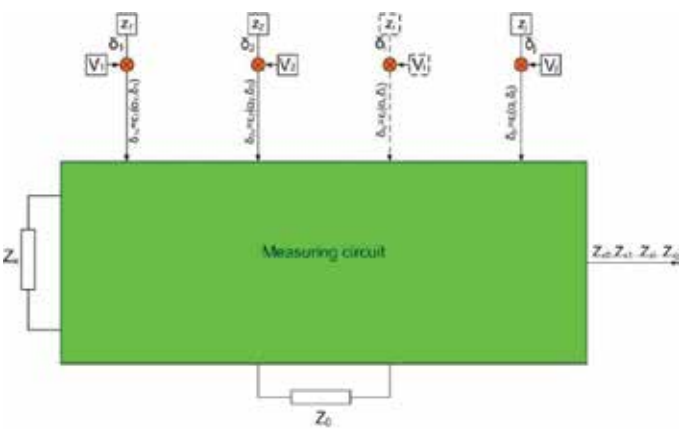

Figure 2. Variational measuring circuit.

Variations could be provided in any order. To simplify the system of equations, it is preferable to perform variations sequentially and to switch ON the variation α_i when all other variations are switched OFF.

Variations could have any law. To simplify the system of equation, it is preferable to provide the multiplicative variation (when we multiply the appropriate uncertainty component δ_i on well-known ratio α_i ($\delta_{iv} = \alpha_i\delta_i$)) or additive variation (when we add the appropriate well-known uncertainty Δ_v to the uncertainty component Δ_{im} ($\Delta_{iv} = \Delta_{im} + \Delta_v$)).

3. After every variation, MC measures the results of the measurement $Z_{x1}\ldots Z_{xi}\ldots Z_{xj}$.

4. The system of Eqs. (5) describes these measurements:

$$\begin{aligned} Z_{x0} &= \gamma\left(Z_x, \delta_1 \ldots \delta_i \ldots \delta_j, \delta_0, \delta_s\right) \\ Z_{x1} &= \gamma\left(Z_x, \delta_1, \alpha_1 \ldots \delta_i \ldots \delta_j, \delta_0, \delta_s\right) \\ Z_{xj} &= \gamma\left(Z_x, \delta_1 \ldots \delta_i \ldots \delta_j, a_j, \delta_0, \delta_s\right) \end{aligned} \tag{5}$$

The system (5) contains j + 1 unknown quantities: Z_x and uncertainties of measurement $\delta_1\ldots\delta_j$, and j + 1 results of measurement $Z_{x0}\ldots Z_{xj}$. Solution (6) of this system gets the true value of the results of measurement Z_x and the values of the uncertainties $\delta_1\ldots\delta_j$ of the measurement:

$$\begin{aligned} Z_x &= \rho_0\left[\left(Z_{x0} - Z_{xj}\right), \left(\alpha_1 - \alpha_j\right), \delta_0, \delta_s\right] \\ \delta_1 &= \rho_1\left[\left(Z_{x0} - Z_{xj}\right), \left(\alpha_1 - \alpha_j\right), \delta_0, \delta_s\right] \\ \delta_j &= \rho_j\left[\left(Z_{x0} - Z_{xj}\right), \left(\alpha_1 - \alpha_j\right), \delta_0, \delta_s\right] \end{aligned} \tag{6}$$

Periodical variation calibration lets us to observe the behavior of every disturbing factor, to determine their stability, to monitor measuring circuit and to ensure precision of the period of the variational calibration.

Let the uncertainty caused by the finite sensitivity of the *i*-measurement be δ_{si} and the uncertainty of the variation α_i be $\delta\alpha_i$. In this case, formula (7) describes the resulting standard uncertainty δ_c of the measurement with variation calibration:

$$\delta_c = \sqrt{\delta_0^2 + \Sigma_0^j\left(\delta_i^2\delta\alpha_i^2 + \delta_{si}^2\right)} \tag{7}$$

Eq. (7) shows that the VM sharply decreases influence of the uncertainty components δ_i on the common uncertainty of measurement (on the $1/\delta\alpha_i$ times).

Let us suppose uncertainty source z_i creates uncertainty $\delta_i = 10^{-3}$ and we need to decrease it to the value 10^{-6}. It means that we have to provide appropriate variation with uncertainty better than 10^{-3} only. It is a very important result of the VM. This effect is restricted only by the stability of the uncertainties $\delta_1\ldots\delta_j$ during the time of measurement.

Let us suppose that time of every measurement is t_i. It means that the common time t_c of measurement increases to the value:

http://dx.doi.org/10.5772/intechopen.74220

$$t_c = \Sigma_0^j t_i \tag{8}$$

Let us suppose that $\delta\alpha_i = 0$ and $\delta_0 = 0$. In this case, formula (9) describes the standard uncertainty of measurement caused by sensitivity of measurements only:

$$\delta_c = \sqrt{\Sigma_0^j \delta_{si}^2}. \tag{9}$$

Formulas (8) and (9) show that the variation method has two disadvantages:

- Variation method needs **n + 1** measurement instead **one** only. It sufficiently increases the time of measurement.
- Variation method increases the contribution of measurement sensitivity δ_{si} in the common uncertainty of measurement.

We can overcome these two disadvantages of the variation method in different ways. Here, we shortly describe *time and space clustering of the thesaurus of the uncertainty sources*.

2.1.1. Time clustering

Usually, different uncertainty sources have different typical speeds of drift. We can divide the thesaurus of **j** uncertainty sources into clusters, which have congruous time of drift. **Figure 3** illustrates this approach. In **Figure 3**, thesaurus of the **j** uncertainty components is divided into three clusters T_1, T_2 and T_3 **(j = m + n + k)**.

The first cluster (T_1) joins ***m*** of the most stable uncertainty sources. It could be instability of the internal standards or arms ratios in transformer bridges, and so on. MC provides their calibration very seldom, for example, one time per year. For this calibration, MC performs sequential

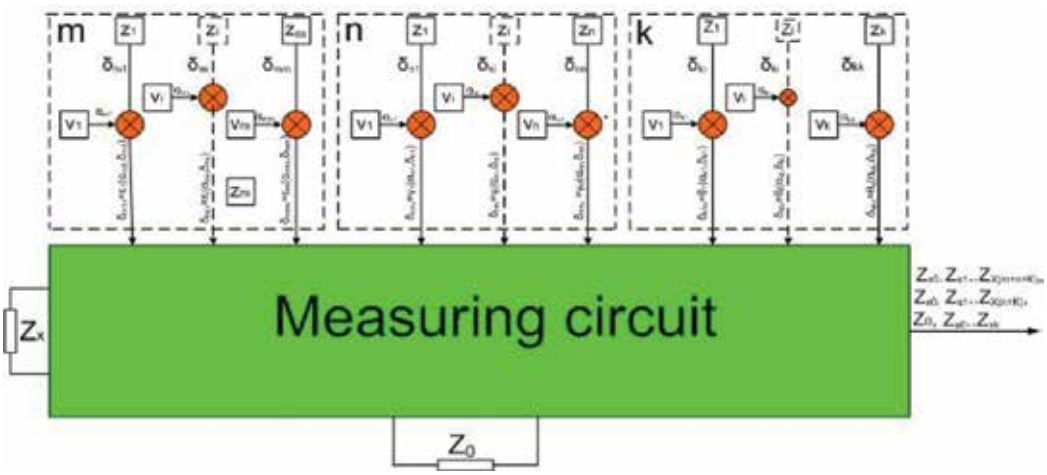

Figure 3. Variation calibration with time clustering.

variation of all sources of uncertainty and provides **m + n + k + 1** measurements. The system (5) of equations describes the results of these measurements. Solution (6) of this system gets us values of the **m** uncertainties of the first cluster.

The second cluster (T_2) joins the **n** less stable sources of the uncertainty. It could be the temperature dependences of the operational amplifiers parameters, and so on. Calibration of these sources is provided more frequently, for example, one time per hour. During this calibration, we suppose that the **m** uncertainties of the first clusters are stable. Values of these uncertainties enter in the system (5) as constants. To find values of the **n** uncertainties of the second cluster, MC varies sequentially the uncertainty sources **n + k**, provides proper measurements and solves the system (5). It needs **n + k + 1** measurements.

The third cluster (T_3) joins the ***k*** uncertainty sources which change most quickly. This cluster mostly includes the sources, which directly depends on the parameters of the object to be measured. This calibration is aimed to find the true results of measurement and values of the last **k** uncertainties. During this calibration, we suppose that uncertainties of the first and second clusters are stable. Their appropriate values are entered in system (5) as constants. Calibration now consists of sequential variation of the **k** uncertainties of third cluster and appropriate measurements. Solution of the system (5) gets us the true results of measurement Z_x and last **k** uncertainties. This calibration needs **k + 1** measurements only.

Let us suppose that any measurement needs time t_i. Formula (10) describes the weighted average t_c of the measurement with variation calibration:

$$t_c = \Sigma_1^k t_i \left(1 + \frac{n+k}{m+n+k}\frac{T_k}{T_m} + \frac{k}{m+n+k}\frac{T_k}{T_m}\right) \tag{10}$$

where $\Sigma_1^k t_i$ is the time of the k cluster calibration and measurement, T_n/T_m is the ratio of the periods of the second T_n and first T_m clusters calibrations and T_k/T_m is the ratio of the periods of the third T_k and first T_m cluster calibrations.

Formula (10) shows that the time of measurement decreases only slightly during the time of calibration of the third cluster. It means sufficient diminution of the time of measurement.

2.1.2. Space clustering

Sometimes, we do not need to separately study every component of the measurement uncertainty. In this case, we use space clustering. During the space clustering, MC is represented as a complex of the **n** quadripoles and standards to be compared. **Figure 4** shows such decomposition of the measurement circuit.

In **Figure 4**, K_1 … K_n are the quadripoles of the MC and the $V_1 \ldots V_n$ are the variators used to vary the transfer coefficient of the proper quadripole.

The following formula describes the decomposed MC:

$$Z_{x0} = f(Z_x, K_1, \Delta K_1 \ldots K_i, \Delta K_i \ldots K_n, \Delta K_n) \tag{11}$$

http://dx.doi.org/10.5772/intechopen.74220

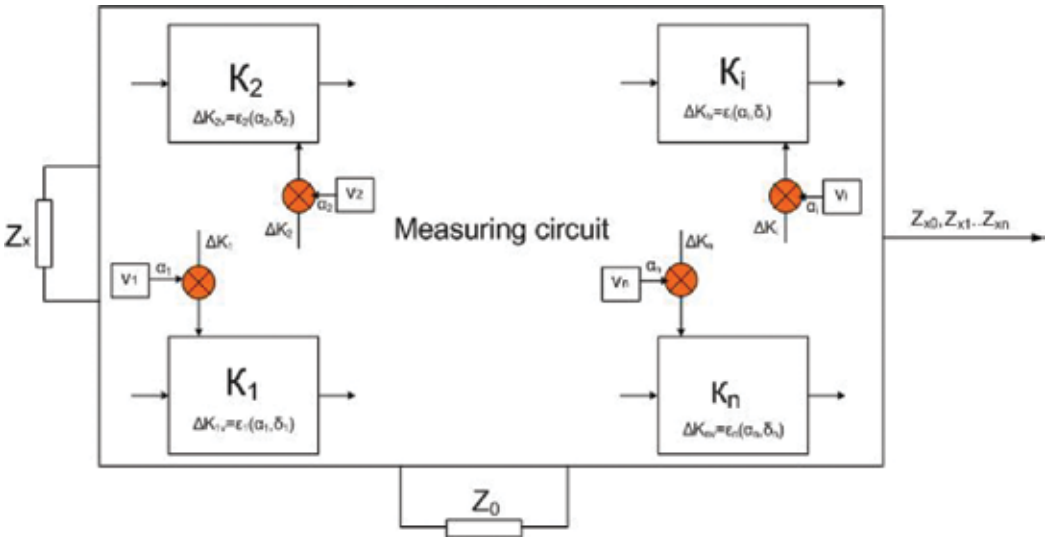

Figure 4. Variation correction with space clustering.

where Z_x and Z_{x0} are the MC input and output values, respectively, $\Delta K_1 \ldots \Delta K_{i\ldots} \Delta K_n$ are the uncertainties of the quadripole transfer coefficients $K_1 \ldots K_i \ldots K_n$.

The following formula expresses the dependence of the measurement uncertainty δ_r on the components of the decomposed MC:

$$\delta_r = \sqrt{\delta_0^2 + \delta_s^2 + \Sigma_1^n \Delta K_i^2} \tag{12}$$

where δ_s is the uncertainty caused by the finite MC sensitivity.

Let us provide **n** well-known variations $v_1 \ldots v_i \ldots v_n$ of the quadripole transfer coefficients $K_1 \ldots K_i \ldots K_n$. MC provides the new measurements $Z_{x0\ldots} Z_{xi} \ldots Z_{xn}$ of the unknown value Z_x after every variation. The system of Eq. (13) describes these measurements:

$$\begin{aligned} Z_{x0} &= f(Z_x, K_1, \Delta K_1 \ldots K_i, \Delta K_i \ldots K_n, \Delta K_n) \\ Z_{x1} &= f(Z_x, K_1, \Delta K_1, v_1 \ldots K_i, \Delta K_i, \ldots K_n, \Delta K_n) \\ Z_{xn} &= f(Z_x, K_1, \Delta K_1 \ldots K_i, \Delta K_i \ldots K_n, \Delta K_n, v_n) \end{aligned} \tag{13}$$

Solution of the system (13) of equations gets accurate results of measurement together with all uncertainties of the quadripoles.

Formulas (8) and (9) describe the uncertainty and time of measurement when using the space clustering as well. However, the number of measurements in case of space clustering is much less. Error accumulation and common time of measurement are much less as well.

We can decompose the measuring circuit in different ways. Optimal decomposition depends on the structure of the measuring circuit. Here, it is impossible to analyze all these possibilities. In most cases, we are forced to use time and space clustering together.

It should be noted that variation method was used earlier in some measurements (e.g., elimination of the uncertainty caused by self-heating of the resistive thermometer in temperature measurements). Here, we consider generalization and dissemination of this method in different areas, first in impedance measurements.

2.2. Experimental developments of the VM

VM was used in several developments. It is too complicated to analyze all these possible applications. Here, we consider only some applications of this method in very important cases of widely used digibridges and in accurate transformer bridges.

2.2.1. Application of the VM in digibridges

Development of the integral operational amplifiers and microprocessors resulted in the new class of measuring devices—digibridges [10–12]. Nowadays, digibridges cover most part of the specific market of the impedance meters. Now many companies manufacture digibridges (HP, Agilent, TeGam, IetLab, Wine Kerr, etc).

2.2.1.1. Operation and analysis

A usual digibridge consists of two serially coupled impedances Z_x and Z_0 (see **Figure 5**) These impedances are connected between outputs of the generator G and the protecting amplifier A. Negative input of this amplifier is connected to the common point of the impedances Z_x and Z_0. Amplifier A creates in this point the potential, close to zero (virtual ground). The same current I_x flows through both impedances Z_x and Z_0 and creates voltages U_x and U_0. Differential vector voltmeter DVV, through switcher S_0, measures these voltages and transfers the

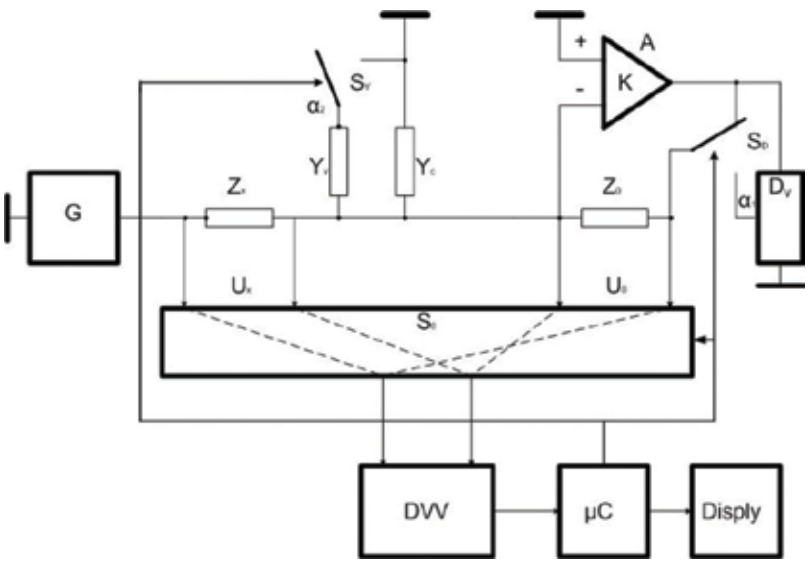

Figure 5. Structure of the digibridge with variational calibration.

results of measurement to microcontroller μC. μC controls the operation of the MC, processes results of the voltages measurements and calculates the ratio of two impedances Z_x and $Z_{0.}$ Display D shows results of measurements.

The amplifier A protects measuring circuit and decreases the influence of the parasitic admittance Y_c between the amplifier inputs on the results of measurement.

In case if gain K is infinite, Eq. (14) describes the process of measurement:

$$Z_x/Z_0 = U_x/U_0 \tag{14}$$

Let gain K be finite. In this case, admittance Y_c between the amplifier inputs cause one of the biggest sources of the measurement uncertainty. This uncertainty (δZ) strongly limits the measurements of the high impedances on high frequencies. δZ is described by the equation:

$$\delta Z = Y_c Z_0/(1 + K) \tag{15}$$

If K » 1, we can write:

$$\delta Z \cong Y_c Z_0/K \tag{16}$$

Here, the values Y_c and K are the disturbing factors. The quotient of the Y_c and K can be considered as the sole source of the uncertainty. Let us provide the multiplicative variation of the gain K of the amplifier A. To vary K on ratio α_1, the divider D_v with transfer coefficient 1 or α_1 (**Figure 5**) is used. After this variation, MC measures the additional voltage U_{0v}.

The system of three equations describes the measurements of the voltages U_x, U_o and U_{ov}.

$$U_x = I_x Z_x; \quad U_0(1 - Y_c Z_0/K) = I_x Z_0; \quad U_0(1 - Y_c Z_0/K) = I_x Z_0 \tag{17}$$

Solution of this system gets the following formula (18):

$$Z_x/Z_0 = U_x[1 - \delta U \cdot \alpha_1/(1 - \alpha_1)]/U_0 \tag{18}$$

where $\delta U = 1 - U_0/U_{0v}$

Analysis of the formula (18) shows that the uncertainty of the variation calibration has minimal if α_1=0.5. Then:

$$Z_x/Z_0 = U_x(1 - \delta U)/U_0 \tag{19}$$

Formula (19) shows that the ratio Z_x/Z_0 does not depend on the quotient of the Y_c and K.

But here increases component of the uncertainty, caused by the increased number of measurements. VV measures quadrature components **a** and **b** of three voltages: U_x, U_o and U_{0v}. Let us suppose that effective input noise of the VV in all these measurement has the same value Δ and the results of measurement are not correlated. In this case, the following formulas are justified:

$$U_x = (a_x + \Delta) + j(b_x + \Delta); U_0 = (a_0 + \Delta) + j(b_0 + \Delta); U_{0v} = (a_{0v} + \Delta) + j(b_x + \Delta) \quad (20)$$

Let us substitute formula (20) in (14) and (19). It gets the following formulas for two cases:

Without variational calibration:

$$\delta_m \approx \sqrt{2}\delta_n \text{ and } \Delta_a \approx \sqrt{2}\delta_n \quad (21)$$

With variational calibration:

$$\delta_m \approx \sqrt{5}\delta_n \text{ and } \Delta_a \approx \sqrt{2}\delta_n \quad (22)$$

where δ_m and Δ_a are the multiplicative and additive uncertainties caused by the relative noise δ_n of the VV.

Formulas (21) and (22) show that the additive uncertainty Δ_a caused by the relative noise ($\delta_n = \Delta/U_0$) in both cases is the same. But these formulas also show that due to the variational calibration, the multiplicative random uncertainty δ_m increases 1.6 times.

Calculation of the uncertainty by the formula (16) has the truncation error δ_t caused by inequality $K \gg 1$ ($\delta_t = Z_0 Y_c/K$). This error sharply increases when K on high frequencies is low, so that calibration practically does not work when $K \to 1$. If amplifier gain K is so low, we cannot consider value Y_c/K as the sole source of the uncertainty. As a result, we have to provide **two** separate variations: multiplicative variation of the gain K and additive variation of the admittance Y_c (using variational admittance Y_v and switcher S_v). DVV measures sequentially voltages U_x, U_0 and $U_0^{'}$, $U_0^{''}$ after multiplicative variation of the gain K and additive variation of the admittance Y_c.

System of three equations describes these four measurements:

$$\begin{aligned} U_x/U_0 &= Z_x/Z_0[1 + Y_c Z_0/(1 + K)] \\ U_x/U_0 &= Z_x/Z_0[1 + Y_c Z_0/(1 + \alpha_1 K)] \\ U_x/U_0 &= Z_x/Z_0[1 + (Y_c + Y_v)Z_0/(1 + K)] \end{aligned} \quad (23)$$

Solution of the system (23) gets following two equations:

$$\begin{aligned} &Y_c Z_0 = \left(A^{'} - 1\right)(\alpha_1 K + 1)(K + 1)/K(1 - \alpha_1) \\ &aK^2 + bK + c = 0 \end{aligned} \quad (24)$$

here: $a = [(1 + \alpha_1) - \alpha_1(A^{'} - 1)](A^{''} - 1)$, $b = (Y_v Z_o + A^{'})A^{''} - A^{'}$, $c = (A^{'} - 1)(A^{''} - 1)$, $A' = U_0^{'}/U_0$, $A^{''} = U_0^{'}/U_0$

Solution of the Eqs. (24) and substitution of these results in (15) gets the accurate results of measurement which absolutely does not depend on the values Y_c and K.

http://dx.doi.org/10.5772/intechopen.74220

The described approach could be used for the accurate calibration of any amplifier with positive or negative gain, followers, gyrators, and so on. It could be used for calibration of any control system as well.

3. Experimental results

The earlier described approach was used in digibridge MNS1200. This digibridge was developed for Siberian Institute of Metrology (Novosibirsk), to be used in working inductance standard. Its short specification is as follows.

MNS1200 operates in frequency range of DC to 1 MHz.

Frequency set discreteness 2×10^{-5}.

Capacitance range of measurement (F) 10^{-17}–10^{5}.

Resistance range of measurement (R) 10^{-6}–10^{14}.

Inductance range of measurement (H) 10^{-12}–10^{10}.

Dissipation factor tgδ (tgφ) 10^{-6}–1.0.

Main uncertainty (ppm) 10.

Sensitivity (ppm) 0.5

Inner standard instability (24 hours, ppm) $\pm$ 2.

Weight (kg) 4

MNS1200 appearance is shown in **Figure 6**.

Instability of the MNS1200 inner standard can achieve 10^{-4} in a long period of time. To get maximal accuracy, MNS1200 can be calibrated by arbitrary R,L,C outer standard. In this case,

Figure 6. Digibridge MNS1200.

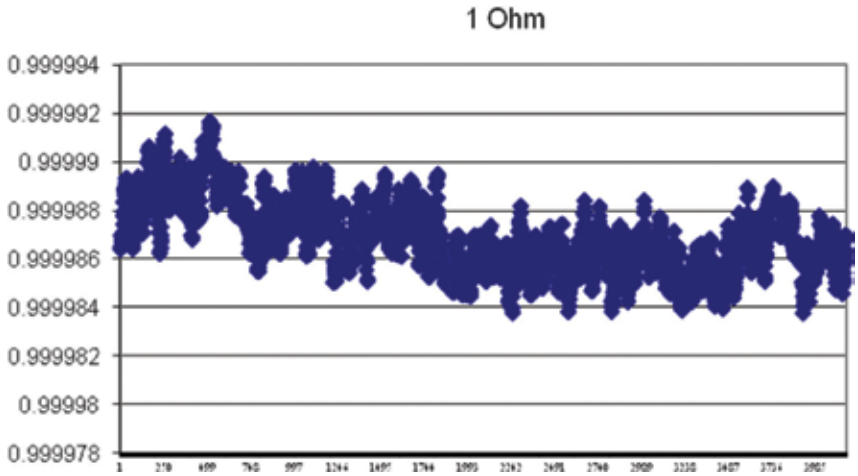

Figure 7. Results of the 24-hour 1 Ohm standard measurements.

uncertainty of measurement depends on short-time stability of inner standards. Results of the 24-hour 1 Ohm standard measurements are shown in **Figure 7**.

3.1. Application of the VM in transformer bridge

Accurate comparison and unit dissemination of the impedance parameters are provided using many different, very complicated manual bridges with numerous different standards. The main world-renowned laboratories (BIPM, NIST, NML, NPL, PTB, VNIIM, etc.) in developed countries have their own primary standards, based on the calculable capacitor [13, 14] and the appropriate transformer bridges [15, 16], on the quantum hall resistance [17] and the appropriate bridges [18, 19] and very accurate quadrature transformer bridges for comparison of different impedance parameters [20, 21], that have original constructions. All these bridges contain complicated set of devices and have long and intricate handle balancing processes. In addition, these bridges and standards are of different kinds and are located in various laboratories. The process of calibration and traceability is, therefore, complicated and very expensive. Uncertainty of the measurement of these bridges achieves 10^{-8}–10^{-9}. It makes them an excellent instrument for fundamental investigations.

For practical needs of the metrologic calibration, it is enough to provide measurements with uncertainty about 10^{-6}. In this case, the equipment have to be universal, to compare arbitrary standards, to have low cost and weight and to be transportable. The complex of bridges described later satisfies these demands. Complex consists of autotransformer and quadrature bridges. Both of them are based on the variational calibration. Autotransformer bridge provides unit transfers in the whole range of the impedance of the C,L,R standards. Quadrature bridge provides cross transfers of the units. Last bridge is described in [22, 23].

This chapter describes the part of the results of this project, covering the development of the transformer bridge-comparators which transfer units of the resistance, inductance, capacitance

http://dx.doi.org/10.5772/intechopen.74220

and dissipation factor in a whole range of measurements and reciprocal transfer of any units. Balance and calibration of these bridges are based on the variational method.

3.1.1. Autotransformer bridge: description and analysis

Early autotransformer bridges were described in [24, 25]. These bridges have been widely used up to now [15, 16]. To eliminate the influence of the cable impedance (yoke) on the results of measurement, double autotransformer bridges are used [3, 5]. The wide-range double autotransformer bridge contains two inductive dividers, simultaneously controlled for bridge balance. For accurate measurements, these inductive dividers usually are of a two-stage design at least. Every stage of these inductive dividers [26] consists of a lot of turns and appropriate complicate switchers. They have to have multidigit capacity (up to seven or eight digits). This quite complicates the bridge.

Development of the variational bridge has to solve two problems:

- to eliminate the Yoke (Z_n) influence on the results of measurement without using the double autotransformer bridge;
- to decrease sharply the number of the autotransformer divider decades without loss in the accuracy of measurement.

The simplified measuring circuit of the automatic variational bridge (PICS) [27], which solves these problems, is shown in **Figure 8**.

The bridge consists of the supply unit (the generator G connected to the voltage transformer TV), the main autotransformer AT and the variationally balanced 90° phase shifter [28], which is calibrated through calibration circuit CC. The vector voltmeter VV (through the preamplifier PA and switchers S_1 and S_2) measures the bridge (U_1, U_2) and the calibration circuit CC (U_c)

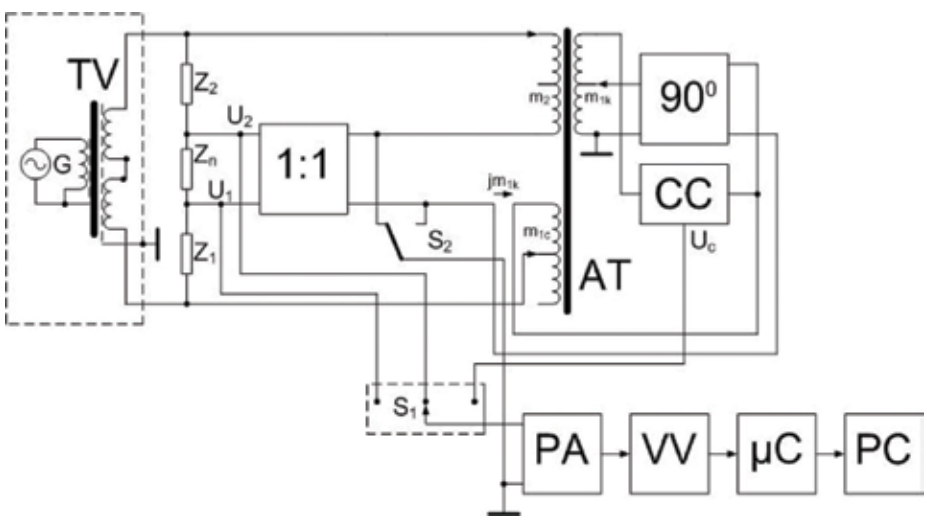

Figure 8. Circuit diagram of the autotransformer bridge.

unbalances the signals. The differential voltage follower 1:1 compensates the voltage drop U_n on the cable impedance Z_n. The microcontroller μC transfers the results of the VV measurements to the personal computer PC and controls the bridge balance and calibration of the phase shifter 90°. The autotransformer AT Carries on its core windings m_2, m_{1c} and m_{1k}. These windings are used to balance the bridge by the main (m_{1c}) and secondary (m_{1k}) parameters. The standards to be compared Z_1 and Z_2 are connected serially by the cable (yoke) and by their high potential ports, to voltage transformer TV and to the windings m_{1c} and m_2 of the autotransformer AT.

The output of the 90° phase shifter is connected in series with the winding m_{1c} to create the balance winding $m_1 = m_{1c} + jm_{1k}$.

The drop of the voltage U_n acts on the impedance Z_n of the cable which connects Z_1 and Z_2. This voltage is applied to the input of the differential voltage follower 1:1.

The two-channel VV has two digital synchronous demodulators, proper LF digital filters and Σ-Δ ADC. It simultaneously measures two orthogonal components of the bridge unbalance signals. This voltmeter has high selectivity (equivalent Q-factor is higher than 10^5). Its integral nonlinearity is better than 10^{-4} and relative sensitivity is better than 10^{-5}. The VV is calibrated automatically and periodically by variational algorithm, described in [29].

On the low impedance ranges, the drop U_n of the voltage on the cable impedance increases. This increases the uncertainty of the bridge unbalance measurement. To decrease this effect, the voltage follower 1:1 is used. This follower places the named drop of the voltage between low potential pins of the windings m_1 and m_2. It decreases the effective cable impedance from Z_n to the equivalent value $Z_{ne} = Z_n\delta$, where δ is the uncertainty of the transfer coefficient of the voltage follower.

To decrease the number of the decades of the autotransformer divider and eliminate the influence of the Z_n on the results of measurement, the bridge operates in a non-fully balance mode and use twice variational balance [27].

In compliance with developed variational algorithm, VV measures sequentially the bridge unbalance signals U_1 and U_2. After that, μC varies the turns of the winding m_1 on Δm_v and VV measures the variational signal U_{2v}.

The system of Eqs. (30) describes these three measurements:

$$\begin{aligned} &U_0(Z_1/Z_c) - U_0[1 - Z_n(1+\delta)/Z_c]m_1/(m_1+m_2) - U_1 = 0 \\ &-U_0[1 - Z_n(1+\delta)/Z_c]m_2/(m_1+m_2) + U_0Z_2/Z_c + U_2 = 0 \\ &-U_0[1 - Z_n(1+\delta)/Z_c]m_2/(m_1+m_2+\Delta m_v) + U_0Z_2/Z_c + U_{2v} = 0 \end{aligned} \tag{25}$$

where $Z_c = Z_1 + Z_2 + Z_n$, and δ is the uncertainty of the voltage follower 1:1, U_0 is the supply voltage.

The formula (26) gives the solution of the system (25):

$$\delta Z = -\frac{\delta_v}{2}\frac{m_1+m_2}{m_2}\left(C + \frac{m_1-m_2}{m_1+m_2}D\right)/[1 + (C+D)\delta_v] \tag{26}$$

where

http://dx.doi.org/10.5772/intechopen.74220

$$C = (U_2 + U_1)/(U_{2v} - U_2); D = (U_2 - U_1)/(U_{2v} - U_2); \delta_v = \delta m/(1 + \delta m); \delta m = \Delta m_v/(m_1 + m_2)$$

μC uses the results of the calculation of the bridge unbalance δZ_c by described algorithm in two stages:

- in the first stage, μC makes quick, automatic balance of the bridge on the four high-order decades (balance stage);
- in the second stage, μC increases the sensitivity of the voltmeter VV on 10^4 and decreases the value of the variation Δm_v of the m_1 turns in the same ratio. Then, μC repeats the measurements by described algorithm. Results of these measurements and calculations by formula (26) determine the balance point coordinates and find the impedance ratio:

$$\frac{Z_1}{Z_2} = \frac{m_1}{m_2} - \delta Z \tag{27}$$

The final result is given in 8.5 digits.

The bridge balance and data processing by described variational algorithm reduce the number of the autotransformer dividers to only one and sharply (twice) reduce the number of the digits of this divider.

The 90° phase shifter and the calibration circuit CC **do not contain accurate internal standards** of capacitance or resistance. To get good accuracy, we use the special phase shifter calibration procedure based on the variational method. Simplified structure of this phase shifter is shown in **Figure 9**.

Phase shifter consists of serially connected inverter I and proper phase shifter PS. Firstly, calibrating circuit (resistors R_1 and R_2) and switchers S_1 and S_2 are used to calibrate inverter I. Secondly, calibrating circuit (resistor R_1 and capacitor C_1) and switchers S_3 and S_4 are used to calibrate the phase shifter PS. Vector voltmeter VV, through switcher S_5 measures unbalance signals of the first or second calibration circuits and translates the results of measurements to microcontroller μC. Finally, one controls all calibration procedure and calculates PS real transfer coefficient.

Calibration procedure consists of two stages.

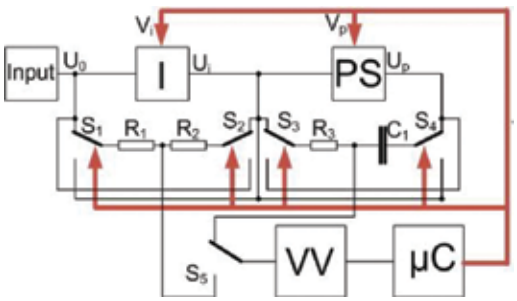

Figure 9. Structure of the phase shifter.

4. Calibration of the inverter I

To calibrate the inverter, the VV measures three signals of the calibration circuit R_1–R_2:

- The initial output signal of the calibration circuit U_{i1};
- The signal U_{i2} after the variation of the inverter transfer coefficient on the value δ_{iv};
- The signal U_{i3} after the inversion of the connection of the calibration circuit between the input and output of the inverter I by the switchers S_1 and S_2.

Complex of these signals is described by proper system of equations. Solution of this system (formula 38) gets the accurate deviation δ_i of the inverter transfer coefficient from its nominal value "1."

$$\delta_i = \delta_{ia}(1 + \delta_{kia}) \tag{28}$$

where.

$\delta_{ia} \approx \frac{\delta_{iv}}{2}\frac{U_{i3}+U_{i1}}{U_{i2}-U_{i1}}$; $\delta_{kia} \approx \frac{\delta_{iv}}{2}\frac{U_{i3}-U_{i1}}{U_{i2}-U_{i1}}$; δ_{ia} and δ_{kia} are the approximate values of the transfer coefficients of the inverter I and calibration circuit R_1-R_2.

5. Calibration of the phase shifter PS

To calibrate the phase shifter PS, the VV measures three signals of the calibration circuit R_3-C_1:

- The initial output signal U_{p1} of the calibration circuit, when calibration circuit is connected between input and output of the phase shifter;
- The signal U_{p2} after the variation of the phase shifter PS transfer coefficient in the value δ_{pv};
- The signal U_{p3} after the inversion of the calibration circuit and connection of this circuit between the input of the inverter I and output of the phase shifter PS by the switchers S_1 and S_2.

Complex of these signals is described by proper system of equations. Solution of this system (formula (29)) gets the accurate deviation δ_p of the phase shifter PS transfer coefficient from its nominal value "j":

$$\delta_p = \delta_{pa}(1 + \delta_{kpa}) \tag{29}$$

where:

$$\delta_{pa} \approx \frac{\delta_{pv}}{2}\frac{jU_{p3} + U_{p1}}{U_{p2} - U_{p1}} - \frac{\delta_i}{2}\frac{1}{1+\delta_i} \text{ and}$$

$$\delta_{kpa} \approx \frac{\delta_{pv}}{2}\frac{jU_{p3} - U_{p1}}{U_{p2} - U_{p1}} - \frac{\delta_i}{2}\frac{1}{1+\delta_i}$$

δ_{pa} and δ_{pka} are the approximate values of the transfer coefficients of the inverter PS and calibration circuit, respectively.

http://dx.doi.org/10.5772/intechopen.74220

After the calibration procedure, we know the real value of the phase shifter transfer coefficient with an uncertainty better than 1–3 ppm. μC makes this calibration procedure automatically at least every hour.

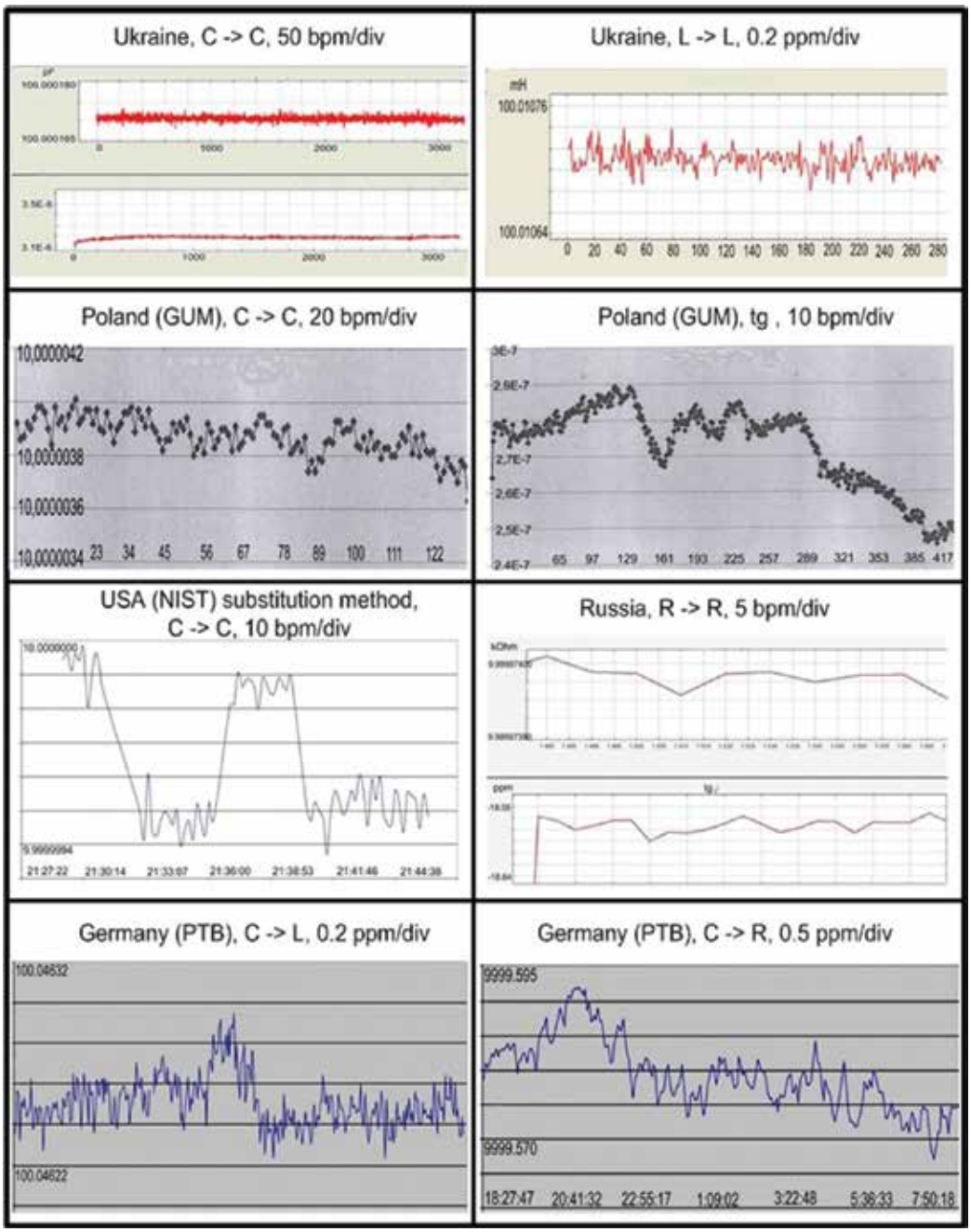

Figure 10. Some results of experimental investigations.

5.1. Experimental results

All results of the theoretical investigations shown earlier were used to develop the comparator PICS.

PICS very short specification is given as follows.

Short PICS Specification.

PICS operates on frequencies 1.00 and 1.59 kHz.

Frequency set discreteness 5×10^{-5}.

Capacitance range of measurement (F) 10^{-19}–10^{-3}.

Resistance range of measurement (R) 10^{-7}–10^{8}.

Inductance range of measurement (H) 10^{-12}–10^{3}.

Dissipation factor tgδ (tgφ) 10^{-6}–1.0.

Main uncertainty (ppm) 1.0.

Sensitivity (ppm) 0.02–0.05

Weight (kg) 5

PICS was tested in USA (NIST) and Russia (VNIIM), in Germany (PTB) and Poland (GUM), in Ukraine (Ukrmetrteststandard) and Byalorussia (Center of metrology).

Some results of these tests are shown in **Figure 10**.

Appearance of the PICS, together with intermediary thermostated standards, is shown in **Figure 11**.

Figure 11. Appearance of the PICS.

6. Conclusion

Variational calibration sharply increases the accuracy of measurement. In case of variation correction, for precision measurements, we can use simple and cheap measuring circuits with rather high uncertainty. Variational calibration diminishes the uncertainty of such circuits on thousands or even more times. It does not need too accurate variational standards. Time and space clustering in significant measure overcomes disadvantages of this calibration—increasing the time of measurement. Experimental investigations of the comparator PICS have shown that uncertainty of measurement on main ranges is lower than 10^{-6} and sensitivity is better than 10^{-7}–10^{-8}. Variational calibration also decreases the weight and cost of the accurate equipment.

Acknowledgements

The author is grateful to Dr. H. Bachmair, Dr. J. Melcher and Dr. M. Klonz (PTB), to Dr. A. Koffman, Dr. J. Kinnard and Dr. Y. Wang (NIST), to Dr. A. Tarlowski (GUM) for their constant support and very useful advice during the project development, to Dr. H. Hall for his very helpful criticism and advice during paper consideration. I would like to specially acknowledge my teacher F. B. Grinevich and colleagues A. Lameko and D. Surdu, who have spent a great part of their life realizing variational ideas.

Author details

Michael Surdu

Address all correspondence to: michaelsurdu1941@gmail.com

Ukrainian Academy of Metrology, Kiev, Ukraine

References

[1] Hall HP. A History of Z Measurement. 64 pp. www.ietlabs.com/pdf/GenRad_History/A_History_of_Z_Measurement.pdf

[2] Ornatsky PP. Automatic Measurements and Instrumentation. Kiev: High School; 1986. p. 310

[3] Kibble BP, Rayner GH. Coaxial AC Bridges. Bristol: Adam Hilger Ltd; 1984. p. 203

[4] Hague B. Alternating Current Bridge Methods. 6th ed. Pitman Publishing; 1971. p. 602

[5] Grinevich FB. Automatic bridges – Novosibirsk. 216 pp. 1964

[6] Kneller JV, Agamalov JR, Desova AA. Automatic impedance bridges with coordinated balance., S.Pt. Energy. 1975:168

[7] Bromberg EM, Kulikovsky KL. Testing methods of the improvement of the accuracy of measurement. Energy, Moskow. 1978:176 pp

[8] Zemmelman MA. Automatic correction of the uncertainty of measurement. Moskow: Standards publishing house; 1972. 200 pp

[9] Grinevich FB, Surdu MN. precision AC variational measuring systems. Kiev: Scientific thinks; 1989. p. 192

[10] Karandeev KB, and all. Quick-acting electronically balanced measuring systems. Kiev-Moskow. Energy. 1978:134 pp

[11] Maeda K, Narimatsu Y. Multy-frequency LCR meter test components under realistic conditions. Hewlett-Packard Journal. February, 1979;**30**(2):24-32

[12] Hall HP. Method of and Apparatus for Automatic Measurement of Impedance or other Parameters with Microprocessor Calculation Techniques. Pat. USA, No 4196475. 1.04; 1980

[13] Thompson AM, Lampard DG. A new theorem in electrostatic and its application to calculable standard of capacitance. Nature. 1956;**177**:888

[14] Fletcher N. The BIPM/NMIA Calculable Capacitor Project. Conference on Precision Electromagnetic Measurements, June 13–18, 2010, Daejeon, Korea. pp. 318-319

[15] Jeffery AM, Shields J, Shields S, Lee LH. New multi-frequency Bridge at NIST, BNM-LCIE, pp. G1-G37. 1998

[16] Delahaye F. AC-bridges at BIMP. BNM-LCIE. pp.C1-C6. 1998

[17] Klitzing v K, Dorda G, Pepper M. New method for high-accuracy determination of the fine-structure constant based on quantized hall resistance. Physical Review Letters. 1980;**45**:494

[18] Fletcher NE, Williams JM, Janssen A. Cryogenic current comparator resistance ratio bridge for the range 10 kΩ to 1 GΩ. Precision Electromagnetic Measurements Digest, CPEM2000 y. 482-483 pp. 2000

[19] MI6800A – Quantum Hall System, technical description

[20] Thompson AM. An absolute determination of resistance based on calculable standard of capacitance. Metrologia. January 1969;**4**(16):1-7

[21] Trapon G, Thevenot O, Lacueille JC, Poirier W. Determination of the von Klitzing constant R_K in terms of the BNM calculable capacitor - fifteen years of investigations. Metrologia. August 2003;**40**(4):159-171

[22] Surdu M, Lameko A, Surdu D, Kursin S. Wide frequency range quadrature bridge comparator. 16 International Congress of Metrology, Paris, 7–10 Okt, 2013

[23] Surdu M, Kinard J, Koffman A, et al. Theoretical basis of variational quadrature bridge design of alternative current. Moscow, Measurement Techniques. 2006;**10**:58-64

[24] Blumlein AD. British Patent No. 323,037. Alternating Bridge circuits

[25] Wenner F. Methods, apparatus, and procedure for the comparison of precision standard resistors. NBS Research Paper RP1323. NBS Journal of Research. 1940;**25**(Aug):231

[26] Brooks HD, Holtz FC. The two-stage current transformer. Transactions of the American Institute of Electrical Engineers. 1922;**XLI**:382-393

[27] Surdu M, Lameko A, Surdu D, Kursin S. An automatic bridge for the comparison of the impedance standards. Measurement. 2013;**46**:3701-3707

[28] Surdu M, Lameko A, Surdu D, Kursin S. Balanced wide frequency range quadrature phase shifter. Conference on Precision Electromagnetic Measurements CPEM2010, Daejeon, Korea, 6–10 July, 2010

[29] Surdu M et al. Peculiarities of the calibration of the two channel vector voltmeter for the digital AC bridge. UMJ. 2011;**1**:25-30

Section 2

Metrological Approaches

Chapter 4

Measuring 'Big G', the Newtonian Constant, with a Frequency Metrology Approach

Andrea De Marchi

Additional information is available at the end of the chapter

http://dx.doi.org/10.5772/intechopen.75635

Abstract

A new approach is described and discussed to the determination of the Newtonian gravitational constant G, which is based on the very powerful measurement of the frequency difference between two similar oscillators. The rate of change of time delay between the two is equal to their relative frequency difference, and small variations of either one can then be detected via delay monitoring with resolution limited only by time resolution and frequency stability of the two oscillators. The latter should be highly sensitive to gravitational field, to measure *G*, which triggers the choice of simple pendulums as field detectors. Since the relative effect on frequency readily obtainable in the lab by well-controlled variations of the gravitational field is on the order of 10^{-7}, stabilities on the order of 10^{-12} are needed of the relative frequency difference if measurement of the fifth decimal digit of *G* is the target of the experiment. It is argued that such high stability is possible with a pendulum properly designed for being locally isochronous and showing an adequately high *Q* factor. The latter is projected to reach possibly 10^7 or more with the discussed design.

Keywords: Newtonian constant, simple pendulum, pendulum frequency stability, time stability, isochronous pendulum

1. Introduction

The presently official value of the Newtonian constant *G* is listed in the most recent CODATA report (2014) as $6.674\ 08 \times 10^{-11}\ m^3\ kg^{-1}\ s^{-2}$, with a quoted relative uncertainty of 4.7×10^{-5}, which still makes it the least well known of all constants of nature, despite improvements derived from a flurry of efforts undertaken in the last decades.

Several different approaches have been followed in the realization of experiments aimed at its determination. A short summary can be found in the introduction of [1], where the experiment illustrated in this chapter was proposed, and for a deeper insight, a well-done recent comprehensive review [2] can be used for reference and comparison. It makes metrological sense to devise different experiments for the purpose, so that the set of possible systematic errors be not the same for all and the risk of undetected coherent biases among various G determinations be minimized. While refurbished and modernized versions of the original Cavendish torsion balance are still the most commonly adopted sensing device and at least one of them has demonstrated extremely high accuracy [3], experiments based on other configurations have also been developed, and a few of them have yielded some of the best results to date. The latter include a measurement based on a beam balance [4] and one based on a pair of simple pendulums used in the static mode [5]. Both achieved accuracy in the low 10^{-5} region. These three determinations of G agree within their stated uncertainty and are the most influential in the 2014 CODATA value, which, however, was attributed higher uncertainty due to the excessive disagreement of other results. A coordinate effort is being led by the recently established working group WG13 of UIAP, stimulated by a NIST initiative, aimed at improving the status of G metrology. The experiments coordinated in this effort are mainly based on the torsion balance approach because of its favorable S/N ratio, hoping to put to fruition the enormous amount of information on systematics affecting it, with the target of improving accuracy by possibly an order of magnitude. However, other approaches are also encouraged, and experiments based differently are monitored or even supported. The free-fall gravimeter [6–8] still appears very promising due to its unique absence of difficult-to-evaluate systematics, but results are still hard to come by, mainly due to the inherently low S/N ratio of these experiments. The experiment presented in this chapter is supported by NIST through its Precision Measurements Grant Program and is based on the adoption of a pair of simple pendulums as a detection device. The target is the determination of G with an accuracy of 10^{-5}. The concept of the experiment has evolved from a pilot experiment carried on at Politecnico di Torino from 1998 to 2005, which used a single pendulum in vacuum and yielded preliminary results at 3% accuracy level [9–11].

2. The dynamic dual simple-pendulum approach

The experiment illustrated here is based on a high-resolution technique, well known in frequency metrology [12], to measure very accurately small frequency differences between two almost synchronous sources. In fact, such small differences Δv produce a variable time delay between the two waveforms, which add up to a full cycle in a time interval $1/\Delta v$. The rate of change of the time delay yields directly the relative frequency difference.

Simple pendulums appear attractive for a G measurement based on this approach, because their small oscillation resonance frequency is directly proportional to the square root of the Earth's gravitational acceleration g, as is well known, which makes them particularly sensitive to a gravitational field variation induced in a controlled way by a displacement of field masses. We will call y the relative frequency change produced in this way. Resolution in this measurement is limited only by time delay resolution and differential frequency stability of

the two sources. For example, if time resolution is 1 ns, a 1000 s run allows to determine the relative frequency difference to 10^{-12}, provided its stability is adequate. This means that the two frequencies can wander around in parallel by more than that but their difference should not. This is important in considering the use of pendulum oscillators, because the gravity acceleration g is not constant in time due to a variety of causes, and so will be their frequency, which will then show instabilities not much below the 10^{-7} level [13]. Nevertheless, since such instabilities affect in a similar way all pendulum oscillators, particularly if they are in the same location, it can be expected to be quite possible that the differential instability of two equal pendulums oscillating not far from each other may be adequate for the projected resolution of the experiment under discussion.

In **Figure 1**, a sketch is shown of the expected evolution of time delay as the active field mass distribution is shifted back and forth between a geometrical configuration in which it increases the frequency of one pendulum and another antisymmetric one in which it increases the frequency of the other one. Suppose one pendulum is slightly slower than the other one (it always will be the case as two exactly equal lengths are very unlikely and even undesirable to avoid coupling). As time goes by, this slower oscillator will show increasing time delay with respect to the other, as indicated in **Figure 1** by the broken trend line. Now, when its frequency is increased by the field masses, it will get closer to that of the faster one, and its time delay rate of change (*DROC*) will decrease. The opposite will happen when the field masses increase the frequency of the other pendulum. The relevant information in this measurement is the difference between *DROC*s in the two configurations.

If v_{s0} and v_{f0} are the undisturbed frequencies of slow and fast pendulums ($v_{f0} - v_{s0} = \Delta v_0 > 0$), their difference will be modified by field masses as in Eq. (1) below, when the latter are next to the slow pendulum, and as in Eq. (2) when they are next to the fast one.

$$\Delta\nu|_s = \nu_{f0}\left(1 + y_{far}\right) - \nu_{s0}(1 + y_{near}) \tag{1}$$

$$\Delta\nu|_f = \nu_{f0}(1 + y_{near}) - \nu_{s0}\left(1 + y_{far}\right) \tag{2}$$

The DROC measurement is performed by measuring the time delay accumulated in n periods of the slow pendulum and dividing it by nT_s, as illustrated in **Figure 2**.

Therefore, it turns out that the relationship between measured DROC and actual frequencies of the two oscillators is.

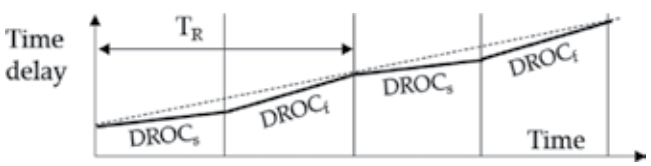

Figure 1. Time delay slope changes as field masses are moved back and forth between the two pendulums with repetition period T_R.

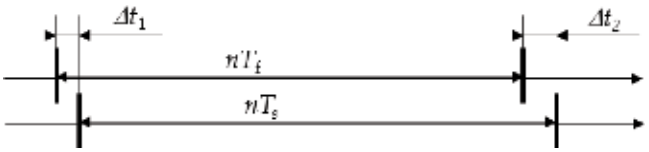

Figure 2. Measurement scheme of the *DROC* (time delay rate of change).

$$DROC = \frac{\Delta t_2 - \Delta t_1}{nT_S} = \frac{n(T_s - T_f)}{nT_s} = \frac{\Delta \nu}{\nu_f}, \tag{3}$$

and the difference between DROCs in the two configurations is then given by.

$$DROC_f - DROC_s = \frac{\nu_{f0} + \nu_{s0}}{\nu_f}\left(y_{near} - y_{far}\right) \approx \left(2 - \frac{\Delta \nu_0}{\nu_f}\right) KG \tag{4}$$

In Eq. (4), the concept was introduced that relative frequency variations induced on pendulums by the field masses are proportional to the Newtonian constant *G* through a proportionality factor *K*. The analysis needed to identify the value of *K* is sketched in the next section. The value of G can be obtained by inverting Eq. (4) and is.

$$G = \frac{DROC_f - DROC_s}{K\left(2 - \frac{\Delta \nu_0}{\nu_f}\right)}. \tag{5}$$

Clearly, *K* must be known with relative uncertainty smaller than the 10^{-5} target *G* accuracy of this experiment. In fact, this may well be the ultimate accuracy limit of this approach.

As for measurement resolution, it is also shown in the next section that the relative effect on pendulum frequency obtainable by a geometrical change in mass distribution around the bob can be on the order of 10^{-7}. It appears therefore clear that a target differential frequency stability of at least 10^{-12} should be looked for in designing the two oscillators. Other than that, the requirements for time interval measurement resolution are instead benign, both because the S/N ratio of pendulum signals is expected to be quite good (more on this in the following) and because the DROC type A uncertainty can be expected to improve as the averaging time to the power 3/2, much faster than the typical power ½ of averaging on white noise [1]. The intuitive explanation for this is in the fact that a linear regression on the scatterplot of delay data versus time will in fact yield a statistical uncertainty improving as the square root of the number of measurements (which is proportional to time), but then the result is divided by elapsed time to get the DROC, which produces the power 3/2 improvement law.

3. Field mass configuration

For the calculation of the gravitational effect on frequency, the relative extra acceleration a_M given to the bob by the system of field masses is the relevant parameter. In fact, for small

oscillations of the bob along x, its angular frequency is given by the square root of $(a_g + a_M)/x$, with $a_g = gx/L$. The relative frequency change y induced by field masses will then be $(a_M/a_g)/2$. A peculiarity of the experiment discussed here, with field masses centered on both sides of the bob, is that both a_g and a_M vanish at rest position, but their ratio does not, as both are linear in x for small displacements. This fact gives this scheme a great advantage over other approaches, because it maximizes the effect exactly where field masses are closest to sensors. For example, this is not the case for free-fall experiments, which see the effect vanish along with a_M where the sensing object spends most of its time, at the apogee of its parabolic flight.

An analysis of the arrangement under discussion, with two equal masses symmetrically centered on either side of the bob rest position, yields for the effect on pendulum frequency.

$$y = \frac{\rho_M}{\rho_E}\frac{L}{R_E}\left(\frac{R}{a}\right)^2 \Gamma(0) \ , \tag{6}$$

where L is the pendulum length, R and a are radius and half distance of field masses between centers, R_E is the Earth's radius, and shown densities are those of the Earth and field masses. $\Gamma(0)$ is the value at $x = 0$ of a geometrical shape factor which is discussed below. It is interesting to point out in Eq. (6) that only the density of field masses is relevant for the size of the effect and not their total mass, other than in the fact that, for a given gap between them, the ratio R/a depends slightly on mass size. Also interesting is to notice that, other than hidden in the size of the gap that must host it, the test mass (which is the bob) does not appear in Eq. (6). This is because neither gravitational acceleration in play, from the Earth or from field masses, depends in any way on the mass of the bob.

The shift of Eq. (6) is expected for small oscillations. However, neither acceleration is strictly linear, which yields the well-known non-isochronism of the simple pendulum plus, relevant for this experiment, a nontrivial tie with the extra gravitational pull. So, while it is easy to find frequency and shift for small oscillations, as the relative extra acceleration can then be considered constant over the swing, nontrivial calculations are necessary for wider swings.

The field masses adopted for the experiment are cylinders of heavy metal positioned, for the "near" configuration, at either side of the bob as shown in **Figure 3a**. The metal could be platinum or, more cheaply, tungsten, but copper is chosen for budget reasons in the preliminary phases. The reason for adopting a cylindrical shape lies in the much higher uniformity of the additional recalling acceleration provided by this shape to a bob displaced from the rest point, with respect to the case of a spherical field mass shape. In **Figure 3b** a plot is given of such additional acceleration (relative to a_g) versus bob displacement in a 1 m pendulum, calculated for two tungsten field masses 85 mm in diameter and 117 mm long, spaced by an 8 mm gap to host a 5 mm spherical bob in between.

The resulting fractional frequency increase y_{near} can be calculated with a suitable integration, which is quite straightforward for oscillation amplitudes not exceeding the uniformity region. The expression of $\Gamma(x)$ used in **Figure 3b**, written with $\eta = w/a$ and $\xi = x/a$, is.

$$\Gamma(x) = \frac{3}{4}\frac{a}{R\xi}\left(\frac{1}{\sqrt{1+(\eta-\xi)^2}} \quad \frac{1}{\sqrt{1+(\eta+\xi)^2}}\right) \ , \tag{7}$$

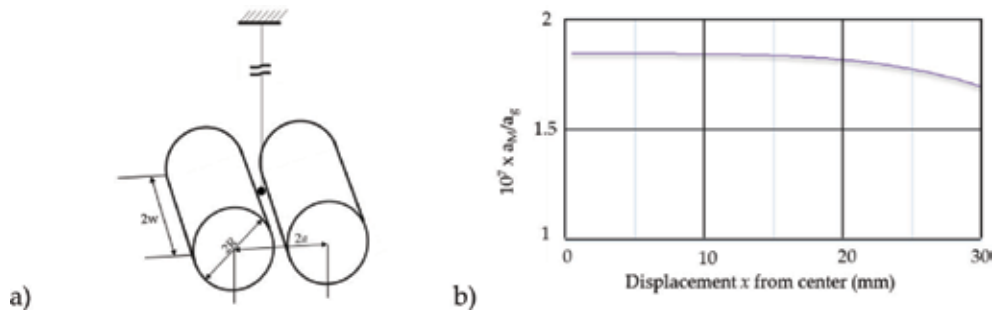

Figure 3. (a) Sketch of the near arrangement of two cylindrical field masses and (b) variations along x, elongation of the bob from rest position, of the recall acceleration a_M produced by the two field masses divided by the relevant *g* component a_g.

It should be pointed out here that shape factor of the cylindrical field masses was chosen in this calculation to optimize the uniformity of the effect, as shown in **Figure 3b**. The absolute dimension of the masses, instead, was designed to best fit the chosen geometry of the vacuum chamber, whose relevant part of the realization is shown in **Figure 4**. The chamber is realized with commercial 10 inch ConFlat flanges for the vertical body assembly, which will host both pendulums. Two thin steel tubes were welded across it to provide tunnels for the passage of the movable field mass system. These tubes are 100 mm in diameter and cannot therefore host cylinders greater than say 90 mm in diameter, together with their cradle which will be necessary for their management.

While the expression of Eq. (7) is valid for one pendulum in the "near" configuration, the effect on the other pendulum of field masses in that position must also be studied because it

Figure 4. Detail of the lower chamber of the UHV vacuum system, showing the two thin steel tubes that allow management of field masses without feedthroughs by keeping them outside the vacuum vessel.

gives raise to the relative frequency change y_{far} of the "far" configuration which appears in Eq. (4). As a matter of fact, this effect is not so small, given the fact that the two pendulums are contained in the same vacuum vessel of **Figure 4**.

In order to facilitate this calculation, while increasing the signal by a factor of two, the idea was conceived to design the field mass system as a periodic structure. In fact, it can easily be shown that increasing w, the length of the field mass cylinders, would cause a signal reduction which would take the signal to vanish if the length is taken to infinity. This happens because such a structure would produce no field gradient in the longitudinal direction. Only a modulation along x of the mass density can produce a field gradient. The periodic structure which is planned, with a density switch between ρ_M and zero (or the lower density of another material) for every length of 2 w, will produce a periodic field gradient along x which vanishes at the center of all regions of uniform density. A pendulum centered at such vanishing gradient points will experience an increased frequency when positioned in correspondence with the higher density material and a symmetrically decreased frequency when positioned in correspondence with the lower density one.

By placing the two pendulums inside the vacuum vessel at a distance 2 w from each other, within a periodic field mass system so conceived, as shown in **Figure 5**, the measured DROC will be doubled because while one pendulum is pulled up, the other one is pulled down. The opposite will then happen after the whole field mass system is displaced by 2 w to invert the centering of the two pendulums.

In practice, an infinite length of the field mass system cannot obviously be deployed, and the structure must be truncated at some point. In **Figure 6**, a calculation is shown of the expected relative gravitational extra acceleration in the case of a nine-mass-long truncated periodic structure. The material of field masses was assumed to be tungsten, dimensions were the same of **Figure 3**, and the density of air in between masses was neglected.

Details of acceleration uniformity around the rest point are given in **Figure 7** for both positions of the two pendulums, at the center of the middle field masses (upper curve) and at the center of the first air gap at their right (lower curve). It can be noticed that the latter is asymmetric. This is because the truncated periodic structure is asymmetric with respect to that point, with five masses on one side and only four on the other one. However, the effect on frequency of such asymmetry is expected to vanish to first order, as long as the rest point of the pendulum is correctly centered. In any case, centering of the pendulums will be important for accuracy as much as uniformity of the extra acceleration. Nevertheless, it can be noticed that a subtraction of the slanting baseline in the lower curve will make it appear very similar

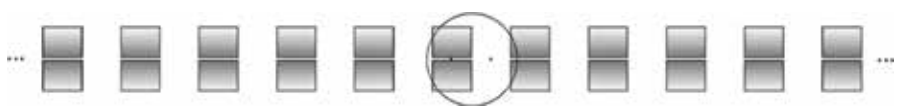

Figure 5. Scheme of the periodic field mass principle. Rest positions of the two bobs are shown (black dots). The circle in the middle represents the outline of the lower vacuum chamber through whose tunnels, shown in **Figure 4**, the field mass systems go.

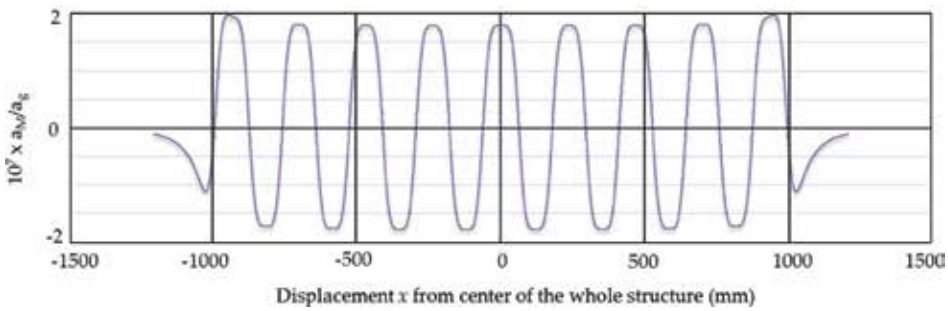

Figure 6. Calculated relative extra acceleration for a pendulum positioned at x from the center of a periodic field mass structure truncated to nine masses.

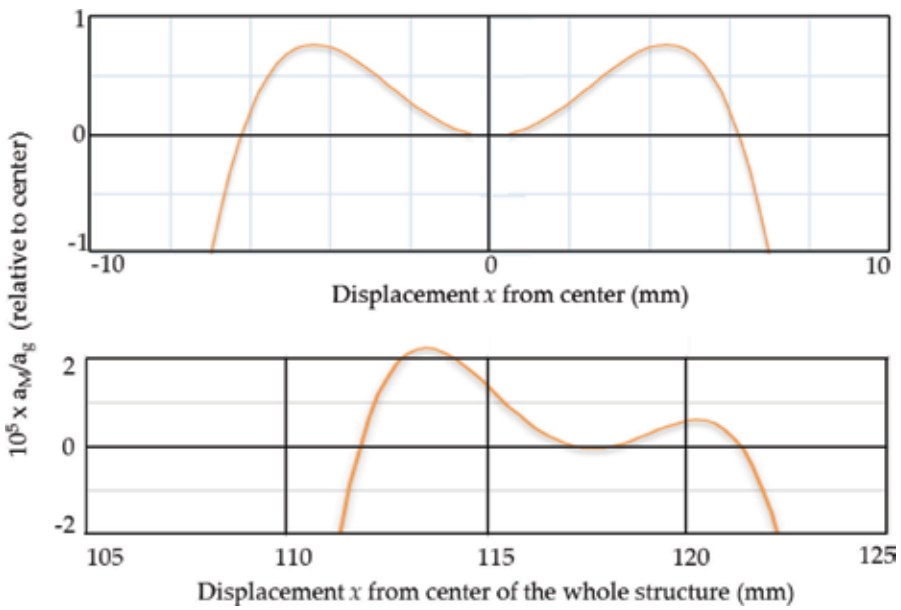

Figure 7. Relative uniformity of the extra acceleration for a pendulum positioned at the center of the middle masses (upper display) and one positioned at the center of the first gap (lower display), as a function of x, distance from the center of a nine-mass-long periodic structure. Uniformity was optimized here by trimming $\eta = w/a$.

to the upper curve for what concerns uniformity. Since both remain within +/− 10^{-5} up to 7 mm either side of the center, integration of the extra gravitational effect will be straightforward for peak pendulum oscillation amplitudes up to 7 mm if the target accuracy is at the 10^{-5} level.

In any case, all geometrical characteristics of the field mass system affect the proportionality constant K of Eq. (4), including the uniformity of their mass density and their stability in operational environmental conditions (like temperature expansion or deformation under mechanical stress). Adequate care must then be taken in design, realization, and handling of the field mass system.

To be truthful, in this respect, the experiment presented here is no different from any other experiment that was or will be tried to measure G. Revisiting the geometry of the field mass system for accuracy optimization will then be necessary after the concept is proven, which

is the real target of the present work. Such an operation will most likely belong to a national metrology institute and not to a university. What this effort wants to prove is that no real obstacle exists in this approach on the way to an accuracy of 10^{-5}, other than problems that may come from accuracy and stability of the field mass system.

More benign is the requirement on positioning of the bob's trajectory with respect to active masses. In fact, it turns out that both in the horizontal and vertical direction, the extra acceleration features an extreme versus trajectory positioning, as shown in **Figures 8** and **9**, respectively: a minimum in the center for the lateral direction and a maximum a little above masses' gravity centers for the vertical.

The vertical displacement of the maximum is due to the extra vertical pull down that field masses exert if they are moved lower than the bob, which adds to Earth's gravity and hence to recall force, until they get too far down to be relevant. Such maximum is $(a^2 + w^2)/3\,L$ above the masses' gravity centers, which turns out to be almost 3 mm for the assumed masses. The

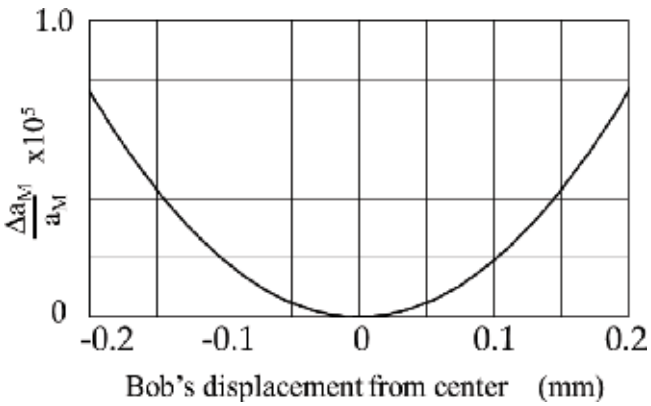

Figure 8. Relative variation of extra pull for lateral displacement of the bob's trajectory from the symmetry plane between field masses.

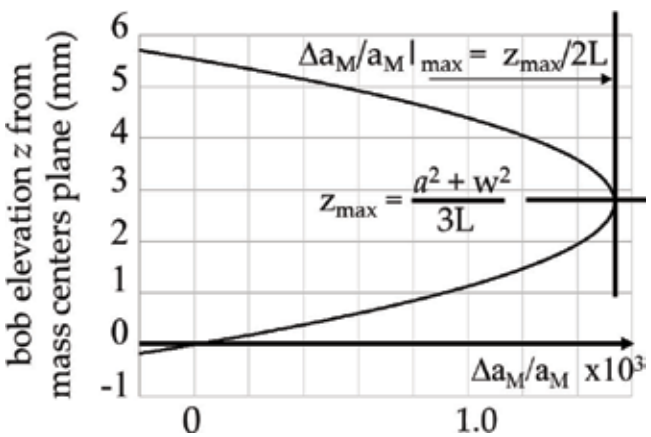

Figure 9. Relative variation of the relevant effect for vertical displacements of the bob's trajectory from the plane of mass centers.

relative shift is below $7 \cdot 10^{-4}$, which must be evaluated only to 1% for an accuracy contribution well below 10^{-5}, and the vertical positioning tolerance is 0.2 mm either side of the maximum, just like that of transverse horizontal positioning.

4. Pendulum design and optimization

The pendulums to be used in the experiment should be designed with the double target in mind of maximizing both accuracy and differential stability.

For accuracy, they should be "ideal," meaning that in their behavior they should not differ from the description that can be made with a mathematical model, supported by an adequate experimental characterization, in a way that can make G measurements uncertain by more than the desired accuracy. To this aim, all non-idealities affecting differential measurements between the two configurations of the field mass system should be considered. The main problem in this respect seems to be the uncertainty in the position of the center of mass of the pendulum given by the nonvanishing mass of the suspension relative to the bob. This shifts high the effective center of mass in a different way for the attraction of the Earth and that of the field mass system.

For differential frequency stability, which should exceed 10^{-12} for a full repetition period T_R, three main characteristics should be optimized in design and realization. They are:

1. Environmental sensitivity, especially versus temperature
2. Amplitude-to-frequency conversion, which induces frequency variations if the oscillation amplitude is not constant
3. Quality factor Q of the resonator, which is relevant in two ways: to obtain a long time constant in case of free decay operation [1] and to maximize stability with a given S/N ratio in case of sustained oscillations

Stability against environmental changes may be particularly critical for temperature, if not addressed, because at least a few ppm per Kelvin must be assumed for the linear expansion coefficient of the suspension, unless some kind of compensation is made. This is a quite common practice in pendulum clocks, but the demand in this application is severe. Even in the case of a successful compensation by a factor of ten of a low-expansion suspension material (e.g., tungsten, with its 4.3 ppm/K), the requirement would still be for a temperature differential between the two pendulums of the order of a few K for the necessary 10^{-12} differential frequency stability. It is true that the two pendulums are contained in the same vacuum vessel, which can be temperature stabilized, but an excellent thermalization scheme must certainly be devised for the purpose. It is assumed here that gold plating of the inner surface of the vacuum vessel or if necessary cylindrical gold-plated mirrors focusing the two suspensions [14] onto each other are the best bet to this aim, but a detailed discussion of the problem is out of the scope of this paper. What instead can be done at the pendulum design phase is implementation of a temperature compensation scheme. To this aim, tungsten is used for the suspension of the bob, and aluminum is deployed in an expansion compensation structure as shown below.

Amplitude-to-frequency (or period) conversion is a well-known problem of pendulum clocks, because period-to-period instability of the kick turns into frequency instability through such connection, and famous in this perspective is the solution proposed by Christiaan Huygens in his 1657 patent of making an initial ribbon section of the suspension wrap on cycloidal profiles each side as it swings back and forth. However, neither Salomon Coster (who built the first such device, still shown in Boerhaave Museum in Leiden) nor anyone later appeared to be able to take full advantage of Huygens' idea, presumably because realizing a faithfully cycloidal profile is very difficult, as its curvature diverges in the cusp, where the shape is most important for small oscillations, which is where pendulum clocks are operated for wear minimization and consequent long-term stability.

In the model chosen for this experiment, pictured in **Figure 10a** with the bob in between field masses, the pendulum suspensions are made of tungsten wires hanging between two cylinders on which they wrap and unwrap. The wires are two for each pendulum, converging on the bob, for removal of the degeneracy of the two orthogonal modes, and the wire section above the cylinders is dimensioned for temperature compensation in a scheme that includes an aluminum structure to fix the length of the upper part of the wires.

Cylinders are technologically very easy to fabricate, contrary to the cycloidal case, and very good ones are common in modern machines, which makes them easy to obtain and cheap. In this work, dowel pins and specifically wrist pins are employed. The latter are very well rectified and have a hard surface because they must bear high forces with little friction in connecting pistons to rods in ICE power trains. As for amplitude-to-frequency conversion, deploying circular profiles does not realize a completely isochronous pendulum like Huygens showed true for a cycloidal profile; nevertheless, they produce a period vs. amplitude curve which shows a minimum at a certain amplitude value which is related to the diameter *D* of the cylinders. For that magic amplitude, the pendulum is then locally isochronous, and operation exactly at that amplitude shows no amplitude-to-frequency conversion. This means that the effect on frequency of amplitude variations vanishes if the amplitude is set correctly and that it depends quadratically on the amplitude error from that magic value in a way that makes it possible to achieve the necessary stability.

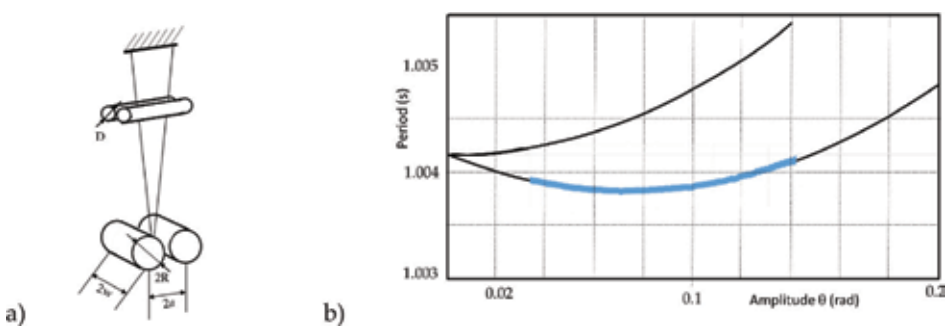

Figure 10. (a) Picture of the pendulum configuration chosen for this work, with the bob hanging between field masses, and (b) period versus amplitude curve of such pendulum compared to the one of a mathematical pendulum. Length is about 250 mm and D is 22 mm. The experimental points are superimposed on the measured section of the curve.

The period versus amplitude curve is compared to that of a mathematical pendulum in **Figure 10b**. The shape is still parabolic, but the vertex is moved from the vanishing amplitude point to an amplitude which can be chosen and adapted to the desired pendulum energy by suitably designing *D*, as shown in [15]. Period measurements, compared to the theory in **Figure 10b**, were taken on a 0.25-m-long pendulum with cylinders of 22 mm in diameter.

In fact, since at the apex of the parabola the two curves of **Figure 10b** show the same curvature, their local description is well known to be

$$\frac{\Delta T}{T_{min}} - \frac{1}{16}(\Delta\theta)^2 \tag{8}$$

which means that amplitude deviations $\Delta\theta$ from the minimum period spot must not exceed 4 μ rad to keep the first term at the 10^{-12} level. On the other hand, a period-to-period amplitude reduction is unavoidable due to energy loss and is related to it by

$$\frac{\Delta E}{E_{min}} = 2\frac{\Delta\theta}{\theta_{min}} = \frac{2\pi}{Q} \tag{9}$$

which means that the minimum pendulum quality factor Q_m necessary to keep the amplitude from decreasing more than the acceptable limit $\Delta\theta$ in one period is

$$Q_m > \pi\frac{\theta_{min}}{\Delta\theta} \tag{10}$$

For example, if θ_{min} = 0.075 rad, as in the case of **Figure 10b**, the quality factor must be greater than about 10^4 to keep the period (and the frequency) within 10^{-12} for one period, and a *Q* of 10^7 will keep the desired frequency stability for less than an hour at most. Luckily, because it's only the differential frequency stability that must be very stable, this requirement applies only to the difference of the two pendulum quality factors, provided they are both oscillating at the sweet amplitude spot. If it can be assumed that both quality factors are the same within say 10%, a *Q* of 10^7 would be enough to guarantee that the desired differential stability is kept for a full working day. This would be a long enough time for two full cycles of the repetition rate of the experiment if the system of field masses is kept in one position for a couple of hours and then moved to the other position for another couple of hours. Such is the situation for an experiment based on a pair of pendulums operated in free decay mode, and it could possibly be improved more if the two quality factors are within 1% of each other, in which case the experiment could go on for almost a week. Modeling out the effect may also be possible to some extent, as silently assumed in [1], and might further increase the useful duration of the experiment between periodic operations of amplitude reset, but this gets more complicated.

Alternatively, at the light of the experimented difficulty in obtaining consistently the extremely high *Q* values which are needed for the discussed reasons if the free decay mode must be adopted, a sustained oscillation approach can be tried for the two pendulums. In this perspective, a synchronous forcing term must be applied to the pendulum, designed to exactly recover the energy lost by friction. The best for stability and most efficient way of doing this would be a sine-wave force *F* applied in phase with the velocity *u* of the bob. This approach

avoids pulse timing and duration problems often encountered in the past by pendulum clock makers. The amplitude of such forcing term can be regulated in closed loop, by an automatic gain control (AGC) arrangement, to exactly compensate the dissipated power P_d at the desired swing amplitude. This requires the average delivered mechanical power $< Fu >$ to be

$$< Fu > \quad P_d \quad \frac{\omega e}{Q}. \tag{11}$$

Since the energy **e** stored in the pendulum swing is proportional to the amplitude squared and u is linear with amplitude, it appears that the desired force is proportional to amplitude, as it might be intuitively expected. However, this is true only if Q is constant with amplitude, which turns out not to be the case for the adopted pendulum design. An analysis of what were felt to be the two main dissipation mechanisms for this structure was given in [1] and showed that in both cases the Q limitation is proportional to some power κ of the amplitude. In detail, periodic stretching of the wires under varying tension and their bending as they wrap and unwrap on the cylinders produce Q limitations which are inversely proportional to the square of the amplitude for the former ($Q_s \propto \theta^{-2}$, where s stands for stretching) and proportional to the amplitude's three-halves power for the latter ($Q_b \propto \theta^{3/2}$, where b stands for bending). Within that simplified theory, cyclic length variations of wires were overlooked, and only stretching under varying tension and bending on the cylinders were analyzed for small oscillations. Expressions obtained for the corresponding Q limitations (Q_s and Q_b, respectively) were

$$\frac{Q_s}{Q_f} = \frac{16}{9\sqrt{\varepsilon_0}\theta^2} \tag{12}$$

$$\frac{Q_b}{Q_f} = \left(\frac{LD}{\phi^2}\varepsilon_0\theta\right)^{3/2}, \tag{13}$$

which shows that $\kappa_s = -2$ and $\kappa_b = 3/2$. Here ε_0 is the static strain imposed on wires by the weight of the bob, ϕ is the wires' diameter, and Q_f is the intrinsic Q of the wire material. The total Q of the pendulum can then be obtained as

$$\frac{1}{Q} = \frac{P_{ds}+P_{db}}{\omega E} = \frac{1}{Q_s} + \frac{1}{Q_b}, \tag{14}$$

and features a maximum Q value at an angular swing amplitude θ_{max} which can both be calculated from Eqs. (12) through (14).

An example of such a Q dependence on amplitude is given in **Figure 11a** as calculated from Eq. (14) for a pendulum which could be suitable for the G experiment (L = 1 m and D = 4 mm), built with 4 μm Tungsten wires and a spherical 4.5 mm tungsten bob. The resulting peak force that is necessary to keep the bob swinging at the given amplitude according to Eq. (11) is shown in **Figure 11b**, where the strange effect appears that, in the branch before the minimum, weaker forcing terms are needed to maintain greater amplitudes.

A comprehensive campaign to confirm the theory in all conditions has not been completed yet as this book is going in press. In particular, Q values in excess of several millions were

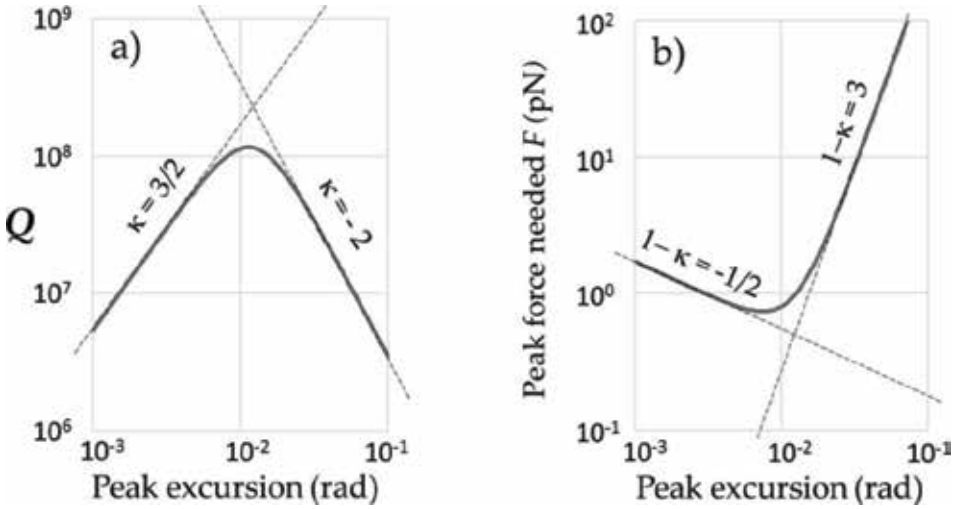

Figure 11. (a) Q as a function of angular oscillation amplitude and (b) peak force value of the sinusoidal forcing term necessary to maintain the corresponding amplitude, calculated for a pendulum with 4-mm-diameter suspending cylinders and 1 m length, made with 4 μm Tungsten wires and a spherical 4.5 mm tungsten bob.

not observed yet in the limited range of configurations that were staged, which suggests that there may be other dissipation mechanisms worth studying, but it seems unlikely that a more complete analysis may not confirm the general shape of these curves. In fact, experimental results obtained by analyzing free decay ringdown amplitude data clearly show that such *Q* maximum exists. Further experiments are in progress, as well as the analysis of such additional dissipative phenomena as belt friction, squeeze film energy loss [16], and more trivially dissipation in the structure holding the experimental arrangement.

What must be underlined here is that, due to the *Q* behavior shown in **Figure 11**, Eq. (11) points to a criticality for AGC stability, because amplitude stabilization cannot be reached if increasing the amplitude requires a reduction of the forcing term. The derivative of the required force with respect to amplitude must be positive for AGC stability, which imposes the selection of a swing amplitude in a region where the dominant dissipation mechanism is such that $\kappa < 1$. If $\kappa > 1$ the AGC will be unstable, and if $\kappa = 1$ it will not be effective because the necessary force does not depend on amplitude. Conversely, given a desired swing amplitude, as dictated, for example, by the range of acceptable field uniformity of **Figure 7**, the design of pendulum suspensions should observe the specification of placing the desired amplitude in a range where AGC stability is guaranteed.

The best choice in this respect appears to be a design which positions the θ_{max} at the desired oscillation amplitude, which is what was tried in the simulation of **Figure 11**, where the amplitude of maximum *Q* was made to correspond at 10 mm with a bob peak excursion which can be judged desirable from the calculated effect uniformity shown in **Figure 7**. However, it must be pointed out here that this design problem is still open because also the minimum of the period, as illustrated in **Figure 8**, must be placed by design at the same oscillation amplitude, which implies a tight restriction on the acceptable values of *D*, the diameter of suspension

cylinders. These values are much smaller than the one adopted in the simulation of **Figure 11** to force the position of the Q maximum. Clearly, full confirmation of the Q theory must be carried out before the pendulum design can be finalized.

Another detail which is obviously relevant to this effect is the material of the suspension wires, because both Q_f and ε_0 in Eqs. (12) and (13) are material dependent, as well as the diameter ϕ of the wires, in its own way. Unfortunately, mechanical characterization of fibers is less than complete in the open literature, particularly for what concerns mechanical losses summarized by Q_f. Therefore, tests were carried out in the laboratory with a purposely built apparatus [17] on promising candidates, mainly aiming at characterization of mechanical losses, creep, and linearity [18]. Para-aramid, SiC, basaltic, and carbon fibers were analyzed [19], as well as steel and tungsten metal wires. Glass and fused quartz are still waiting in line. No doubt, a final decision on this important item must be integrated with the whole design of the pendulum, as both analyzed loss mechanisms depend on ε_0, and hence on ϕ, while the bending loss, in particular, depends also explicitly on ϕ.

Three more very important items must be considered in the design of the pendulum because they have an impact on the operation of the device, if not on its effectiveness in detecting the gravitational field modulation. They are the mode map of the pendulum, the oscillation detection system, and the excitation mechanism in case of forced oscillations' operation mode.

The first one may affect obtainable Q values and introduce fastidious coherent noise in the detection signal. In fact, if undesired oscillation modes get excited, albeit weakly, they can easily increase the effective total damping by sucking energy into dissipative mechanisms which do not belong to the main pendulum mode, lowering its Q as a consequence, and on the other hand, they force detection data processing to face spurious coherent signals which may reduce S/N ratio and ultimately affect resolution. Getting rid of spurious signals is impossible by the Nyquist theorem because of aliasing if the sampling frequency is not at least double the highest undesired mode frequency, which forces the handling of a massive amount of data in a full sine-wave detection system. The most difficult undesired modes to deal with, however, are the ones that are closest in frequency to the pendulum mode [20], because they are the ones that are most easily excited. In particular, the transverse mode, whose degeneracy with the pendulum mode is removed by the double-wire suspension structure, remains close to it in frequency if the angle between wires is not too big.

Other modes that should be focused on are the double pendulum mode and the similar balance wheel mode, which are more separated in frequency but are easily excited as soon as some imperfection appears in the suspension structure or in the excitation system, if present.

Given the boundary conditions emerging from the panorama spelled out here, care must be taken in designing and realizing excitation and detection systems for the two pendulums, to minimize the risk of getting undesired modes excited and affecting in this way damping and measurement resolution. Both optical and electromagnetic methods have been analyzed for both. All tested methods have their own advantages and problems, but all can serve the purpose if well implemented.

5. Attitude control

One final problem must be addressed here to give a complete picture of the complexity of this apparently very simple experiment: the attitude of the whole apparatus with respect to the vertical direction, as defined by the Earth's local gravity vector, can affect the operation of pendulums and must therefore be guaranteed to be adequately accurate and stable in time, if necessary by active attitude control. Two different problems must be addressed in this respect as both the absolute tilt and its stability are relevant, in different ways.

The absolute verticality is important because the two cylinders must be guaranteed to be horizontal for the symmetry of the swing, which in turn guarantees the positioning of the minimum period in amplitude space (the curve of **Figure 10** was calculated for the case of two cylinders at the same level). Because the pendulums are two, this issue is complicated by the need to have both pairs of suspension cylinders aligned on the same horizontal plane.

The attitude stability is particularly critical in the case of low sampling-rate detection, like simple flyby time stamping at half periods, because of the heavy aliasing of seismic angular noise [1] that it produces. In **Figure 12**, a series of background seismic power spectrums is reported, as collected in different locations of the global seismographic network [21]. A peak at about 0.2 Hz appears in all of them, which is produced by low damping surface Rayleigh waves excited by ocean waves hammering the shores, extended with reduced intensity at higher frequencies. Because of their low frequency, it is very difficult to filter out such seismic angular noise contributions.

Work done to attack this problem includes passive and active attitude control [22, 23]. However, passive filtering was quickly understood to be inadequate for the purpose, not only because of its awkwardness at such low frequencies but also because of the need for stiffness of the structure holding pendulums to prevent detrimental effects of recoil from pendulums on attitude stability and damping itself. Active stabilization was then decided to be necessary, and work

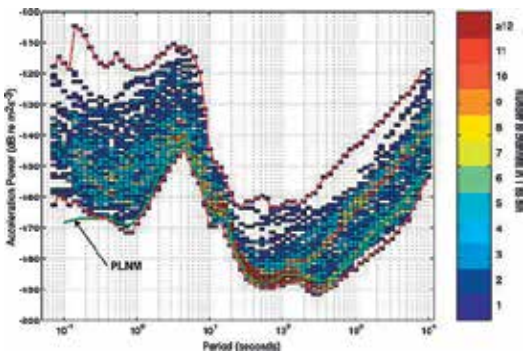

Figure 12. Background seismic power spectrums, as collected in different locations of the global seismographic network. High noise at periods above 1s (i.e. Fourier frequencies below 1 Hz) is caused by far travelling Rayleigh surface-waves excited by ocean waves.

was done to realize for the purpose a high-sensitivity tiltmeter [24] with sub-nanoradian resolution and special half-pole actuators based on thermoelectric devices [25]. The problem of substantial angular stability improvement by active control is not trivial because a tiltmeter with the necessary sensitivity was never seen with resonance-limited bandwidth above, say, 10 Hz, which provides not much more than a decade range in the Fourier frequency domain for open-loop gain increase from the zero-dB level of the loop bandwidth allowed by a typical 45° phase margin to the desired open-loop gain at the seismic peak sub-Hertz frequency. The half-pole actuator was developed for this reason, so that a loop-gain roll-off of 30 dB/dec could be achieved without resorting to a digital control, allowing in this way a guaranteed-stability servo operation with low-frequency open-loop gain in excess of 40 dB.

Nevertheless, the seismic angular noise problem is expected to be much more benign in case of acquisition of the whole sine-wave swing signal at a conveniently high sampling rate. For this reason, and because acquisition of the full sine wave is necessary anyway for oscillation support, unless the free ringdown approach is adopted, the choice was made to develop a suitable detection method for this purpose. The latter can be electromagnetic, based on the generation of an e.m.f. in a wire swinging through a magnetic field together with the suspenders of the bob, or optical, based on a linear position-sensitive detector deployed to translate the bob's position in an electrical signal.

The first approach has the advantage of measuring the bob's velocity, with which the forcing term should be in phase, and is therefore to be preferred for phase accuracy of the oscillation loop but implies the risk of introducing in the experiment undesired electromagnetic forces which could be greater than the weak gravitational force that must be measured.

The second approach, on the contrary, is less risky of introducing undesired forces but requires the generation of a sine-wave signal in quadrature with the detected position for the implementation of the forcing term. This must be performed very accurately to obtain oscillations at exactly the resonance frequency because any error from quadrature would introduce a frequency shift, which in turn may build an error on G if it's not adequately common moded between the two pendulums.

Similar considerations hold for the forcing sine wave, which can be realized with just a current-carrying wire attached to the suspenders in a voice coil type of device in the first approach and if Q is high enough could be implemented by radiation pressure in the second.

6. Accuracy budget

A tentative accuracy budget for the experiment described here is given in [1]. Because of the highly efficient time and frequency metrology approach, only geometrical uncertainties are expected to be relevant at the level of 10^{-5}, provided the necessary differential stability of 10^{-12} can be achieved. This is clearly a big "if," as discussed above, because it assumes that seismic and mode leakage problems are adequately solved. However, it can be in principle obtained if the limitation is electronic noise. It must be noted here for completeness that the

Effect	Relative bias	Uncertainty	Conditions
Shift at bob's vertical position	$6.7 \cdot 10^{-4}$	$<10^{-6}$	< 50 μm uncertainty in *a*, w
Bob's vertical position	0	$2 \cdot 10^{-6}$	0.2 mm full tolerance
Bob's lateral position	0	$1.7 \cdot 10^{-6}$	0.2 mm full tolerance
Non-isochronism	$-1.8 \cdot 10^{-5}$	$< 10^{-7}$	Operation at minimum period
Spacing between twin masses	0	$6 \cdot 10^{-6}$	0.4 μm gap uncertainty
Field masses' dimensions	0	$6 \cdot 10^{-6}$	1 μm uncertainty
Field masses' density	0	$5 \cdot 10^{-6}$	

Table 1. Accuracy budget projection based on 1-m-long 4 μm tungsten fibres, 6-mm-diameter suspension cylindrical profiles, a swing amplitude of 0.01 rad, and a 5 mm tungsten bob. The position of field masses' gravity center is assumed known with <300 nm uncertainty.

best pendulum clocks ever realized [13] were probably not differentially stable better than 10^{-9} at the target 10^4 s averaging time, which means that 60 dB improvement is necessary. Although this is granted on paper by projected S/N and *Q*, actually achieving it is still a big challenge. On the positive side, it is worth pointing out here that energy-induced amplitude changes [11] do not affect frequency if operation is kept at the minimum period isochronous point and that an approach to oscillation support aimed at overcoming pulse stability problems by moving to a sine-wave excitation system similar to that employed in high-stability quartz oscillators will remove one of the worst contributions to instability.

This said, it can be seen in **Table 1** that most geometrical contributions to uncertainty impose quite loose requirements at the target accuracy level of 10^{-5}, with the sole exception of size and positioning of field masses, which must be guaranteed at high accuracy. While other contributions enjoy relaxed specifications granted by parabolic minima which are specific of this configuration, the latter do not and must comply with specs which are similar to any other big G experiment. However, the expectation that accuracy on G may be limited by control on this single geometry contribution ushers the possibility of doing even better than 10^{-5} if resources were to become available to improve the accuracy of field masses. A summary of such uncertainties is reported in **Table 1**, as listed in Ref. [1], where the reader can find more details and a deeper discussion on accuracy.

7. Conclusions

A new experiment was presented for the determination of the Newtonian constant. It is based on a time and frequency metrology approach consisting in the measurement of the small frequency difference between two freely oscillating pendulums via their time delay rate of change. A system of dense field masses is moved back and forth between the two, alternately increasing one frequency and reducing the other and vice versa. The increase in resolution by averaging is fast in this case because the limiting noise is white delay noise, which yields $\sigma_y(\tau)$

proportional to $\tau^{-3/2}$. This fact is unique among experiments for the determination of G and offsets the poor signal size problem allowing to focus the design on accuracy rather than S/N ratio. It remains to be shown that differential stability in the 10^{-12} region can be obtained with consistency for two similar pendulums of the design which has been sketched here. This seems to be a long shot when considering the absolute stability achieved by the best Shortt clock [13], because it requires an improvement of more than three orders of magnitude with respect to it, at the target few hours (T_R) averaging time. However, it is not unreasonable to think that two adequately similar pendulums can be realized, and if they are within 100 mm of each other, it can be expected that g uniformity may be adequately stable in time to support the assumption. A description of the apparatus and a discussion of pendulum design optimization for this experiment were offered in detail, pointing out problems and possible solutions. Work is in progress on the preparation of the experiment, considering both a free decay solution and pendulum operation with active support of oscillations and amplitude control. It is expected that an accuracy of 10^{-5} may be obtained for G with the proposed approach, limited only by the accuracy of field masses' size and positioning, and that it may be possible in a metrology laboratory to reduce limiting geometrical uncertainties enough to push it into the 10^{-6} range.

Acknowledgements

The author wishes to thank for encouragement and discussions Robert Drullinger, Stephan Schlamminger, and Bill Phillips of NIST and Valter Giaretto, Mario Lavella, and Lamberto Rondoni of the Politecnico di Torino. Special thanks go to Luca Maffioli for his master's thesis on the pendulum analysis and to Meccanica Mori of Parma for the TIG welding of the thin steel tubes to the experimental chamber. The author also wishes to acknowledge the support of the US Department of Commerce and NIST through the Precision Measurements Grant Program, Award ID number 70NANB15H348.

Author details

Andrea De Marchi

Address all correspondence to: andrea.demarchi@polito.it

Department of Electronics and Telecommunications, Politecnico di Torino, Torino, Italy

References

[1] De Marchi A. A frequency metrology approach to Newtonian constant G determination using a pair of extremely high Q simple pendulums in free decay. Journal of Physics: Conference Series. 2016. DOI: 10.1088/1742-6596/723/012046

[2] Rothleitner C, Schlamminger S. Measurements of the Newtonian constant of gravitation, *G*. Review of Scientific Instruments; **88**(11):111101. DOI: 10.1063/1.4994619

[3] Quinn T, Speake C, Richman S, Davis R, Picard A. A new determination of *G* using two methods. Physical Review Letters. 2001;**87**:111101

[4] Schlamminger S, Holzschuh E, Kundig W, Nolting F, Pixley RE, Schurr J, Straumann U. Measurement of Newton's gravitational constant. Physical Review D. 2006;**74**:082001

[5] Parks HV, Faller JE. Simple pendulum determination of the gravitational constant. Physical Review Letters. 2010;**105**:110801

[6] Schwarz JP, Robertson DS, Niebauer TM, Faller JE. A free-fall determination of the Newtonian constant of gravity. Science. 1998;**282**:2230

[7] Fixler JB, Foster GT, McGuirk JM, Kasevich MA. Atom interferometer measurement of the Newtonian constant of gravity. Science. 2007;**315**:74

[8] Lamporesi G, Bertoldi A, Cacciapuoti L, Prevedelli M, Tino GM. Determination of the Newtonian gravitational constant using atom interferometry. Physical Review Letters. 2008;**100**:050801

[9] De Marchi A, Ortolano M, Berutto M, Periale F. Simple pendulum experiment for the determination of the gravitational constant G: Progress report. In: Proceedings of 6th Symposium on Frequency Standards and Metrology; September 10-14, 2001; Fife. 2002. p. 538

[10] Berutto M, Ortolano M, Mura A, Periale F, De Marchi A. Toward the determination of *G* with a simple pendulum. IEEE Transactions on Instrumentation and Measurement. 2007;**56**:249. DOI: 10.1109/TIM.2007.890785

[11] Berutto M, Ortolano M, De Marchi A. The period of a free-swinging pendulum in adiabatic and non-adiabatic gravitational potential variations. Metrologia. 2009;**46**:119

[12] Sullivan D, Allan D, Howe D, Walls FL. Characterization of Clocks and Oscillators. NIST Technical Note. Obtainable from NIST, US Department of Commerce. Vol. 1337. 1990

[13] Van Baak T. A Dream Pendulum Clock. 2009. leapsecond.com

[14] Giaretto V. Private Communication. 2008

[15] Maffioli L. Mathematical modelization and experimental validation of a simple pendulum for the measurement of the Newtonian constant *G* [Master Thesis]. Politecnico di Torino; 2013

[16] Schlamminger S, Hagedorn CA, Gundlach JH. Indirect evidence for Lévy walks in squeeze film damping. Physical Review D. 2010;**81**:123008

[17] Ceravolo R, De Marchi A, Pinotti E, Surace C, Zanotti Fragonara L. A new testing machine for the dynamic characterization of high strength low damping fiber materials. In: Experimental Mechanics. Vol. 57. New York: Springer LLC; 2016. p. 10. ISSN: 0014-4851. DOI: 10.1007/s11340-016-0208-4

[18] Zanotti Fragonara L, Pinotti E, Ceravolo R, Surace C, De Marchi A. Non-linearity detection and dynamic characterisation of aramid and silicon carbide fibres. International Journal of Lifecycle Performance Engineering. 2016;**2**:15. Interscience Publishers. ISSN: 2043-8656. DOI: 10.1504/IJLCPE.2016.082708

[19] Ceravolo R, De Marchi A, Pinotti E, Surace C, Zanotti Fragonara L. Measurement of weak non-linear response of Kevlar® fibre damaged by UV exposure. Composite Structures. Elsevier; 2017. p. 12. ISSN: 0263-8223. DOI: 10.1016/j.compstruct.2017.10.056

[20] Ortolano M: Misura della costante gravitazionale con pendolo in vuoto [PhD thesis]. Politecnico di Torino; 2001

[21] Berger J, Davis P, Ekstroem G. Ambient earth noise: A survey of the global seismographic network. Journal of Geophysical Research. 2004;**109**. DOI: B11307

[22] Berutto M. Isolamento da trumore meccanico di una piattafoma [PhD thesis] Politecnico di Torino; 2004

[23] Mura A. Measurement of the Newtonian gravitational constant with dynamic pendulum [PhD thesis]. Politecnico di Torino; 2009

[24] Berutto M, Ortolano M, Periale F, De Marchi A. Realization and metrological characterization of a compact high-resolution pendulum tiltmeter. IEEE Sensors Journal. 2005; **5**(1):26-31

[25] De Marchi A, Giaretto V. The elusive half-pole in the frequency domain transfer function of Peltier thermoelectric devices. Review of Scientific Instruments. 2011;**82**:034901. DOI: 10.1063/1.3558696

Chapter 5

Optical Radiation Metrology and Uncertainty

Manal A. Haridy and Affia Aslam

Additional information is available at the end of the chapter

http://dx.doi.org/10.5772/intechopen.75205

Abstract

Metrology is the science of measurement. The chapter contains introductory material, terminology and units used in the optical radiation metrology. Optical radiation metrology provides an applied understanding of essential optical measurement concepts, techniques and procedures. In this chapter, we focus on electromagnetic radiation with wavelengths from approximately 100 to 2500 nm. We describe the principles used to measure photometry and radiometry quantities such as total flux, intensity, illuminance, luminance, radiance, exitance and irradiance. Measurement results should be expressed in terms of estimated value and an associated uncertainty, we provide an explanation to how to estimate and build the uncertainty budget of measurements. Metrology is based on measurements and comparisons. The unit is a unique name we assign to the measures of that quantity. Base standards must be both accessible and invariable. The metrological traceability chain is the sequence of measurement standards and calibrations that were used to relate the measurement result to the reference. The uncertainty budgets for photometric and radiometric quantities are represented in this chapter.

Keywords: photometry, radiometry, illuminance, luminance, total flux, radiance, irradiance intensity, luminous intensity, irradiance, traceability, accreditation laboratory, uncertainty

1. Introduction

Optical radiation metrology is the radiometry and photometry science of measurements. Optical radiation metrology provides an applied understanding of essential optical measurement concepts, techniques and procedures. In this chapter, we focus on electromagnetic

radiations with wavelengths from approximately 100 to 2500 nm. We describe the principles used to measure photometry and radiometry quantities such as total flux, intensity, illuminance, luminance, radiance, exitance and irradiance. Measurement results should be expressed in terms of estimated value and an associated uncertainty, we provide an explanation how to estimate and build the uncertainty budget of measurements. Metrology is based on measurements and comparisons. We measure each quantity in its own units, by comparison with a standard. The unit is a unique name we assign to the measures of that quantity. Base standards must be both accessible and invariable. The metrological traceability chain is the sequence of measurement standards and calibrations that were used to relate the measurement result to the reference.

Optical radiations bathe the world in which we live [1]. Very early in our history, it was observed that light can be produced by different means depending upon the daily rotation of the earth. New ways of using light were discovered to effect changes upon many of the materials we found in the world around us. In this chapter, we discuss some of the procedures and equipment necessary to obtain accurate measurements of the amount of optical radiation that will act on our activities. The principal purpose of the science of photometry is to evaluate visible radiation or light, so the results match as closely as possible with a normal human observer exposed to that radiation. In order to achieve this aim, one must take into account the light stimulus, the radiation entering the eye and the characteristics of the visual organ that produce the relevant sensation of light [2]. Light is essential for vision, the world is only visible when light reflected or emitted by objects reaches our eye. Light is a kind of energy and is portion of a broad range of the electromagnetic spectrum. The visible light spectrum is a little part of this spectrum, between 380 and 760 nm (see **Figure 1**). The total light energy emitted from a source or falling on a surface can be measured. This total energy can cover a part of the visible spectrum, including ultraviolet and infrared energy. The branch of science in which we study light measurement is known as photometry and a subset of the broader field is radiometry.

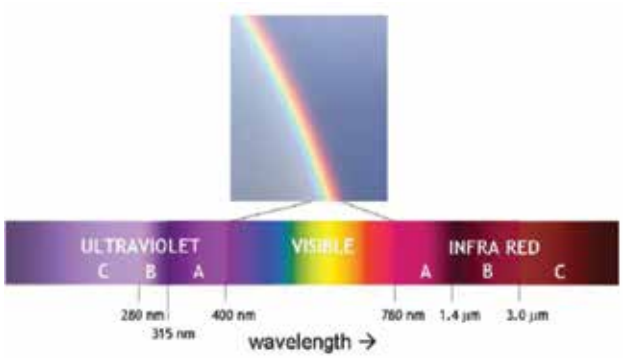

Figure 1. Electromagnetic radiation spectrum [3].

http://dx.doi.org/10.5772/intechopen.75205

2. Optical radiation quantities

To understand the measurement of several basic optical radiation quantities used to determine absolute amounts of optical radiation, it is useful to study the two aspects of quantitative optical radiation measurements: the geometrical optical radiation that we wish to measure and the spectral components of this special geometrical compound of radiation [1]. Our discussion concentrates on electromagnetic radiation with wavelengths from approximately 100 to 2500 nm, which is an extension from the visible wavelength range, which is approximately from 380 to 760 nm.

2.1. Solid angle (ω)

A solid angle (ω) is defined by the surface area of a sphere subtended by the lines and by the radius of that sphere, as shown in **Figure 2**. The dimensionless unit of solid angle is the steradian, with 4π steradians in a full sphere [4].

2.2. Radiometry

Radiometry is the science of electromagnetic (EM) radiation measurement. The spectrum covered by the science of radiometry is the range from 100 to 2500 nm.

2.2.1. Radiant flux (Φ_e)

Radiant flux is defined as power emitted, transmitted or received in the form of radiation as shown in **Figure 3** [4]. The International System of Units (SI unit) of radiant flux is Watt.

2.2.2. Radiant intensity (I_e)

Quotient of the radiant flux ($d\Phi_e$) leaving the source and propagated in the element of solid angle ($d\omega$) containing the given direction divided by the element of solid angle. The SI unit for radiant intensity is Watt/steradian (Watt/sr) as shown in **Figure 4** [4].

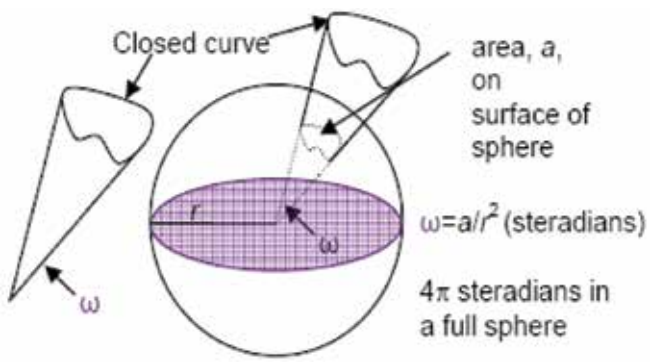

Figure 2. Solid angle [5].

Figure 3. Radiant flux [6].

Figure 4. Radiant intensity [6].

$$I_e = \frac{d\Phi_e}{d\omega} \tag{1}$$

2.2.3. Radiance (L_e)

Quotient of the radiant flux **(Φ_e)** leaving, arriving at or passing through an element of surface at this point and propagated in directions defined by an elementary cone containing [7]:

$$L_e = \frac{d^2\Phi_e}{d\omega \cdot dA. \cos\varepsilon} \tag{2}$$

where is the angle between the normal *of* the surface element and the direction *of* propagation under question. The SI unit for radiance is Watt/square meter steradian (Watt/m^2 sr), as shown in **Figure 5**.

2.2.4. Irradiance (E_e)

Flux per unit area passing through a plane from all directions in one hemisphere [7].

http://dx.doi.org/10.5772/intechopen.75205

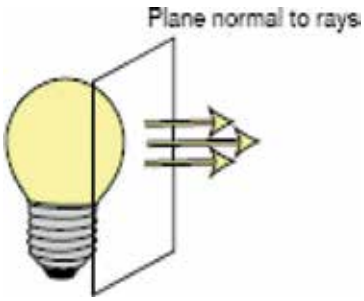

Figure 5. Radiance.

$$E_e = \int_{2\pi} L_e(\varepsilon, \varphi) \cos \varepsilon \, d\omega(\varepsilon, \varphi) = \int_{\varphi=0}^{2\pi} \int_{\varepsilon=0}^{2\pi} L_e(\varepsilon, \varphi) \cos \varepsilon \sin \varepsilon \, d\varepsilon \, d\varphi \, \omega_0 \quad (3)$$

ω_0= 1 sr unit of solid angle.

where the angles ε and φ are as shown in **Figure 6**.

The amount of incident radiant flux per unit area of a plane surface in Watt/square meter (Watt/m^2), as shown in **Figure 7**.

2.2.5. Exitance (M) [4]

It is the radiant flux emitted by a surface per unit area. The SI unit of radiant exitance is the amount of radiant flux per unit area leaving a plane surface in W/m^2, as shown in **Figure 8**.

2.3. Photometry

Photometry has a unique position in the science of physics. It is influenced by vision science and is a branch of optical radiometry. The science of photometry has been developed to quantify light and its properties accurately [9, 10]. The human eye reacts to electromagnetic

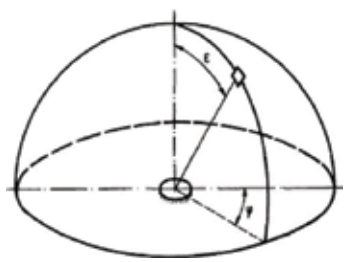

Figure 6. Illustrating the definition of the irradiance produced on a plane by a distributed source [7].

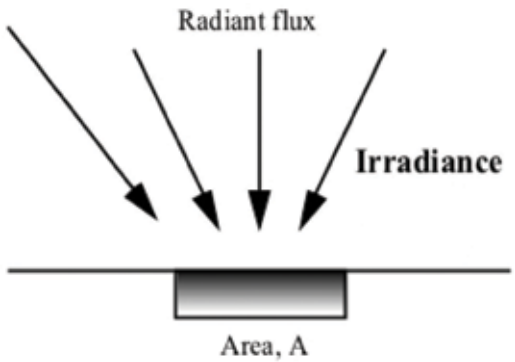

Figure 7. Irradiance [8].

radiation only in a certain part of the spectrum, that is, to a limited range of wavelengths or frequencies. The radiation of sufficient power within a wavelength range of approximately 380–830 nm only can stimulate the eye, and it is called light. Light enters the human eye through the cornea, a tough transparent membrane on the front of the eye as shown in **Figure 9**. It is refracted by the cornea and lens to form an image on the retina at the back of the eye. The sensitivity of the human eye to radiation is not the same for each of the wavelengths. This subjective nature of the visual system sets photometric quantities apart from purely physical quantities.

2.3.1. Photopic and scotopic vision

The human eye adapts to the changes in brightness and color conditions, but a lux meter does not. [12]. CIE measured the light-adapted eyes of a sizeable sample group and compiled the data into the CIE standard luminosity function. During the daytime, the cones of the eye are the primary receptors and the response is called photopic vision, . During the nighttime, the rods become the primary receptors, and the eye's response changes to scotopic vision,. Relative spectral sensitivity here means the ratio of the perceived optical stimulus to the

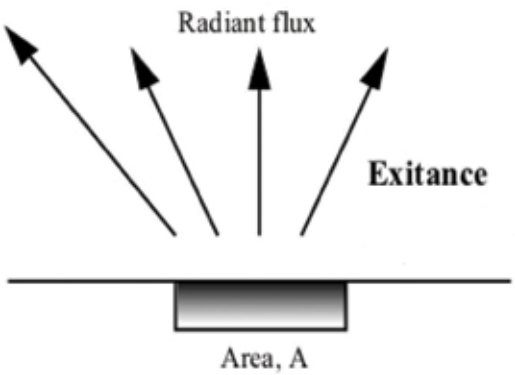

Figure 8. Exitance [8].

http://dx.doi.org/10.5772/intechopen.75205

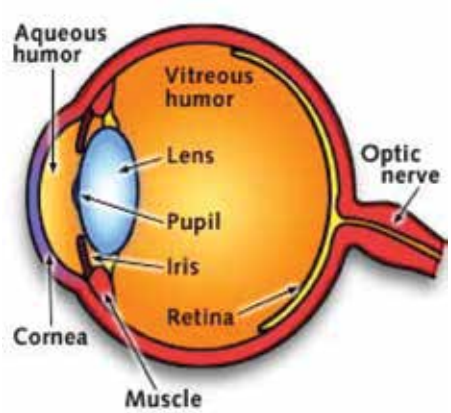

Figure 9. Human eye structure [11].

incident radiant power as a function of wavelength, normalized to unity at the maximum of the function [13] (see **Figure 10**). Special optical filters are used to give photometers nearly the same response as the average eye.

The photometric quantities are related to the corresponding radiometric quantities by the CIE standard luminosity function. We can think of the luminosity function as the transfer function of a filter which approximates the behaviors of the average human eye as shown in **Figure 11**.

2.3.2. Luminous flux (Φ_v)

Quantity derived from radiant flux **(Φ_e)** by evaluating the radiation according to its action upon the **CIE** standard photometric observer, as shown in **Figure 12** [4]. The unit is lumen (lm) = 683 × W (Watt) × V(λ).

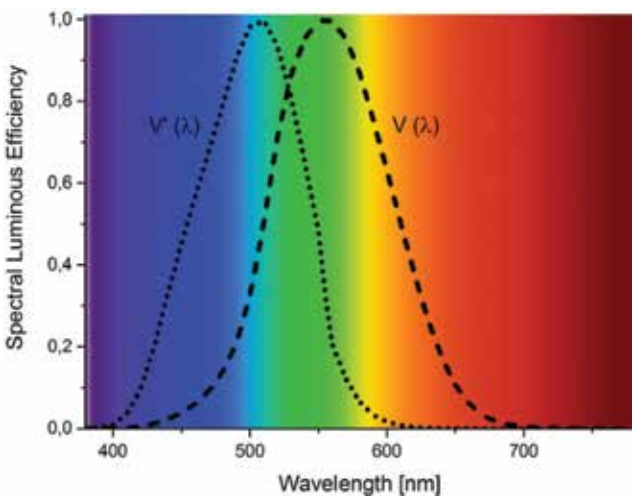

Figure 10. The photopic vision $V(\lambda)$ and the scotopic vision $V'(\lambda)$ functions [14].

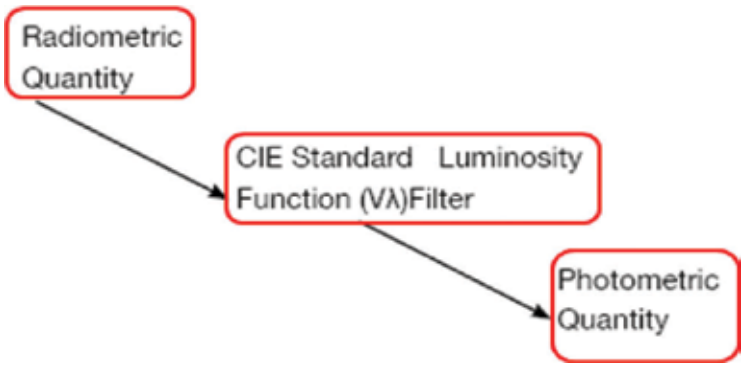

Figure 11. Relationship between radiometric units and photometric units.

2.3.3. Luminous intensity (I_v)

Quotient of the luminous flux **(Φ_v)** leaving the source and propagated in the element of solid angle $d\omega$ containing the given direction divided by the element of solid angle, as shown in **Figure 12** [4]. The unit is candela (cd).

$$I_v = \frac{d\Phi_v}{d\omega} \tag{4}$$

2.3.4. Illuminance (E_v)

Quotient of the luminous flux Φv incident on asurface divided by the area dA of that element, as shown in **Figure 12** [4]. The unit is lux (lx) and is equal to lumen per square meter (lm/m^2).

$$E_v = \frac{d\Phi_v}{dA} \tag{5}$$

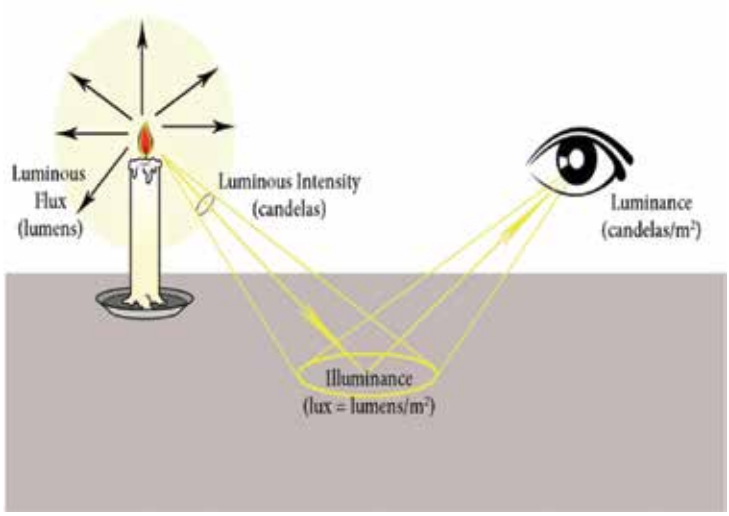

Figure 12. Luminous flux, luminous intensity, illuminance, and luminance [15].

http://dx.doi.org/10.5772/intechopen.75205

2.3.5. Luminance (L_v)

Quantity defined by the formula [4]:

$$L_v = \frac{d\Phi_v}{dA.\cos\theta.\, d\omega} \tag{6}$$

where $d\Phi_v$ is the luminous flux transmitted by an elementary beam passing through the given point and propagating in the solid angle $d\omega$ containing the given direction, dA is the area of a section of that beam containing the given point, B is the angle between the normal to that section and the direction of the beam. The unit is candelas per square meter (cd/m^2).

3. Traceability and the accreditation of the laboratories

The traceability to the SI unit through a National Metrology Institute (NMI) is defined as the property of the result of measurement or the value of a standard whereby, it can be related to stated references, usually national or international standards, through an unbroken chain of comparisons all having stated uncertainties [16], as shown in **Figure 13**. Traceability only exists when metrological evidence is collected to document the traceability chain and quantify its associated measurement uncertainties. In most cases, the ultimate reference for a measurement result is the SI definition of the appropriate unit and the stated reference is usually a national laboratory that maintains a realization of the unit. This is a practical way of stating traceability and reflects the usual chain of measurement comparisons.

Figure 13. The traceability chain [17].

Generally, goods and services are produced by a process that operates under a quality system. Nowadays, people are more conscious about quality more than before. In modern economy, calibration and testing activities play important roles in assuring the quality of goods, services and purchasing decisions. Currently, quality system registration seems to be a popular method of providing assurance of product quality, but it has become quite clear that, for testing and calibration activities, this is not good enough. The internationally recognized standard for the accreditation of laboratories is ISO 17025: General Requirements for the Competence of Testing and Calibration Laboratories [18]. Accreditation is verification that a laboratory has executed a featured system appropriate for its operations. It is verification of measurement uncertainty claims and of traceability to the International System of Units (SI). Accreditation facilitates trade and commerce by eradicating technical barriers to trade. The accreditation of calibration laboratories is particularly important through its impact on international commerce. A final benefit is that an accredited laboratory has been found to perform better in interlaboratory comparisons than unaccredited laboratories, providing additional assurance to users of accredited services [19].

4. Evaluating and expressing uncertainty

Accurate measurements and associated uncertainty propagation are the backbone of science and industry [20]. Measurements have been the cornerstone of the quantitative sciences since antiquity. However, concepts, terms, units and methods for expressing measurement results [21] and their uncertainties are still contested despite extensive and successful attempts at international consensus resulting in the International Vocabulary of Metrology (VIM) and Guide to the Expression of Uncertainty in Measurement (GUM) more than a decade ago [22–26]. The philosophy of measurement also continues to be a dynamic field of enquiry [27–30] rekindled since the early 2000s [31–34] when the Bureau International des Poids et Mesures (BIPM) began to engage in chemical measurements in addition to physical measurements.

The concept of uncertainty as a quantifiable attribute is relatively new in the history of measurement, although error and error analysis have long been a part of the practice of measurement science or metrology. It is now widely recognized that, when all of the known or suspected components of error have been evaluated and the appropriate corrections have been applied, there still remains an uncertainty about the correctness of the stated result, that is, a doubt about how well the result of the measurement represents the value of the quantity being measured. The uncertainty of the result of the measurement reflects the lack of exact knowledge of the value of the measurand. The result of a measurement after correction for recognized systematic effects is still only an estimate of the value of the measurand because of the uncertainty arising from random effects and from imperfect correction of the result for systematic effects.

The ideal method for evaluating and expressing the uncertainty of the result of a measurement should be applicable to all kinds of measurements and to all types of input data used in measurements. Also, the actual quantity used to express uncertainty should be directly derivable from the components that contribute to it. A measurement is a set of operations having the object of governing values of a particular quantity called the measurand. In general, the result

of a measurement is only an estimate of the value of the measurand and thus is complete only when accompanied by a statement of the uncertainty of that estimate [35]. In general, a measurement has imperfections that give rise to an error in the measurement result. Traditionally, an error is viewed as having a random component and a systematic component. Random error presumably arises from unpredictable variations of influence quantities. It is not possible to compensate for the random error of a measurement, but increasing the number of observations can usually reduce it. A systematic error arises from a recognized effect of an influence quantity on a measurement; it can be quantified and a correction can be applied to compensate for the effect. According to GUM [35], it is assumed that the result of a measurement has been corrected for all recognized significant systematic effects and that every effort has been made to identify such effect. Uncertainty components are grouped into two categories based on their method of evaluation "A" and "B." Both types are based on probability distributions, and the uncertainty resulting from either type is quantified by variances or standard deviations. Type A standard uncertainty is calculated from series of repeated observations and is the square root of the statistically estimated variance (i.e., the estimated standard deviation). Type B standard uncertainty is also the square root of an estimated variance, but rather than being evaluated by repeated measurement, it is obtained from an assumed probability density function based on the degree of belief that an event will occur. This degree of belief is usually based on a pool of comparatively reliable information such as previous measurement data, experience, manufacturer's specifications, calibration certificates, and so on. Once all the uncertainty components, either Type A or Type B, have been estimated, they are used to calculate the combined standard uncertainty, which equals the square root of the combined variance obtained from all variance and covariance components using what is termed as the law of propagation of uncertainty. When reporting expanded uncertainty instead of combined standard uncertainty, the multiplying factor k should be stated as well as the approximate level of confidence associated with the interval covered by the expanded uncertainty.

The Joint Committee for Guides in Metrology (JCGM) provides authoritative guidance documents to address measurement needs and is currently developing an expanded Guide to the Expression of Uncertainty in Measurement (GUM) that will provide measurement uncertainty propagation methods for a range of applications. Therefore, a comprehensive set of new worked examples to support modern industrial and research practices and to promote the consistent evaluation of measurement uncertainties are needed for this document [36].

4.1. Type A evaluation

In the simplest case (and fortunately the most usual one) of Type A evaluation, the input quantity X_i is treated as a random variable and is reasonably well approximated by the normal distribution [10]. The best estimate of the expected value of the random variable is denoted by x_i and is obtained from the arithmetic mean of a series of n independent observations obtained under the same conditions of measurement:

$$x_i = \frac{1}{n}\sum_{k=1}^{n} x_{i,k} \tag{7}$$

The individual observations $x_{i,k}$ differ in values because of random variations in the influence quantities or random effects. The experimental variance of the observations, which estimates the variance of the probability distribution of X_i, is given by:

$$s^2(x_{i,k}) = \frac{1}{n-1}\sum_{k=1}^{n}(x_{i,k} - x_i)^2 \tag{8}$$

This estimate of variance and its positive square root, $S(x_{i,k})$ termed as the experimental standard deviation, characterize the variability of the observed values $x_{i,k}$.

According to statistical theory, the best estimate for the variance of the mean x_i is given by:

$$s^2(x_i) = \frac{s^2(x_{i,k})}{n} = \frac{1}{n(n-1)}\sum_{k=1}^{n}(x_{i,k} - x_i)^2 \tag{9}$$

The Type A standard uncertainty for that component is then defined as the positive square root of this last quantity:

$$u(x_i) = \sqrt{\frac{1}{n(n-1)}\sum_{k=1}^{n}(x_{i,k} - x_i)^2} \tag{10}$$

The number of observations n should be large enough to ensure that x_i provides a reliable estimate of the expectation for X_i and that $u^2(x_i)$ provides a reliable estimate of the variance of the expectation for X_i. The number of degrees of freedom, defined as $v_i = n - 1$ should always be given when Type A evaluations of uncertainty components are documented.

4.2. Type B evaluation

With Type B evaluation, an estimate x_i of an input quantity X_i has not been obtained from repeated observations and the associated standard uncertainty is evaluated by scientific judgment based on all of the available information on the possible variability of X_i [10]. This information may include previous measurement data, experience, manufacturer's specifications, calibration certificates, and so on. Type B evaluation calls for insight based on experience and general knowledge; it is, however, as reliable as Type A evaluation.

4.3. The typical uncertainty budget for measurements

4.3.1. The components of a typical uncertainty budget for luminous intensity calibrations (detector-based method) [9]

The following are the descriptions of the abovementioned uncertainty budget items [9] (**Table 1**):

- **Calibration of reference photometers:** The uncertainty of reference photometer is stated in the calibration report issued by the national laboratory or the calibration laboratory that conducted the calibration.

- **Long-term drift of the reference photometers between recalibrations:** Estimated maximum drift of the reference photometer between calibrations.
- **Photometer temperature variation:** If the photometer has no temperature controller or temperature sensor, and the laboratory temperature is kept within
- **Distance scale of the bench (0.5 mm in 3 m)**
- **Alignment of the lamp distance (1 mm in 3 m)**
- **Spectral mismatch correction**
- **Lamp-current regulation (0.01%)**
- **Lamp-current measurement uncertainty (0.01%)**
- **Stray light**
- **Random noise (lamp drift, etc.)**
- **Repeatability of the test lamp (including alignment)**

4.3.2. The typical uncertainty budget for total luminous flux measurements

The components of a typical uncertainty budget for total luminous flux measurements are shown in **Table 2** [9].

Uncertainty factor	Type	Relative standard uncertainty (%)
Calibration of reference photometers	**B**	
Long-term drift of the reference photometers between recalibrations	**B**	
Photometer temperature variation	**A**	
Distance scale of the bench (0.5 mm in 3 m)	**B**	
Alignment of the lamp distance (1 mm in 3 m)	**A**	
Spectral mismatch correction	**B**	
Lamp-current regulation (0.01%)	**A**	
Lamp-current measurement uncertainty (0.01%)	**B**	
Stray light	**B**	
Random noise (lamp drift, etc.)	**A**	
Repeatability of the test lamp (including alignment)	**A**	
Relative combined standard uncertainty		
Relative expanded uncertainty (k = 2)		

Table 1. Typical uncertainty budget for luminous intensity calibrations (detector-based method).

The following are the descriptions of the abovementioned uncertainty budget items:

- **Calibration of luminous-flux standard lamps:** The uncertainty of the luminous-flux standard lamps is stated in the calibration report issued by the national laboratory or the calibration laboratory that performed the calibration. This uncertainty normally includes the repeatability of the lamp.
- **Aging of standard lamps:** This uncertainty is calculated from the aging rate of the standard lamps and their calibration intervals. For example, if the aging rate is 0.02% per hour and the lamp is recalibrated every 50 h of its burning time, the uncertainty due to aging of the lamp is estimated to be 1.0%.
- **Self-absorption correction:** Uncertainty of the determination of the correction factor.
- **Spectral mismatch correction:** Uncertainty of the determination of the spectral mismatch correction factor u(SCF) which can be determined regarding Eq. (11) and according to reference [29] by the following Equation [10, 37]:

$$SCF = \frac{\int_{360}^{830nm} P_e^T(\lambda) \times V(\lambda)\, d\lambda \int_{all-wavelengths} P_e^S(\lambda) \times R(\lambda)\, d\lambda}{\int_{all-wavelengths} P_e^T(\lambda) \times R(\lambda)\, d\lambda \int_{360}^{830nm} P_e^S(\lambda) \times V(\lambda)\, d\lambda} \tag{11}$$

where

is the relative spectral output of the test source;

is the relative spectral output of the standard source;

is the relative spectral responsivity of the photometer; and.

is the spectral luminous efficiency function that defines a photometric measurement.

$$u^2 = \sum_{variable} \left(\frac{\partial SCF}{\partial\, variable}\right) \times u^2(variable) \tag{12}$$

Uncertainty factor	Type	Relative standard uncertainty (%)
Calibration of primary standard lamps	**B**	
Aging of standard lamps	**B**	
Self-absorption correction	**A**	
Spectral mismatch correction	**B**	
Repeatability of test lamps	**A**	
Spatial nonuniformity of the sphere response	**B**	
Lamp electrical control	**A**	
Relative combined standard uncertainty		
Relative expanded uncertainty (k = 2)		

Table 2. Typical uncertainty budget for luminous intensity calibration (source-based method) [9].

- **Repeatability of test lamps:** Calculated as the standard deviation of the all measurements for each lamp.
- **Spatial nonuniformity of the sphere response:** This uncertainty is associated with differences of the angular intensity distribution of the test lamps and the standard lamp.
- **Lamp electrical control [10]:** The uncertainty of less than 0.01% in the calibration of voltmeter and standard resistor used for measuring and setting the electrical operating conditions of the lamps may result in 0.08% uncertainty in the lamp output.

5. Conclusion

In this chapter, we concentrate on the measurement of absolute amounts of optical radiation, which requires careful definition for the photometric and radiometric quantities such as total flux, intensity, illuminance, luminance, radiance, exitance and irradiance. Also, it was necessary to distinguish between the difference of the exitance and irradiance quantities in the physical meaning. The metrological traceability chain is the sequence of measurement standards and calibrations that were used to relate the measurement result to the reference. To produce accurate, reproducible and international acceptable results, the measurement of absolute amounts of optical radiation needs careful and detailed consideration of a broad range of physical concepts. A measurement has imperfections that give rise to an error in the measurement result. Therefore, measurement results should be expressed in terms of estimated value and an associated uncertainty. Actually, an error is viewed as having a random component and a systematic component. Random error presumably arises from unpredictable variations of influence quantities and is not possible to compensate for the random error of a measurement, but increasing the number of observations can usually reduce it. We provide an explanation to how to estimate and build the uncertainty budget of measurements for the most important quantities. The components of a typical uncertainty budgets for luminous intensity calibrations (detector-based method) and total luminous flux measurements are represented and explained in detail in this chapter.

Abbreviations

ω	solid angle
ω_0	Steradian unit of solid angle
EM	electromagnetic radiation
SI unit	International system of units
L_e	radiance
Φ_e	radiant flux
I_e	radiant Intensity

E_e	irradiance
ε	the angle between the normal *of* the surface element and the direction *of* propagation
E_e	irradiance
M	exitance
CIE	Commission Internationale del'Eclairage
$V(\lambda)$	photopic vision (CIE Standard Luminosity Function)
$V'(\lambda)$	scotopic vision
Φ_v	luminous flux
I_v	luminous intensity
E_v	illuminance
L_v	luminance

Author details

Manal A. Haridy[1,2]* and Affia Aslam[2]

*Address all correspondence to: manal_haridi@yahoo.com

1 Physics Department, Photometry and Radiometry Division, National Institute of Standards (NIS), Giza, Egypt

2 College of Science, University of Hail (UOH), Hail, Kingdom of Saudi Arabia (KSA)

References

[1] Gaertner AA. In: Cocco L, editor. Optical Radiation Measurement, Modern Metrology Concerns. Croatia: InTech; 2012 Available from: http://www.intechopen.com/books/modern-metrologyconcerns/optical-radiation-measurements. ISBN: 978-953-51-0584-8

[2] CIE. The Basis of Physical Photometry. 3rd Edition, PUBLICATION No 18.2 (TC-I .2) ISBN: 92-9034-01 8-5 ed. Vienna, Austria: Commission Internationale deL'Eclairage; 1983

[3] https://www.slideshare.net/OSRAMLEDlight/osram-os-led Fundamentals radiometry photometry v281111

[4] CIE: 1987, International Lighting Vocabulary", Publication No 17.4, Commission Internationale deL'Eclairage, Vienna, Austria.

[5] https://spie.org/publications/fg11_p02_solid_angle?SSO=1

[6] http://www.writeopinions.com

[7] CIE: 1982, Methods of Characterizing The Performance of Radiometers and Photometers, Publication No: 53. ISBN: 92-9034-053-3, Commission Internationale deL'Eclairage, Vienna, Austria

[8] https://www.slideshare.net/naresh29/l3-emr

[9] DeCusatis C, editor. Handbook of Applied Photometry. Woodbury, New York: American Institute of Physics; 1997

[10] Haridy MA. The Realization of Luminous Flux Scale and its Application in Preparing Calibrated and Tested Lamps, Doctoral Thesis, College of Women. NIS Egypt and NRC Canada: Ein Shams University; 2008

[11] http://www.meritnation.com/ask-answer/question/explain-structure-of-human-eye/human-eye-and-colourful-world/6729689

[12] CIE: 1983, The Basics of Physical Photometry, Publication No. 18.2, Commission Internationale deL'Eclairage, Vienna, Austria

[13] Köhler R. Handbook of Applied Photometry, Photometric and Radiometric Quantities. Woodbury, New York: American Institute of Physics; 1997

[14] http://www.chemistryviews.org/details/ezine/7897011/The_Future_of_Lighting.html

[15] http://rsagencies.co.za/lumens-for-the-laymen/:

[16] Traceability, NORAMET Document No. 7 (1997-04-23)

[17] http://www.accl-calibration.com/acclnews/19-Traceability-Chart/

[18] ISO/IEC 17025-1999 (International Standards Organization). General requirements for the competence of testing and calibration laboratory

[19] Canadian Association of Environmental Analytical Laboratories, Laboratory Accreditation – Proof of Performance, 1997 CAEAL Study

[20] EMPIR Call 2017, Industry, Fundamental, Normative and Research Potential. Advancing measurement uncertainty - comprehensive examples for key international standards. SRT-n02, Version: 1.0

[21] Marciano JB. Whatever Happened to the Metric System? How America Kept its Feet. 1st ed. New York: Bloomsbury; 2014

[22] JCGM. Evaluation of measurement data — Guide to the expression of uncertainty in measurement. Paris: Joint Committee for Guides in Metrology; 2008. JCGM 100:2008, GUM 1995 with minor corrections. Available at: http://www. bipm.org/utils/common/documents/jcgm/JCGM_100_2008_E.pdf. [Accessed February 15, 2016]

[23] Dybkaer R. ISO terminological analysis of the VIM3 concepts 'quantity' and 'kind-of-quantity'. Metrologia. 2010;**47**:127-134

[24] JCGM. International vocabulary of metrology—Basic and general concepts and associated terms (VIM 3). 3rd edition. 2012. Available at: http://www.bipm.org/ utils/common/ documents/jcgm/JCGM_200_2008.pdf. [Accessed February 15, 2016]

[25] Zender R. Whims on VIM. Journal of International Federation of Clinical Chemistry. 1992;**4**:115-116

[26] Page CH, Vigoureux PE. The International Bureau of Weights and Measures 1875-1975. Paris: National Bureau of Standards; 1975. Vol NBS Special Publication 420

[27] Tal E. Measurement in Science. In: Zalta EN, editor. Stanford Encyclopedia of Philosophy; 2015. Available at: http://plato.stanford.edu/entries/measurementscience/#Bib. [Accessed February 16, 2016]

[28] Boumans M, Hon G, Petersen AC. Error and Uncertainty in Scientific Practice. London: Pickering &Chatto; 2014

[29] Mari L, Giordani A. Modeling measurement: Error and uncertainty. In: Boumans M, Hon G, Petersen A, editors. Error and Uncertainty in Scientific Practice. London: Pickering &Chatto; 2014. pp. 79-96

[30] Giordani A, Mari L. Measurement, models, and uncertainty. IEEE Transactions on Instrumentation and Measurement. 2012;**61**(8):2144-2152

[31] Psillos S. Scientific Realism: How Science Tracks Truth. London: Routledge; 1999

[32] Giere RN. Explaining Science: A Cognitive Approach. Chicago: University of Chicago Press; 1988

[33] Giere RN. Cognitive Models of Science. Minneapolis: University of Minnesota Press; 1992

[34] Giere RN. Scientific Perspectivism. Chicago: University of Chicago Press; 2006

[35] Guide to the Expression of Uncertainty in Measurement, First Edition, International Organization for Standardization (ISO), 1995

[36] EMPIR Call 2017 – Industry, Fundamental, Normative and Research Potential, SRT-n02, Version: 1.0

[37] Haridy MA. Uncertainty estimation of spectral mismatch correction factor for incandescent lamps. International Journal of Current Research and Academic Review. 2015;**3**(7):262-273

Chapter 6

A New Statistical Tool Focused on Metrological Tasks

Eugene Charnukha

Additional information is available at the end of the chapter

http://dx.doi.org/10.5772/intechopen.74872

Abstract

A set of mathematical tools based on the principle of probability of origin are presented and intended to directly account for all a priori and experimental information. The principle of determining the probability of data origin, relatively the model of the experiment for evaluating the result of this experiment, is proposed. The application of this principle and its properties are described using the example of the trivial model of the direct experiment. Estimates of the result of the experiment are compared for various algorithms, including normative ones, and for various types of experiments.

Keywords: stochastic models of metrology, uncertainty, probability metrics, range measure, calibration experiment, repeated, multiple, work measurements, a priori information

1. Introduction

The key point of the text is the principle of the probability of the origin of the data. We believe that it is useful before exposition of this principle and its consequences spell out some general speculations about the situation in metrology. Metrology as a technology needs a simple, well-established and understandable procedure for implementing its tasks. Metrology as a business tries to canonize and protect its methods from strangers. These peculiars prevent the use of new mathematical tools. Metrology in a narrow sense begins with the creation of the standard, continues by the construction of a calibration hierarchy, and ends with the calibration of the working instrument of measurement. Metrology in a broad sense is a component of the experiment everywhere where its main tools are used, namely, traceability to the standard and an estimation of uncertainty.

Uncertainty is estimated using statistical tools. The peculiarity of statistical instruments applicable in metrology is the essential role of a priori information in their work. The best way to obtain a priori information is a specially performed calibration experiment. In an ideal metrological experiment, the values of all model parameters are known and controlled except for one single parameter whose value is estimated.

Statistics without a priori information cannot be used as the metrological tool. But the origin of the a priori information can be different. For example, certain object does not in any way depend on the will of the observer, and, consequently, a calibration experiment is impossible. But it is possible to collect a lot of different data about this object and similar ones. Data can only be used to classify them and to monitor the evolution of the object. On the other hand, if we reformulate the accumulated database as a priori information for identifying an object class from new data, then this is already a metrological formulation of the problem. The estimation of the absolute value characterizing the object is difficult because there is no direct traceability to the standard. But recognizing an object and estimating the magnitude of relative changes from a small amount of data can be formulated as a metrological task.

Usually, the data of the working experiment on the subject of observation are not numerous, but there is a priori information obtained in the calibration experiment. It is assumed that by the time of the working experiment this information is still relevant. Comparing the data and the model, we can estimate the observed state of the object.

An effective method—to compare the model used and the available data—is to estimate the probability that the data is generated by a source corresponding to the model. This probability is interpreted, in particular, as an estimate of the reliability of a particular value of the investigated quantity, described in the a priori model as an adjustable parameter. In other words, as an argument for the criterion to choose, one of the many variants of the measurement model provides a description of the object under study.

In this text, an analysis of the features of traditional statistical tools [1] and some new tools to replace them is proposed. The dignity of new tools (in particular the rank measure) is significantly a better universality, but its disadvantage is a large computing expenses.

The rank measure was first proposed and intuitively grounded in [2]. In paper [3], it was formally justified. Some aspects of its application were discussed in Ref. [4]. Paper [5] describes the main tools and their applications for the method of converting the densities (MCD). In paper [6] the application of a rank measure to the type of experiment rarely used by metrology but widespread in technical disciplines is discussed. This is a simple interpretation of dynamic experiment. Its main features are as follows: enough data is collected, and a minimum number of observable factors are required to evaluate the values of many parameters of the model.

2. Models

Habitual models of the measurement experiment are constructed from the principal f and stochastic η components, formally $M\ (f, \eta)$. The principal component is a mathematical description

of the physical principle of the experiment. Usually, this is an arithmetic formula, but sometimes the algorithm decides equation or even numerical simulation.

The stochastic component is a description of the random (or considered to be) influence on the result of the experiment. Often, this description consists of a system of equivalent noise sources with some specified characteristics.

The components of the model are formalized as headings of procedures whose variables are divided into two parts—the variable values of which must be determined quite accurately by the time of the working experiment, and the variable X whose values are estimated from the data D is obtained as a result of the experiment $(M, D) \rightarrow X$, where both the experimental data and the evaluated variables can be either simple or complex data structures.

The main purpose of the model is to formulate a prediction. For metrological tasks, we set the value of the controlled parameters of the model, and from it we obtain a data structure modeling experimental data. Two modeling methods that can be compared with the definitions of probability have been distributed. The Monte Carlo method (MCM) is comparable to a countable probability, and the method of converting the densities (MCD) is comparable with the axiomatic probability.

In metrological statistics the most widespread one is the simple additive noise model (additive random error model) $d_i = x + \eta_i$, where d_i is the observed process; x is the value under measurement (measurand) (is constant throughout the experiment); and η_i is a random impurity, at each time of measurement i having a different value. It is the simplest model of a direct measurement experiment. It is also called the trivial model.

It is important that it is a priori known about a random component. It is usually assumed that only the form of distribution of probability of the source of chance is known. It is necessary to estimate the value of the constant component (as a shift parameter of a known distribution) over a small number of data affected by a random error with zero shift (for simplicity of interpretation) but with a scattering magnitude of unknown magnitude. It is also assumed that the time between measurements is so large that the data sampling elements are statistically independent.

3. Normative identification of the trivial model

3.1. Sectorial formula

A trivial model with an unknown scattering parameter in accordance with mathematical statistics and normative documents of metrology is identified according to the formula (we call it the sectoral formula) $\bar{x} = s(D) \pm kS(D)$, where $\bar{x}$ is the estimate of the value of the measured quantity in the form of a confidence interval, D is experimental data, $s(D)$ is the statistics used to estimate the value of the shift parameter of the distribution given by the model, $S(D)$ is the statistics applied to estimate the scattering parameter and k is the coverage coefficient, which in general depends on the distribution law (both model and real) of the source of randomness, the number of repetitions of the experiment, both statistics, confidence and correction factors.

The property of the formula is illustrated in **Figure 1**. In this figure, by MCM the cloud of possible results of a multiple experiment is calculated and is delineated by means of a formula. The formula is linear, therefore divides the cloud of estimates into two regions by oblique boundaries.

The change in the coefficient of coverage will lead to a shift in the boundaries of the blue and red sectors, and a corresponding change in the confidence probability is due to a change in the ratio of the shares of estimates within and outside the confidence interval.

The advantage of the formula is that whatever the dispersion of the source of chance, you will still get your 95% of correct estimates. This is illustrated by the superposition of clouds with different dispersions.

The disadvantage is the strong dependence of the error probability on the standard deviation. If by will of chance the data is close, then the probability of error is large, greater than the confidence probability. If the data is very scattered, then the confidence interval is too wide, with that the actual probability of making a mistake is negligible. The confidence interval is located at the level value of statistics from the border blue/red to the border red/blue. But in the statistical limit, the confidence probability will be met. Intuitively, it is believed that, namely, the extreme values of the cloud of estimates are discarded, but in reality, it is not so. The paradox is that the probability of error is more there when the data seem better and vice versa.

The illustration is given for normal distribution and normative statistics. For other distributions and for other statistics, the scattering clouds of the results are different, sometimes quite bizarre. Coefficient of coverage should also have its own value different from Student; however, it is

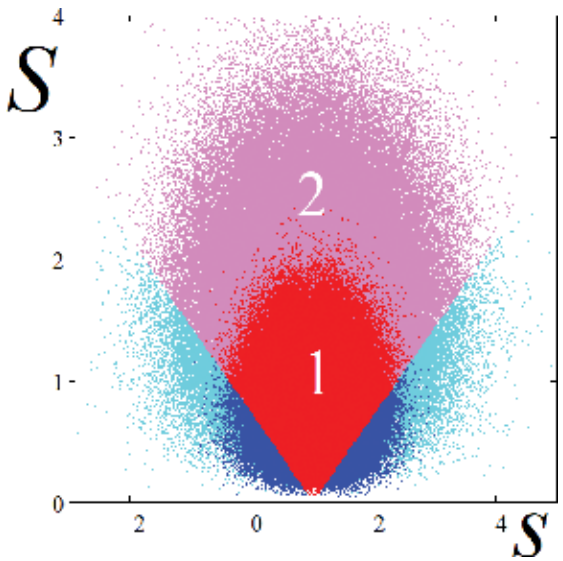

Figure 1. Clouds of scattering of results of estimates. The number of tests is 10^6, the multiplicity of the experiment is 5, the source of chance has the normal distribution with $\mu = 1$ and $\sigma = 1$ and 2 (the notations in the figure by different transparency) and the color markings for the confidence probability of 0.95 are blue (erroneous estimates) and red (correct $\mu \in \bar{r}$). Statistics are used (the arithmetic mean and the standard deviation) and the coverage coefficient is the Student's coefficient, now depending only on the number of repetitions and the confidence level.

quite simple to calculate. Here are just several simple illustrations. Let us replace the normal distribution to a very important uniform distribution. First, we apply to it normative statistics [**Figure 2** (left and central)] and then more suitable statistics of extrema $s = \frac{1}{2}(max(D) + min(D))$ and $S = \frac{1}{2}(max(D) - min(D))$ [**Figure 2** (right)].

Without going into numerical details, we give a few qualitative remarks on the illustrations given. Although the scale of both the distributions and clouds of assessments is comparable, coverage coefficients are distinctly different. It can be judged from the tilt of the colored borders.

Clouds differ not only in form but also in size. The most compact cloud gives set of a normal distribution with of normative statisticians [**Figure 2** (left)] because this combination is optimal. The combination of a uniform distribution and normative statistics (central) is not optimal; hence, the cloud is scattered more. This loss of efficiency is not catastrophic, so this combination is used in practice. Normative statistics provide acceptable estimates for many finite distributions and many distributions with light tails, but there are such distributions where the efficiency is too small, for example, distributions with heavy tails. The combination of uniform distribution and statistics of extrema (right figure), although not optimally but somewhat more efficient than in the previous example. But in practice this combination is not used because the sectoral formula of the cloud cross section leads to an unacceptably overestimation of the confidence interval value. The reason is that the maximum cloud density of this example is at the vertex, when, as in the previous examples, the maximum density is closer to the centres of the clouds. An effective algorithm for estimating the distribution of the scattering parameter could help, but because of the variability of the distribution form, mathematical statistic could not offer such an algorithm.

De facto, the distribution form and both statistics are used as a single set. The situation can be interpreted in two ways. On the one hand, having the form of distribution, we can choose or synthesize statistics more or less effectively. On the other hand, selecting statistics from a certain set of tools, we actually choose a class of distribution forms for which the statistics are still effective. However, neither the value of efficiency nor the form of distribution can be precisely determined.

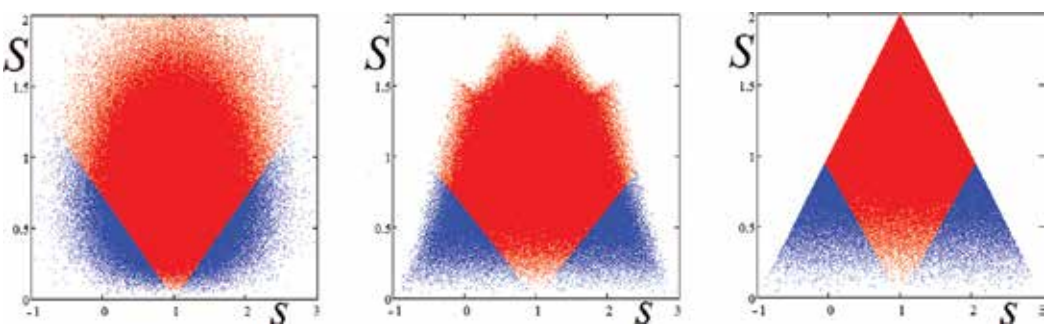

Figure 2. Clouds of scattering of results of estimates. For normal $N(x, \mu = 1, \sigma = 1)$ (left) and uniform $U(x, min = -1, max = 3)$ (central and right) distributions. The number of tests is 10^6, the multiplicity of the experiment is 5 and the color markings for the confidence probability of 0.95.

3.2. Corrections coefficients

The normative tool has yet a problem that we call a mysterious amendment to deviation. Deviation is recommended to be used not in a pure form, but with a correction coefficient (the so-called standard deviation). It is explained that this amendment allegedly eliminated deviation from the dispersion of the normal random source. But very few noticed that this is not quite true.

Firstly, the distribution of deviation is asymmetric, its form changes, and is especially strongly at small amounts of repeated experiments. And only to an infinite number of experiments it approximates to normality and, accordingly, to symmetry.

Secondly, because of the nonsymmetric form of deviation distribution, it is not entirely clear in which its characteristic should be adjusted. It is customary to correct the mode, but with the same success, it is possible to correct a centre of gravity or some kind of composite criterion composed of the moments of this distribution.

Thirdly, even for the mode, the recommended corrections only partially eliminate the problem. The reason lies in the desire to describe the correction factor by a simple formula. While its magnitude is simply calculated, the result does not fit into any of the proposed theoretical constructions (**Figure 3**). The reason is the complex and contradictory changes in the form and position of the cloud of estimates as the number of repeated experiments is changing.

The idea of the correction is that, a priori knowing its magnitude, we correct the estimate made by the statistics that measures the scattering parameter so that in the statistical limit the estimate coincides with the value of the dispersion. The question arises: what for? The quality of the estimate of the measured quantity is determined by the sectoral formula, and the coefficient

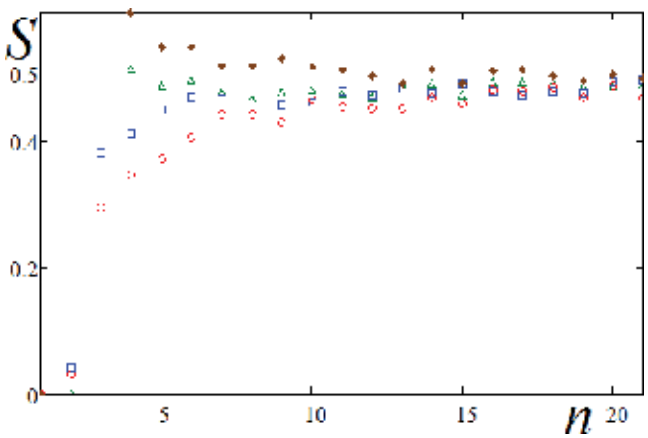

Figure 3. Estimates of the scattering parameter and the effect of corrections as a function of the number of repetitions of the experiment. The source of randomness is the normal distribution with $\mu = 2$ and $\sigma = 0.5$. The statistics for estimating the scattering parameter is the deviation. MCM is used for obtaining data by two 10^7 tests. Each point is the result of an independent experiment. Legend on the figure field: ○ is estimate without correction, □ with correction factor $\sqrt{\frac{n}{n-1}}$ (standard deviation), △ with correction $\sqrt{\frac{n-2}{n-3}}$ and ◆ with correction $\sqrt{\frac{n-1}{n-3}}$.

of coverage of which is calculated even more easily than the correction. A reasonable way is to abandon the amendments and the coefficients of coverage numerically computed, but this will no longer be the coefficients of the Student.

The sectoral formula is useful, but the rank measure copes with similar tasks of metrology better.

4. The principle of measuring of probabilities of origin

The principle says that the important instrument of metrological research should allow to estimate the probability of obtaining a certain sample of data from the selected model.

According to the principle—using the model and experimental data—the joint probability distribution for all values of each of the estimated variables is calculated. Each point of this distribution is interpreted as the probability that the data is obtained in accordance with the model and, moreover, with specific values of its parameters. Evaluation of the result of the experiment is given as $\hat{X} \coloneqq \{(x, p)\}$ (the value of each of the estimated variables, the corresponding probability of this value). Of course, differences in the parameters of the model lead to different probabilities for a particular value of the evaluated value; the same can be said if the model is the same and the experimental data are different.

The task of constructing the estimation algorithm is solved in the general form of both MCM and CDM. The results are comparable, although the algorithms are different. To solve this, we need a consistency of the numerical model and also a metric for the data structures that model the results of the experiment.

Formally, this sequence of operations must be performed: $\bar{x} \xrightarrow{dis} \{x\} \to \{M(x)\} \to \{Pr|x\} \to \{\mu(Pr, D)|x\} \to u(x)$. The range of possible values of the estimated parameter x^- must be broken one way or another into a set of possible values $\{x\}$. Using the model for each possible value, a prediction of the possible data values $\{Pr\}$ (it also is a set) should be obtained. Each prediction is compared with the experimental data by means of the metric μ. The results of the comparison are collected in the uncertainty function $u(x)$. And, only after this based on the uncertainty function, simplified formal estimates are performed.

The numerical consistency of the model is understood as the ability of the model (if all the adjustable variables are given) in a numerical experiment to generate model data indistinguishable (quite similar) from the data obtained in the experiment.

The metric should evaluate the magnitude of the difference between the same type of data in both experimental and simulation origin. The metric is constructed based on the modeling method and also on features of the application where it is used.

When using MCM, the 'natural' metric consists of counting the (approximate) matches of the data set to be checked and the extensive database generated for the given parameter values. In order to estimate the probability to the value of the parameter being evaluated, the model is launched many times (at example N), at this value of the parameter x, and the fraction of coincidences

with the experimental data is counted in this series of numerical experiments, formally $\{M(x) \rightarrow Pr{=}{=}D\}_N \xrightarrow{count} C$; sequence metric is $\mu \stackrel{\text{def}}{=} \frac{C}{N}\Big|x$. Repeating a series of experiments for other values of the same parameter, we obtain the required estimate, which looks like a density of probability distribution. If it is required to evaluate number of the factors more than have been considered, then they are evaluated by the same algorithm by performing similar operations.

When using MCD, the estimation algorithm solves the deconvolution problem in the general formulation $M(u(x)) \rightarrow Pr{=}{=}D \rightarrow u(x)$. The model parameters are specified as densities for both the stochastic component and the parameters to be evaluated (as objective function $u(x)$). The prediction of the model will be obtained as a certain n-dimensional density describing the possible values of the data. It is required to choose both the dimensions and the form of the density of the evaluated parameters so that the metric points out the maximum similarity of the experimental data and the prediction of the model. The natural metric in this approach is the magnitude of the overlap of the prediction density and the actual experimental data, namely, $\mu \stackrel{\text{def}}{=} \int_{\pm\infty} Pr(x, D(x))dx$ in general and in a case of point data as $\mu \stackrel{\text{def}}{=} Pr(D)$.

Obviously, the solution in general form, without taking into account the structure of the model and data, is very labour-consuming by both methods. But for simple models and data, the situation is so simplified that it leads to simple algorithms.

5. Rank measure

The concept of a rank measure was proposed years ago and analyzed from both the intuitive and the formal points of view. Here, we propose an approach which can be regarded as justification as rationale in constructive style.

Statement. For a trivial metrological model, if the source of randomness is described only by its distribution, and the data elements are statistically independent, the implementation of the 'principle of measuring the probability of origin' leads to a simple 'rank measure'.

Proof. From the assumption of data independence, the value of the metric is independent of the permutation of the data elements in the data sample used to identify the trivial model.

In fact, suppose that for two data samples of the same length, all elements are the same. Should the metric distinguish them? It is obvious enough that it is not necessary to distinguish and there is no possibility to do this.

Now, in each sample, one element by element of a different but identical value and in the same position is replaced. As before, the samples are indistinguishable.

Now, in one of the data samples, we change the positions of any two elements. If the data elements are equal, then the samples are indistinguishable. If the data elements are different, then the samples can be distinguished, but should this be done?

If the data is independent, then any position of each element is equally probable. Thus, the probability of origin is unchanged. The metric must be such that a simple permutation of data elements within one of the samples does not change the value of the metric. Consequently, neither the number nor the step of internal permutations on the value of the metric is affected.

This creates an equivalence class for data samples formally different as records of the data acquisition process, but within the class, those samples are indistinguishable by the metric. Data sample after simple sorting in ascending order (rank statistics) is a natural representative of each of these classes and can be used instead.

Each of the data sample elements $d_k | k = 1 \ldots n$ in its ordered sample has its own order density of distribution $p_{k/n}(x) = \frac{n!}{(k-1)!(n-k)!} P(x)^{k-1} (1 - P(x))^{n-k} p(x)$ different from the distributions in each of elements in other positions, where $p(x)$ and $P(x)$ are the probability distribution density and the cumulative distribution function of a model random source, respectively.

The probability of the origin of the value of each data element d_k is calculated from the corresponding order distribution density as $p_{k/n}(d_k)$. The probability associated with the entire sample of data $\{d_k\}_n$ is naturally calculated as the multiplication of the origin probabilities of each of the elements of data $m\left(\{d_k\}_n\right) = \prod_{k=1}^{n} p_{k/n}(d)$ because the event of obtaining a sample of data is considered single. We call this result the 'rank measure'. *End of proof.*

An important feature of the algorithm for identifying a trivial statistical model with the assumptions made is that there is no need to explicitly define the metric. You can immediately go to the estimation of the demanded probability of origin by comparing the prediction of the model in the form of the densities of the distributions of each of the data elements and the sorted experimental data. The formula of a rank measure can be dissected to three factors:

$$m(\{d\}_n, \mu, \sigma) = \left(\prod_{k=1}^{n} \frac{n!}{(k-1)!(n-k)!}\right) \times \left(\prod_{k=1}^{n} \left(P(d_k, \mu, \sigma)^{k-1} \left(1 - P(d_k, \mu, \sigma)\right)^{n-k}\right)\right) \left(\prod_{k=1}^{n} p(d_k, \mu, \sigma)\right)$$

Their interpretation is obvious: the latter is the formula of the likelihood method, the second is the correction to the likelihood method and the first is the normalizing factor. For this reason, the rank measure can be considered as a corrected likelihood method.

The rank measure is the simplest solution of the identification problem for the simplest model that can be obtained within the framework of calculating the probability of origin. The reason is in the availability of an analytical formula for calculating the model's prediction. For more complex models, there is no such formula. At least we need to compute the prediction of the model numerically. Studies were conducted and it was revealed that for two important particular models' explicit formulation of a metric is not required too. It is multifactor expansion of the trivial model and model where the parameters of the dynamic deterministic function are identified against the background of noise.

6. Using rank measure in metrology

In this section we give examples of the application of a rank measure in some basic types of experiments. Let us compare the results obtained by algorithms using a rank measure and the results of normative algorithms. In this section, several varieties of direct measurement experiment and one generalization are considered.

6.1. Calibration experiment

Calibration experiment is main type of experiments in metrology. There is no means of measurement which one way or another would not undergo calibration. The purpose of the calibration experiment is to compare the measuring instrument with the standard, collect the data and describe a correction function that will be used as a priori information in the working measurement experiment.

In the calibration experiment, the values of the standard and the readings of the measuring instrument are juxtaposed. In this case, the measuring means is used to estimate the value of the standard used. The results are collected and form a data structure, for example, as in **Figure 4** (left).

The correction function is constructed as a regression at the calibration data. The obvious representation is the density stretched over the whole measurement range and accumulating all the calibration information [**Figure 4** (right)]. The more calibration data and the more carefully the regression, the more reliable the results. The replacement of the abscissa axis from the value of the reference value to the unknown means that the probability of the value of the standard corresponding to the experimental data is estimated.

The quantity and quality of the information collected in the calibration experiment and the information stored in the correction function largely determine the capabilities of the working measurement experiment. Although modern regulatory documents allow the use of a correction function in this form, for example, IEEE 1451, historically, the systematic error is eliminated separately, and the uncertainty of the measurement tool is described as an interval approximation of the density function in the form of a two-term formula or its simplifications.

6.2. Single experiment

The correction function is used in a working experiment to fully evaluate the result of the experiment. If the data comes in the form of a point estimate (number), then the corrected measurement result is calculated as cross section of correction function, which is interpreted

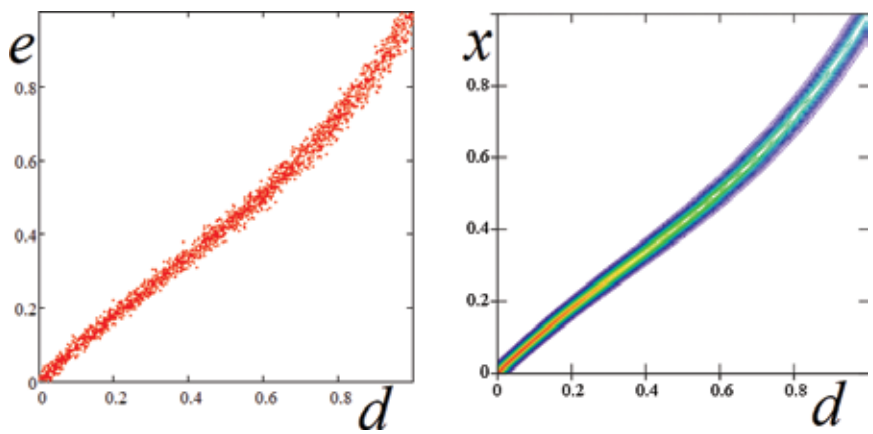

Figure 4. The structure of the calibration data in graphical form (left) and the correction function (right) as the regression of these data $p(x) = \hat{f}(d)$.

as the distribution density of the possible values of the measured value. That is, the systematic error is eliminated, and an estimate of the uncertainty of the values of the measurand is given (**Figure 5**).

On the other hand, the data may already contain a description of the uncertainty, for example, in the form of a probability density $g(d)$. In this case, the joint probability density distribution of the data and the estimate is calculated $p(d,x) = g(d) \cdot \left(\hat{f}(d) = x\right)$. Note that this is a joint distribution and does not refer to independent distributions because of the large correlation (**Figure 6**). The projection of this joint density will lead to a final evaluation of the measurement result $p(x) = \int_{\pm\infty}\left(g(d) \cdot \hat{f}(d)\right)dd$. Thus, a complete and natural synthesis of the available a priori and a posteriori information about this measurement experiment was made without any assumptions and approximate calculations.

6.3. Multiple experiment

Measuring the same physical quantity repeatedly, in principle, we get the opportunity to deal with errors and thereby improve the accuracy of the evaluation of the result. The problem of normative statistical tools is that it was far from always possible to use data efficiently, and sometimes efficiency was reduced to zero. From this point of view, since the rank measure uses the form of a specific distribution, it will always be optimal in efficiency with respect to this distribution.

6.3.1. The scattering parameter is unknown and is estimated from experimental data

The greatest effect of using the rank measure as statistics for estimating the distribution parameters is observed in a multiple experiment with unknown scattering. According to the principle of probability of origin, the probability of obtaining experimental data from a

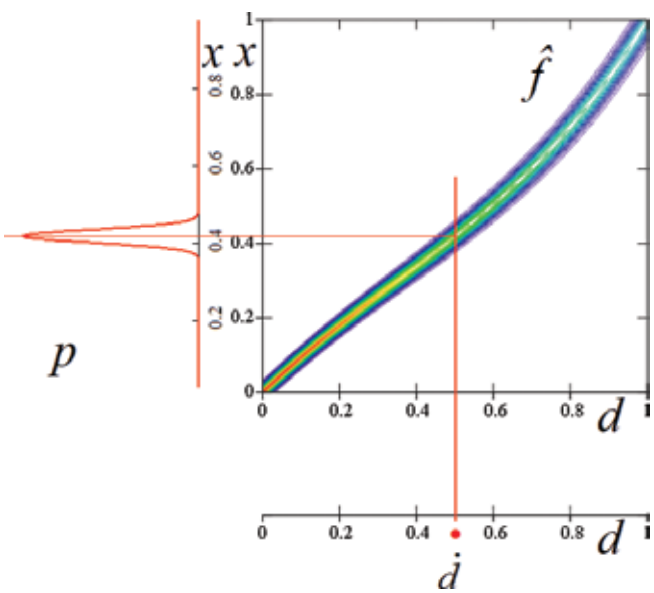

Figure 5. The transition from point experimental data $\dot{d}$ to a full evaluation of the experimental result, taking into account a priori information about the property of the measuring instrument $p(x) = \hat{f}(\dot{d})$.

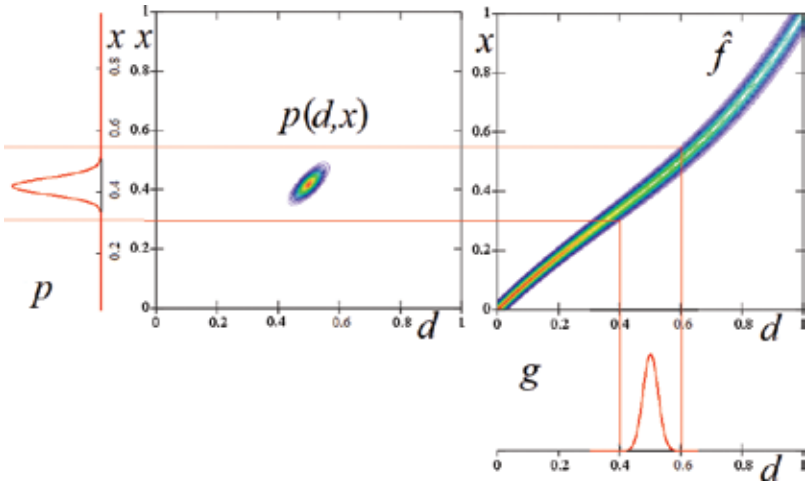

Figure 6. The transition from experimental data with uncertainty $g(d)$ to a full evaluation of the experimental result $p(x) = \int_{+\infty} p(d, x)dd$. In the middle of the figure, an intermediate result is presented $p(d, x) = g(d) \cdot \hat{f}(d)$.

random process model with a known form of the distribution density is estimated, but the parameters of the shift μ and scattering σ must be estimated from the experimental data. Note that the form of the distribution can be arbitrary, but it shall be a priori known, for example, obtained from a calibration experiment. We seek a joint distribution of the values of parameters that are estimated $u(\mu, \sigma) = m(\{d\}_n, \mu, \sigma)$, and the distribution density of error source is also described in terms of the values of these parameters $p(x, \mu, \sigma)$.

For example, we estimate the shift parameter from the data for normal and uniform distributions $\{d\}_n = \{-0.125, -0.044, 0.183, 0.349, 0.404\}$. It is convenient to designate the desired joint distribution as $u(\mu, \sigma) \mid p$ with an explicit indication of the distribution form used in the model and interpret it as a function of the uncertainty of estimates with respect to the distribution used (**Figure 7**).

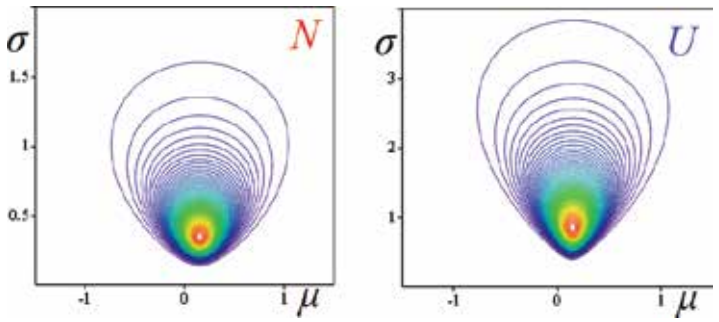

Figure 7. Uncertainty functions $u(\mu, \sigma) \mid N$ for the normal distribution (only the form is used) and $u(\mu, \sigma) \mid U$ for the uniform distribution. For a correct comparison, distribution densities are scaled to the law 2σ.

The uncertainty functions for different distributions differ in varying degrees by form but mainly by the scattering estimate. The distributions used in the example are both symmetric for this reason, and the difference in the estimation of the shift parameter is small.

Now, it became possible to move from a joint estimation of parameters to only an estimate of the shift parameter (usually interpreted as an estimate of the measured quantity). At this stage, it is possible to take into account a priori information about the scattering parameter. This information can be different. One of the polar cases is its complete absence; the scattering can be any $u(\mu) = \int_{\pm\infty} u(\mu, \sigma)d\sigma$ (**Figure 8**).

If, for joint uncertainty function, the influence of the form of the model distribution is obvious, then the integral estimates of only the shift parameter differ insignificantly. Small differences can be interpreted as evidence of the prevalent thesis 'if there is a small number of data the form of the distribution is unimportant'. More precisely, when identifying only the shift parameter for a small number of data, the form of the distribution has no important significance and does not introduce significant errors in addition for a wide class of distributions. However, it is possible to construct counterexamples that show that this is not always so, for example, using distributions having a significant displacement.

The form of the uncertainty function of the result for a number of reasons has heavier tails than the original distribution. Briefly, there are two main reasons. There is still a high probability of obtaining compact data from the distribution with a large value of the scattering parameter, which heavies the tails of the uncertainty function. On the contrary, the probability of compact distributions is concentrated in a small space, which leads to a high probability density near the vertex of the uncertainty function and sharpens it.

Now, we can write an interval estimate of the measurement result as a quantile of the uncertainty function. For the confidence probability of 0.95 by the normal distribution model, result estimation with uncertainty is 0.153 ± 0.869 and by the uniform distribution model is 0.149 ± 0.94. Uncertainty function has less scattering than the original distribution (at example for normal distribution ±1.96 and for uniform ±2.0), which is actually the goal of increasing the multiplicity of the experiment. The recording of the result by the form is the same as the

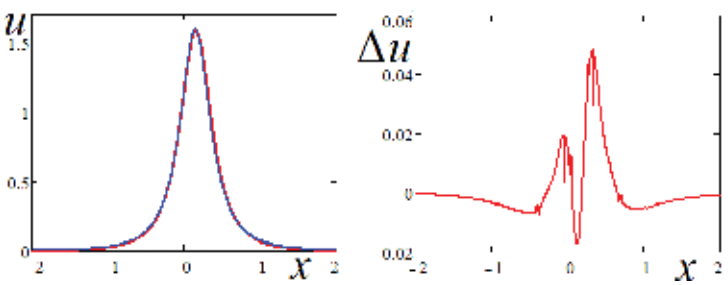

Figure 8. The uncertainty functions of estimating the shift parameter (left) and their difference (right). The notations on the left figure are a red line for the normal distribution and blue for the uniform, respectively. For a correct comparison, the uncertainty functions are normalized, which is interpreted as an assumption of the validity of both models simultaneously.

normative one, but in fact it has a more rigorous meaning. Tails of joint distributions (as well as clouds of estimates) are cut vertically, but not by the sector as in the normative case.

6.3.2. The scattering parameter is known fully or partially

There are many cases when the scattering parameter is known a priori with greater or lesser accuracy. The direct way to take into account information about the value of the scattering parameter is to solve the estimation problem for an unknown parameter and only then to use a priori information $u(\mu,\sigma)\xrightarrow{\sigma?}u(\mu)$. The algorithm for solving the problem formally depends on the form of the representation of this information but at the heart of all algorithms lies an integral that somehow projects the joint uncertainty function to the shift parameter uncertainty.

The most often known is the range of possible values of the scattering parameter $\bar{\sigma}$. The solution reduces to a simple integral $u(\mu) = \int_{\sigma} u(\mu,\sigma)d\sigma$. Two polar variants are evident. It is complete ignorance $\bar{\sigma} = \pm\infty$ and exact knowledge $\sigma = \dot{\sigma} \pm 0$ which are solved analogically. The case of a known density distribution $g(\sigma)$ of the scattering parameter $u(\mu) = \int_{\pm\infty} g(\sigma)u(\mu,\sigma)d\sigma$ is slightly more complicated (**Figure 9**).

6.3.3. Repetitive experiment

Under favorable conditions, instead of the joint uncertainty function of the parameters, one can use the fact that the correction function itself is a distribution. Consequently, one complete correction function can be replaced by a set of ordinal correction functions with the same external characteristics. This is done either experimentally in a calibration experiment or analytically from the formulas of the densities of ordinal distributions for each value of the measured quantity in the entire measurement range. We obtain a family of correction functions passing along and partially overlapping $\{f_{k_n}(d)\}_n$. Each of these functions is used to correct its data element from an ordered data sample [**Figure 10** (left)]. The uncertainty function with

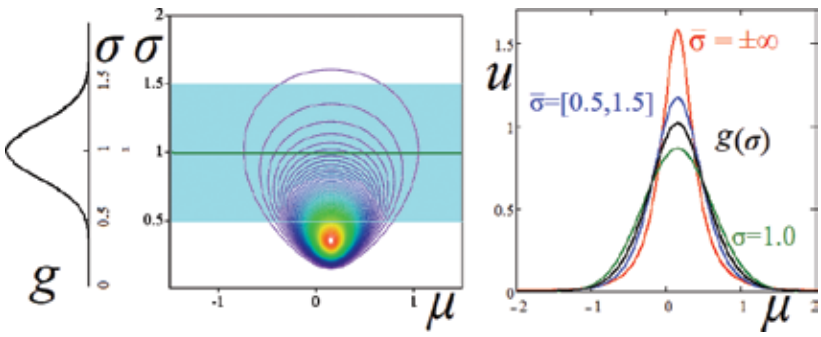

Figure 9. Illustration of the use of a priori information on the scattering parameter in order to convert joint uncertainty to uncertainty function of the shift parameter. Legend on the right picture field: The green line is the exact knowledge of the scattering parameter $\sigma = 1.0$; black line corresponds to the normal distribution $g(\sigma) = N(\sigma, 1{,}0.2)$ (graph on the left); blue line corresponds to the interval number $\bar{\sigma} = [0.5{,}1.5]$; and red line for complete ignorance $\bar{\sigma} = \pm\infty$. Legend on the Centre picture field: The joint uncertainty distribution with respect to both parameters is the same as in **figure 7** on the left; the green line is the exact knowledge of the scattering parameter; and blue wideband is the image of the scattering parameter interval.

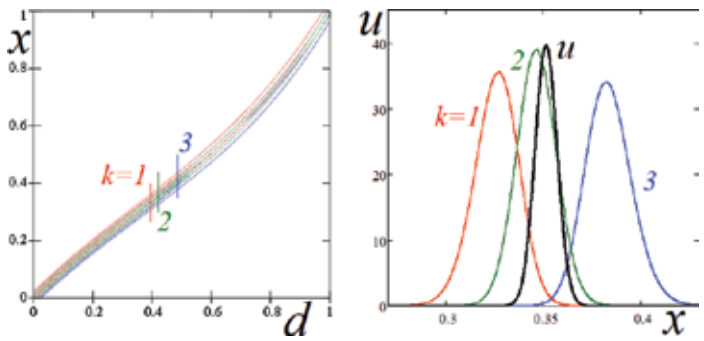

Figure 10. Illustration of the use of the set of ordinal correction functions. On the left is a set of correction functions for a triple experiment, and on the right is an example of estimating the value of the measured parameter for data {0.4, 0.41, 0.44} each of the three ordinal estimations (color lines) and resultant estimation (black line).

respect to the shift parameter is calculated directly as the product of these functions $u(x) = \prod_{k=1}^{n} f_{\nu_k}(d_k)$. The formula is interpreted as uncertainty of a repetitive measurement of the same physical quantity by an imperfect means of measurement but with a known scattering parameter of it stochastic model. It is assumed that new sources of randomness, not accounted for by the calibration experiment, are not added. This is what distinguishes the repeated experiment from a multiple experiment.

This tool is more refined because it can take into account the change in the form of the distribution of the correction function for different elements from the data set. But it is more vulnerable because it does not provide for any additional sources of randomness that cannot be the taken into account in the calibration experiment.

The situation where the scattering parameter is known sufficiently accurately is not so rare, although it is hidden inside the measuring instrument. At best, the user can adjust the 'accumulation time'. If the accumulation of information is made in digital form, then this is a direct analogue to the number of repeated measurements, but in the analogue form, the accumulation is not fundamentally different from the effect of repeated measurements.

6.3.4. The uncertainty of the experimental data is known

The abstraction of point data is very useful from a practical point of view. Its application seriously simplifies both calculations and their interpretation, and the results are of quite satisfactory quality. In most cases, it should be used. However, in the strict approach, each data element must be assigned to its own individual uncertainty. For many applications, including the case of multiple measurement experiments, an adequate form of describing the uncertainty of the experimental data is the probability density of the obtained value $D := \{g_k(\delta)\}_n$ interpreted as the reliability of the point fragment of this estimate. It is because the basis is the single experiments in which the initial data are obtained.

Normative documents including GUM solve this problem taking into account uncertainties apart, for example, preliminarily dividing the uncertainties into type A and type B and then

combining them in a specific way. The method is simple but strictly adequate only for normal distribution and simple models. For distributions similar to normal distribution, the deterioration in the result still is quite acceptable.

To strictly take into account the uncertainty of the measuring instrument, it is sufficient to slightly upgrade the rank measure to.

$$m(D) = \int_{\pm\infty}^{n} \left(m\left(sort\left(\{\delta\}_n\right)\right) \cdot \prod_{k=1}^{n} g_k(\delta) \right) d\delta^n.$$

The formula is interpreted as an n-fold integral of a rank measure from deviation to point data with their joint probability. The complexity of applying the formula is the multiplicity of the integral and the need to constantly check the order of the data if the density of the data distribution overlaps. When the distribution density of data is reduced to the delta function, the upgraded measure reduces to the original measure. The delta function is the model of point data. From this point of view, uncertainty function for point data is the most likely, but for data deviations it is a less likely alternative.

In a more general case, all sources of uncertainty are taken into account in a natural way when calculating the model's predictions and when a comparison of the prediction and an adequate data model is made.

Let us explain this with an example (**Figure 11**). The data is the same as for **Figure 10**. We will supplement the data with uncertainty ±0.05. The uncertainty is the same for all data elements, but it can also have an individual value. The law of distribution of uncertainty will be assumed to be uniform. The model of the measurement experiment being studied differs from the trivial model only in the presence of two sources of randomness. One source has a normal distribution law, for example, the error of manufacturing samples from the same material whose property is being investigated. Another source has a uniform distribution of, for example, uncertainty of a digit measuring instrument.

The work of the algorithm can be interpreted as the creation of a film. Each frame is an estimate of the parameters from a given set of point data $\{\delta_k\}_n$. Each frame is similar to the one in **Figure 11** (left). The difference between frames is a consequence of the differences in the data. Data is selected from specified distributions either randomly (MCM) or according to a

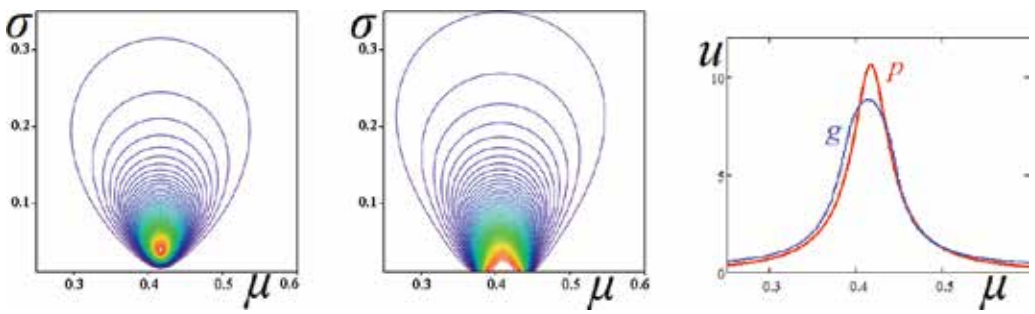

Figure 11. Illustration of identification of a trivial model with two different sources of randomness. The left figure is obtained for point data, and the central figure is obtained for data with uncertainty. The right figure shows the uncertainty functions of the estimates for the two preceding figures: *p*, without data uncertainties, and *g*, with uncertainties.

regular grid (MCD) (in example used 12 grid knots for each data distribution). Each frame corresponds a probability that is calculated by formula $\prod_{k=1}^{n} g_k(\delta_k)$. When all data distributions are uniform and equal, then probabilities of frames are equal. At the end of the algorithm, all frames (in example $12^3 = 1728$ frames) are summed according to their probability. The result is shown in **Figure 11** in the centre.

The uncertainty is large compared to the distance between data; hence, the probability of accidental coincidence of data is large, which leads to a touch of the uncertainty function of the estimates to the abscissa axis [**Figure 11** (centre)]. The uncertainty of the data, as it was, 'smears out' the uncertainty function of the estimate. Uncertainty is greater in all respects but especially strongly affects the top of the uncertainty function of the estimate of the measured parameter and often changes the form of the evaluation function.

This allows us to build a logical chain from the interpretation of data by interpreting possible estimates to the final estimate of the uncertainty of the measurand. For example, $D \xrightarrow{\hat{f}(d)} \{d(x)\} \xrightarrow{\{p(x)\}} \{u(x)\} \to \overline{x}$, where D is the initial experimental data given in point form, $\hat{f}(d)$ is the correction function obtained from a calibration experiment, $\{d(x)\}$ is the data in the form of densities that have adjusted by the calibration experiment, $\{p(x)\}$ is the set of admissible types of distributions in measurement model, $\{u(x)\}$ is the set of densities of estimates measurand and $\overline{x}$ is the final evaluation, for example, obtained for the worst case.

6.3.5. Multifactor multiple experiment

The purpose of the multifactorial experiment is to estimate the value of several quantities in the form of a joint uncertainty function by factors. The number of factors considered varies easily, so in the examples we confine ourselves to two. And so, $u(\xi, \upsilon)$ is estimated by the data structure $\Xi\Upsilon$ for each of the factors. The result of the evaluation and the complexity of the algorithm are essentially determined by the relationships within the data structure. The simplest solution is obtained when the data for different factors are not related to each other. For example, a data structure is simply a list of independent data differing only belonging to its factor $\Xi\Upsilon \coloneqq \Xi, \Upsilon$. The solution consists of a multiplication of uncertainty functions for each of the factors calculated independently $u(\xi, \upsilon) = u(\xi)u(\upsilon)$. The number of data for each factor can be different.

Another solution is obtained if the experimental data are obtained synchronously $\Xi\Upsilon \coloneqq \{\xi, \upsilon\}_n | \xi \in \Xi, \upsilon \in \Upsilon$. If the statistical relationships between the factors do not manifest themselves $r(\xi, \upsilon) = p(\xi) \cdot g(\upsilon)$, then it is possible to express the densities of order distribution $r_{i,j,n}(\xi, \upsilon) = p_{i/n}(\xi) \cdot g_{j/n}(\upsilon)$.

For example, if the multiplicity of experiment is 3, the number of factors is 2, $p(\xi)$ is a normal distribution and $g(\upsilon)$ is the uniform distribution, then the figure of the set of ordinal distributions will look like in **Figure 12**.

The rank measure is constructed as follows. The data structure (in the example this is three data pairs) is ordered by one of the factors, for example, by ξ. This predefines the selection of the columns of the set of ordinal distributions. The rows are selected in accordance with the order of the data for the second factor. As a result, for each experiment of the nine distributions, three will be chosen. Using them as a function of the data values, we get three probabilities for each

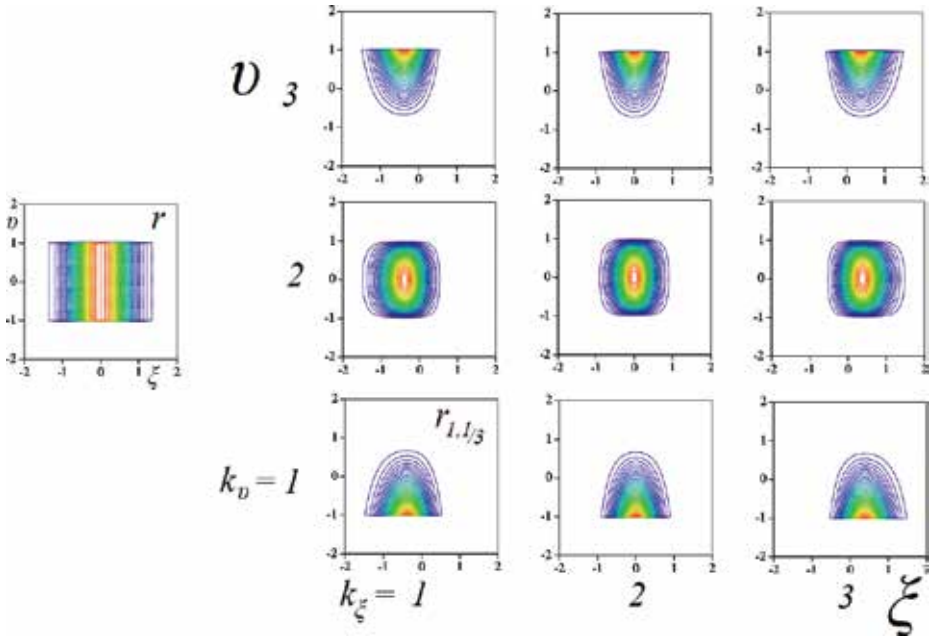

Figure 12. Initial joint distribution and set of ordinal joint distributions.

rank. Multiplying them we get the value of a rank measure. You can take advantage of this in a working experiment when the data about the same physical quantity comes in completely different ways.

For example, let's use the model whose distribution is shown in **Figure 12**. The received data is {(−0.5,0.5), (0.1, −0.4), (0.5,0.7)}. Their order is {(1, 2), (2, 1), (3, 3)}. The values of probabilities from the densities of ordinal distributions are {(0.578), (0.841), (1.114)}. Hence the value of a rank measure is 0.542. Next, it is possible to identify the shear and scattering parameters of the model in the usual way.

In the event that the statistical links between the factors are significant, the task is solved only numerically. For MCM, this is a direct numerical experiment. MCD is a search for direct and inverse transformations of such that make the distribution of the model independent by factors.

6.4. Indirect experiment

In order to pass from the model of direct measurement to the model of the indirect measurement experiment, it is necessary to replace the measurand of trivial model by a more complex measurement principle model $x = f(\xi, \upsilon)$, where ξ and υ are the quantities measured from the direct measurement experiment. In a simple formulation, the problem of an indirect experiment consists in calculating the uncertainty function of the new measurand $u(x)$, starting from the uncertainties obtained from the experimental data $u(\xi)$ and $u(\upsilon)$. As a rule, the problem is easily solved by both MCM and MCD.

Although in the natural sciences and in technology one can find very complex principal models of the experiment, metrology strives to avoid indirect experiments. This is achieved through the creation of new standards and the construction of suitable calibration schemes (calibration hierarchy). Even if the measurement tool uses inside the complex indirect model but being calibrated in the target units, then it realizes direct experiment. All that metrology can afford is the use of an indirect experiment as a temporary means in cases where a direct reference to the standard is not yet possible. Of course, one can complicate the formulation of the problem of indirect experiment in different ways, for example, in the analogy of Section 6.3.5, complicating the data structure, but it is unlikely that metrologists will be interested in this.

7. Conclusion

The tools that metrology now uses have been created by statisticians at the beginning of the last century. By the middle of the century, metrology had mastered them. Over the years, the goals and circumstances of their creation and some of the properties have been forgotten. This creates some misunderstandings when interpreting the results of their application. Attempting to implement the GUM has been useful by simplifying and standardizing their application, but the tools themselves remained the same.

As a result of the application of new tools, a direct and obvious chain of information gathering and use is built up in the performance of metrology tasks from calibration to the final result.

Author details

Eugene Charnukha

Address all correspondence to: charnukha@tut.by

A. V. Luikov Heat and Mass Transfer Institute, National Academy of Sciences of Belarus, Minsk, Belarus

References

[1] Uncertainty in Measurement (GUM). https://www.bipm.org/en/publications/guides/

[2] Chernukho EV. Estimation of arbitrary-distribution parameters from the data of a repetitive experiment. Journal of Engineering Physics and Thermophysics. 2010;**83**(2):431-437

[3] Chernukho EV. Substantiation of the rank measure as an efficient statistic for estimating distribution parameters of arbitrary form. Journal of Engineering Physics and Thermophysics. 2012;**85**(1):239-248

[4] Chernukho EV. Uncertainty principle in metrology and statistics: Algorithms and applications. Journal of Engineering Physics and Thermophysics. 2014;**87**(2):498-506

[5] Chernukho EV. Analysis of uncertainties with the example of direct and inverse heat metering problems. Journal of Engineering Physics and Thermophysics. 2016;**89**(2): 518-527. DOI: 10.1007/s10891-016-1405-9

[6] Chernukho EV. Regression algorithm using the rank measure. Journal of Engineering Physics and Thermophysics. 2015;**88**(4):1034-1043. DOI: 10.1007/s10891-015-1282-7

Edited by Anil Akdogan

Metrology, the science of measurement, is crucial for many sciences and technological developments. Since metrology helps to improve many other sciences, the book reflects in general metrology and some special metrological approaches at different fields such as radiation and frequency measurements in detail. This book also focuses on technical testing and control applications in the industry. It also intends the fundamentals of metrology concerning the related standards and systems of units. In addition, the book considers the calibration of measurement instruments and measurement uncertainties as the basic requirements of the related quality standards.

Published in London, UK

IntechOpen

ISBN 978-1-83881-517-2